NASA/TM-20240000941

Analyses of the MISSE 9-15 Polymers and Composites Experiment 1-4 (PCE 1-4) Contamination Samples

Kim K. de Groh
Glenn Research Center, Cleveland, Ohio

Dorothy Lukco
HX5, LLC, Brook Park, Ohio

Sylvie F. Crowell and Skyler J. Gregor
Glenn Research Center, Cleveland, Ohio

Bruce A. Banks
Science Applications International Corporation, Cleveland, Ohio

February 2024

NASA STI Program Report Series

Since its founding, NASA has been dedicated to the advancement of aeronautics and space science. The NASA scientific and technical information (STI) program plays a key part in helping NASA maintain this important role.

The NASA STI program operates under the auspices of the Agency Chief Information Officer. It collects, organizes, provides for archiving, and disseminates NASA's STI. The NASA STI program provides access to the NTRS Registered and its public interface, the NASA Technical Reports Server, thus providing one of the largest collections of aeronautical and space science STI in the world. Results are published in both non-NASA channels and by NASA in the NASA STI Report Series, which includes the following report types:

- TECHNICAL PUBLICATION.
  Reports of completed research or a major significant phase of research that present the results of NASA Programs and include extensive data or theoretical analysis. Includes compilations of significant scientific and technical data and information deemed to be of continuing reference value. NASA counterpart of peer-reviewed formal professional papers but has less stringent limitations on manuscript length and extent of graphic presentations.

- TECHNICAL MEMORANDUM.
  Scientific and technical findings that are preliminary or of specialized interest, e.g., quick release reports, working papers, and bibliographies that contain minimal annotation. Does not contain extensive analysis.

- CONTRACTOR REPORT.
  Scientific and technical findings by NASA-sponsored contractors and grantees.

- CONTRACTOR REPORT.
  Scientific and technical findings by NASA-sponsored contractors and grantees.

- CONFERENCE PUBLICATION.
  Collected papers from scientific and technical conferences, symposia, seminars, or other meetings sponsored or co-sponsored by NASA.

- SPECIAL PUBLICATION.
  Scientific, technical, or historical information from NASA programs, projects, and missions, often concerned with subjects having substantial public interest.

- TECHNICAL TRANSLATION.
  English-language translations of foreign scientific and technical material pertinent to NASA's mission.

Specialized services also include organizing and publishing research results, distributing specialized research announcements and feeds, providing information desk and personal search support, and enabling data exchange services.

For more information about the NASA STI program, see the following:

- Access the NASA STI program home page at http://www.sti.nasa.gov

NASA/TM-20240000941

Analyses of the MISSE 9-15 Polymers and Composites Experiment 1-4 (PCE 1-4) Contamination Samples

Kim K. de Groh
Glenn Research Center, Cleveland, Ohio

Dorothy Lukco
HX5, LLC, Brook Park, Ohio

Sylvie F. Crowell and Skyler J. Gregor
Glenn Research Center, Cleveland, Ohio

Bruce A. Banks
Science Applications International Corporation, Cleveland, Ohio

National Aeronautics and
Space Administration

Glenn Research Center
Cleveland, Ohio 44135

February 2024

Acknowledgments

We are grateful to the NASA Flight Opportunities program, the International Space Station Program Office and Aegis Aerospace for making these flight opportunities possible. We would also like to thank Diane Malarik of NASA Headquarters, along with Craig Robinson and Kelly Bailey of NASA Glenn Research Center for their long-term support of these MISSE-FF experiments. This work is supported by the Biological and Physical Sciences Division.

Level of Review: This material has been technically reviewed by technical management.

This report is available in electronic form at https://www.sti.nasa.gov/ and https://ntrs.nasa.gov/

NASA STI Program/Mail Stop 050
NASA Langley Research Center
Hampton, VA 23681-2199

Contents

Analyses of the MISSE 9-15 Polymers and Composites Experiment 1-4 (PCE 1-4) Contamination Samples

Kim K. de Groh
National Aeronautics and Space Administration
Glenn Research Center
Cleveland, Ohio 44135

Dorothy Lukco
HX5, LLC
Brook Park, Ohio 44142

Sylvie F. Crowell* and Skyler J. Gregor†
National Aeronautics and Space Administration
Glenn Research Center
Cleveland, Ohio 44135

Bruce A. Banks
Science Applications International Corporation
Cleveland, Ohio 44135

Abstract

Spacecraft in low Earth orbit (LEO) are subjected to harsh environmental conditions, including radiation (cosmic rays, ultraviolet (UV), x-ray and charged particle radiation), micrometeoroids and orbital debris, temperature extremes, thermal cycling, and atomic oxygen (AO). These environmental exposures can result in erosion, embrittlement and optical property degradation of susceptible materials threatening spacecraft performance and durability. To increase our understanding of environmental effects such as AO erosion and radiation induced embrittlement of spacecraft materials, NASA Glenn Research Center developed a series of experiments that were flown as part of the Materials International Space Station Experiment (MISSE) missions on the exterior of the International Space Station (ISS). Recently, four Glenn experiments with 365 flight samples were flown on ISS's MISSE-Flight Facility (MISSE-FF). These experiments are the Polymers and Composites Experiment-1 (PCE-1) flown as part of the MISSE-9 mission, the PCE-2 flown as part of the MISSE-10 mission, the PCE-3 flown as part of the MISSE-12 and MISSE-15 missions, and the PCE-4 flown as part of the MISSE-13 mission. Each of these experiments included passive contamination witness samples in each flight direction for post-flight molecular contamination analyses. A total of 13 contamination flight samples were flown. The post-flight analyses of the PCE 1-4 contamination samples include X-ray Photoelectron Spectroscopy (XPS) analyses (surface and ion sputter depth analyses) and optical properties (total reflectance, total transmittance and solar absorptance). This paper provides results of post-flight

*Summer 2023 Pathways Intern at NASA Glenn Research Center
†Summer 2022 Pathways Intern at NASA Glenn Research Center

analyses of the PCE 1-4 contamination samples and their corresponding control samples. Knowledge of on-orbit contamination is important for the PCE 1-4 flight data interpretation.

1.0 Introduction

Spacecraft in low Earth orbit (LEO) are subjected to harsh environmental conditions, including radiation (cosmic rays, ultraviolet (UV), x-ray and charged particle radiation), micrometeoroids and orbital debris, temperature extremes, thermal cycling, and atomic oxygen (AO). These environmental exposures can result in erosion, embrittlement and optical property degradation of susceptible materials threatening spacecraft performance and durability. In addition, on-orbit spacecraft contamination is a serious spaceflight issue, with silicone contamination being a particular concern.

Silicones are used as adhesives, potting compounds and lubricants for various spacecraft components. An example of this is the adhesive for bonding cover glass to solar cells. Although spacecraft designers generally use silicones that meet outgas requirements, silicone fragments can still be evolved in the vacuum environment in LEO and the process is enhanced with AO and/or radiation-induced bond breaking.[1] Silicone fragments that deposit on surfaces with accompanying AO exposure are oxidized, lose hydrocarbons, and convert to a hardened, often crazed, silica-based oxide layer.[2,3] In addition, UV can react with silicone fragments, causing a polymerized contaminant layer to build up. If the silicone deposition is also accompanied by hydrocarbon deposition, a far more optically absorbing coating can result.[1] Examples of darkened silicone contamination have been reported on the Long Duration Exposure Facility (see Figure 1)[4,5] and the Russian space station Mir (see Figure 2)[6]. Figure 1 shows an example of AO and UV radiation darkened silicone contamination from LDEF's Passive Solar Array Materials Experiment.[4,5] Figure 2 shows silicone darkened components from a Russian solar array panel retrieved after more than ten years exposure to the orbital space environment on the Russian space station Mir.[6] On-orbit contamination can negatively affect spacecraft components (optical and thermal properties, etc.) and spaceflight experiment results. For example, the accumulation of an oxidized

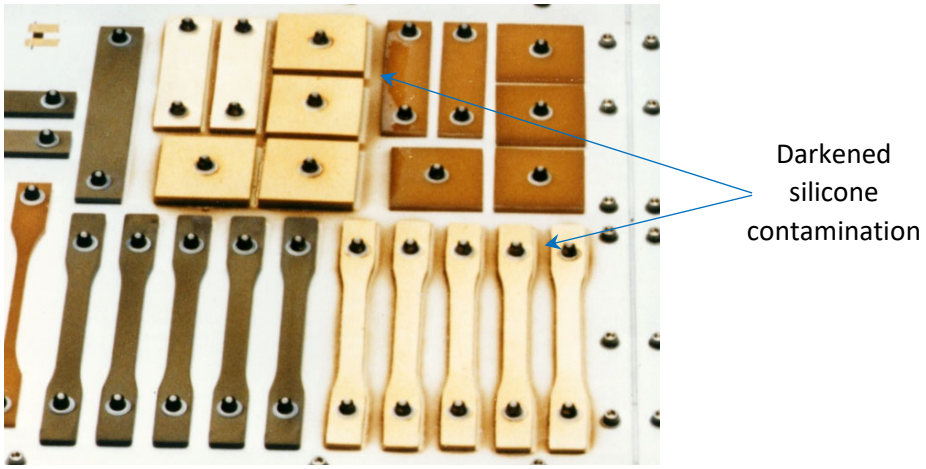

Figure 1. Atomic oxygen and UV darkened silicone contamination on LDEF (arrows point to areas with the dark contamination layer).[4,5]

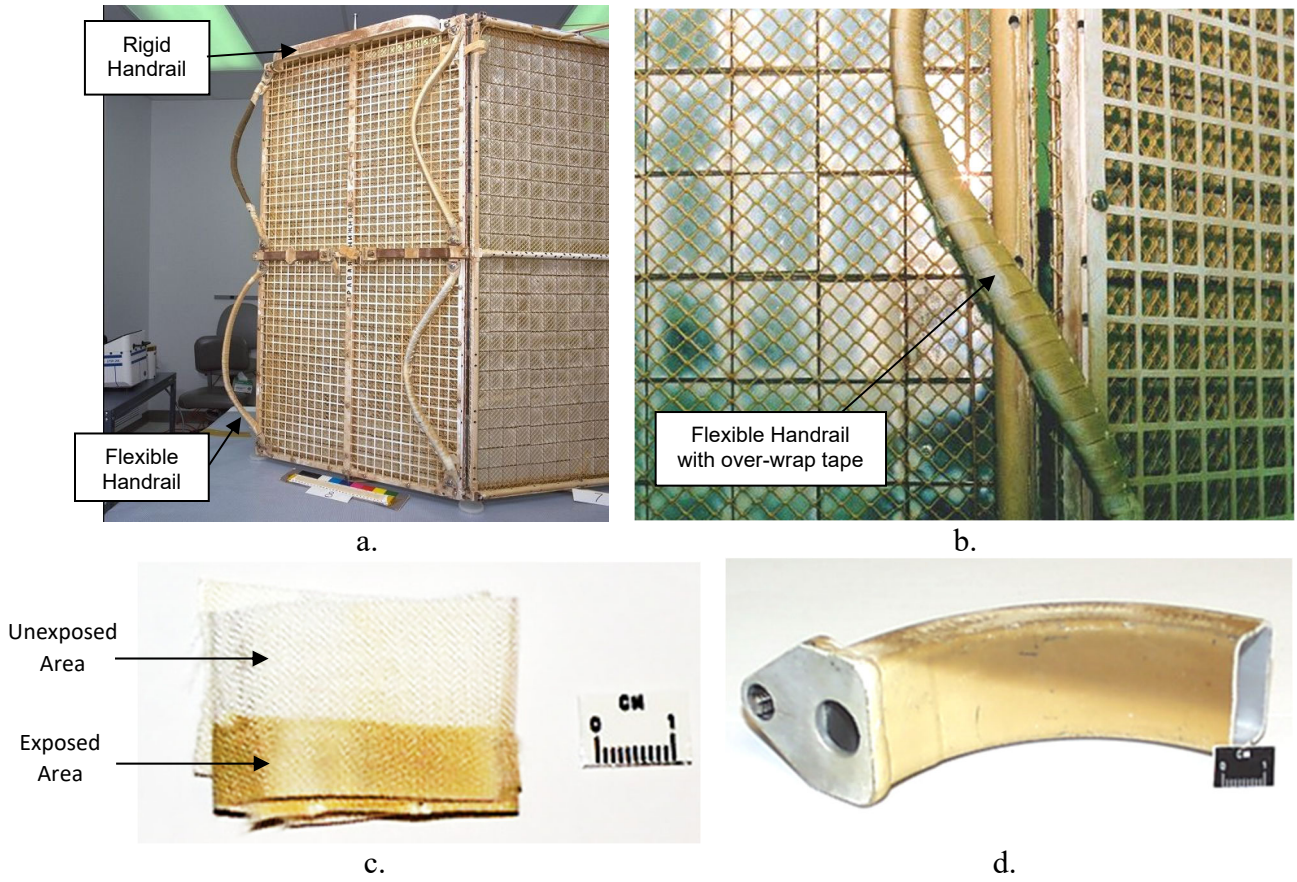

Figure 2. Examples of silicone darkened components from a retrieved Russian space station Mir solar panel: (a). Backside of the solar array panel, (b). Close-up section showing a flexible handrail with darkened over-wrap tape, (c). Flexible handrail over-wrap tape sample showing exposed and unexposed areas, and (d). The array-facing side of a darkened curved rigid handrail sample.

silicate layer can negatively affect AO erosion experiments. An example is provided by Kimoto for Japan Aerospace Exploration Agency's Micro-Particles Capturer and Space Environment Exposure Device (MPAC&SEED) space materials exposure experiment flown on the exterior of the ISS's Russian Service Module (SM).[7] One of the monitoring samples flown on MPAC&SEED had an estimated 90 nm layer of silicone contamination that prevented the sample erosion.[7]

To increase our understanding of effects such as AO erosion and radiation induced embrittlement of spacecraft materials, NASA Glenn Research Center developed a series of experiments that were flown as part of the Materials International Space Station Experiment (MISSE) missions on the exterior of the International Space Station (ISS). These experiments have provided critical space environmental durability data such as AO erosion data of polymers and composites, and radiation induced mechanical property degradation of spacecraft insulation materials, after long term space exposure. Four Glenn experiments with 365 flight samples were flown on ISS's MISSE-Flight Facility (MISSE-FF). These experiments are the Polymers and Composites Experiment-1 (PCE-1) flown as part of the MISSE-9 mission, the PCE-2 flown as part

of the MISSE-10 mission, the PCE-3 flown as part of the MISSE-12 and MISSE-15 missions, and the PCE-4 flown as part of the MISSE-13 mission.[8,9]

Each of the PCE 1-4 experiments included passive contamination witness samples in each flight direction for post-flight molecular contamination and optical property analyses. A total of 13 contamination flight samples were flown. The post-flight analyses included X-ray Photoelectron Spectroscopy (XPS) analyses (surface and ion sputter depth analyses) and optical properties (total reflectance, total transmittance and solar absorptance) of flight and corresponding control samples. This paper provides a brief overview of the PCE 1-4 experiments, a summary of the MISSE 9-15 mission environmental exposures, and detailed results of the post-flight analyses of the PCE 1-4 contamination samples and their corresponding control samples.

2.0 MISSE-Flight Facility (MISSE-FF)

The PCE 1-4 flight experiments with 365 flight samples were flown on ISS's MISSE-FF. MISSE-FF samples are flown in MISSE Sample Carriers (MSCs) also referred to as MISSE Science Carriers. The MISSE-FF is operated by Aegis Aerospace, Inc.[10] It is a modular and robotically serviceable external facility that is located on ISS Express Logistics Carrier-2 Site 3 (ELC-2 Site 3). Figure 3 provides an on-orbit photograph showing the location of the MISSE-FF on ELC-2. The MISSE-FF provides ram, wake, zenith, and nadir space exposures. Figure 4 provides a diagram of these flight orientations on the ISS. Figure 5 shows a close-up of the wake side of the MISSE-FF with one MSC open. The MISSE-FF is rotated 8° "pitch up" such that the zenith direction is 8° away from ram and the nadir direction is 8° towards ram. Thus, the nadir samples will get slightly more grazing AO fluence and the zenith samples will get slightly less grazing AO fluence during the MISSE-FF missions. Additionally, the ram surface is off-set 8° from true ram.

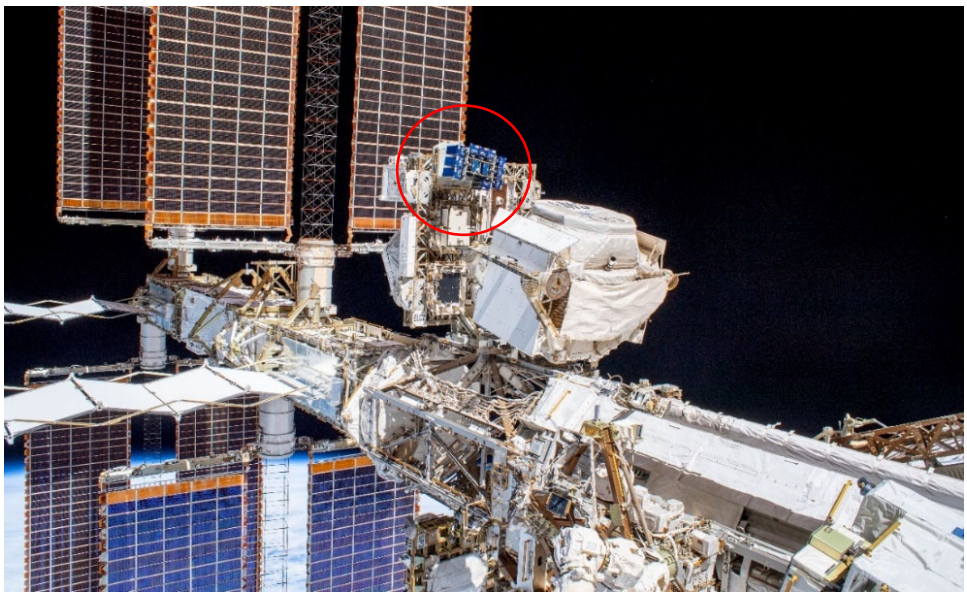

Figure 3. A view of the MISSE-FF on ELC-2 Site 3 as photographed during an EVA on November 15, 2019 (iss061e040917).

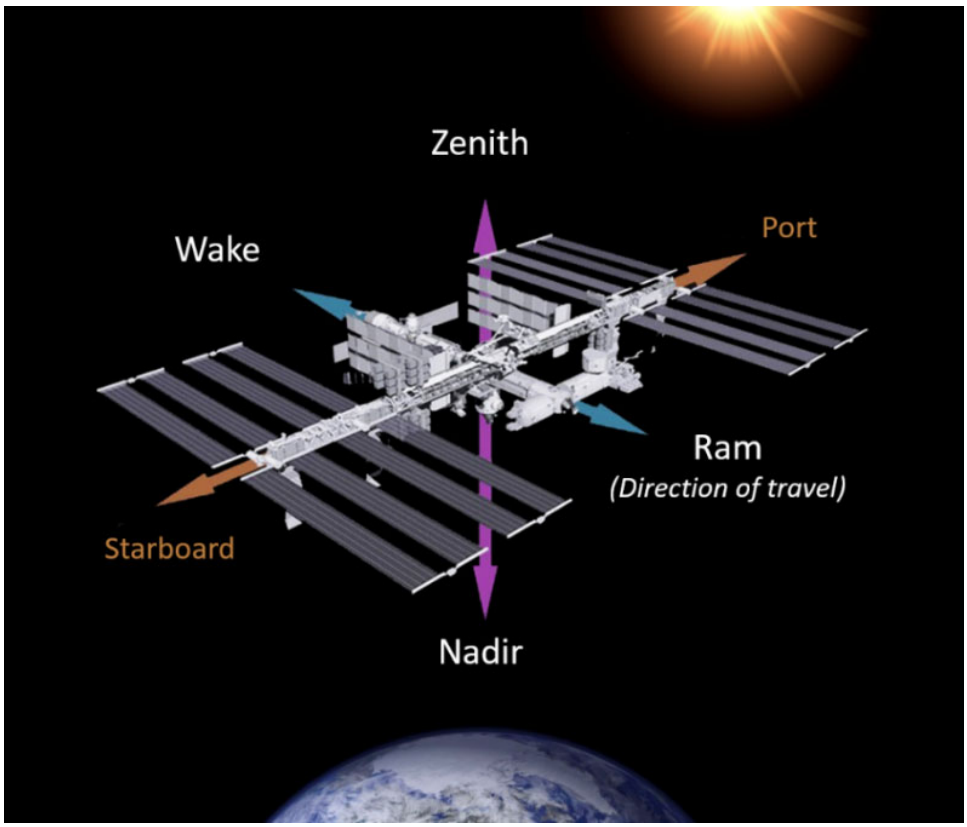

Figure 4. Diagram showing ram, wake, zenith, and nadir directions on the International Space Station.

Figure 5. The wake side of the MISSE-FF with the MISSE-10 PCE-2 and MISSE-12 PCE-3 MSCs as photographed on January 25, 2020 during an EVA. The MSCs are closed, except for the central wake MSC which is open (iss061e143021).

3.0 MISSE 9-15 Mission Exposures

Reference 9 by de Groh and Banks provides a detailed review of the space environmental exposure for the PCE 1-4 flight samples. Table 1 provides the mission environmental exposure summary table for the PCE 1-4 experiment samples as reported in Reference 9. The table provides the MISSE mission and flight experiment, on-orbit flight direction (also referred to as flight orientation), MSC details including mount side (MS) or swing side (SS) deck, launch and return missions, and the dates of MSC installation onto the MISSE-FF along with the MSC retrieval dates from the MISSE-FF. Table 1 also provides for each MSC the direct space vacuum duration, direct space exposure duration (total time the MSC was open and exposed to the space environment), the computed AO fluence, and the total mission ESH (provided by Aegis Aerospace). The AO fluence values were computed from Kapton H® AO Fluence Witness sample dehydrated mass loss, except for MISSE-12 zenith where the AO fluence was based on the erosion morphology of a zenith Photographic AO Fluence Monitor (M12Z-S1 F).[9]

Typical on-orbit temperatures are also provided by de Groh and Banks in Reference 9 and are listed below. These MISSE-FF MSCs temperature ranges were provided by Aegis Aerospace and can vary during each mission depending on the Sun's Beta angle and ISS orientation.

- Ram: -30 °C to 45 °C
- Zenith: -20 °C to 50 °C
- Wake: -26 °C to 45 °C
- Nadir: -7 °C to 40 °C

It should also be noted that all MSC decks loaded with flight samples underwent a pre-flight thermal vacuum bake-out at Aegis Aerospace. The thermal vacuum bake-out was conducted at 60 °C for 24 hours while under vacuum (approximately 3×10^{-5} torr).

Table 1. Polymers and Composites Experiment 1-4 (PCE 1-4) Mission Exposure Summary[9]

MISSE Mission and Experiment	Flight Direction	MISSE Sample Carrier (MSC)	Launch Mission	Installed on MISSE-FF	Retrieved from MISSE-FF	Return Mission	Space Vacuum Duration (Years)	Time on MISSE-FF (Years)	Direct Space Exposure Duration (Years)	Atomic Oxygen Fluence (atoms/cm^2)^	Mission Equivalent Sun Hours (ESH)^^
MISSE-9 PCE-1	Ram	R2 (MSC 3) MS	SpaceX-14 April 2, 2018	April 18, 2018	Nov. 11, 2019	SpaceX-19 Jan. 7, 2020	1.59	1.57	0.77	3.44E+20	952.3
	Wake	W3 (MSC 8) MS		April 18, 2018	April 26, 2019	SpaceX-17 June 3, 2019	1.07	1.02	0.54	4.46E+16	634.6
	Zenith	Z3 (MSC 5) MS		April 19, 2018			1.07	1.02	0.54	3.19E+18	555.7
MISSE-10 PCE-2	Ram	R1 (MSC 11) MS	NG-10 Nov. 17, 2018	Jan. 4, 2019	Nov. 25, 2020	SpaceX-21 Jan. 13, 2021*	1.93	1.90	1.17	3.93E+20	1445.4
	Zenith	Z2 (MSC 10) MS			March 18, 2020	SpaceX-20 April 7, 2020	1.25	1.20	0.69	4.84E+18	702.0
	Nadir	N3 (MSC 13) MS					1.25	1.20	0.48	6.94E+18	102.3
MISSE-12 PCE-3	Ram	R2 (MSC 4) SS	NG-12 Nov. 2, 2019	Nov. 11, 2019	Nov. 25, 2020	SpaceX-21 Jan. 13, 2021*	1.07	1.04	0.89	2.97E+20	1104.0
	Wake	W3 (MSC 6) MS			Nov. 27, 2020		1.07	1.05	0**	0	0
	Zenith	Z1 (MSC 18) MS			Nov. 26, 2020		1.07	1.05	0.45	*≈1.67E+18*	465.4
MISSE-13 PCE-4	Wake	W1 (MSC 5) MS/SS	SpaceX-20 March 6, 2020	March 18, 2020	Nov. 27, 2020	SpaceX-21 Jan. 13, 2021*	0.72	0.70	0.44	2.65E+18	515.6
	Zenith	Z2 (MSC 19) MS			Nov. 26, 2020		0.72	0.70	0.46	2.24E+18	467.9
MISSE-15 PCE-3 Wake Re-flight**	Wake	W1 (MSC 10) MS	SpaceX-23 Aug. 29, 2021	Dec. 28, 2021	Aug. 2, 2022	SpaceX-25 Aug. 20, 2022	0.71	0.60	0.44	4.77E+18	511.7

MS: Mount side deck; SS: Swing side deck

*January 13, 2021 EST (January 14, 2021 UTC)

**The PCE-3 wake samples were re-flown as part of the MISSE-15 mission

^ AO fluence was computed from dehydrated Kapton H mass loss, except for MISSE-12 zenith which was based on erosion morphology of the M12Z-S1 Photographic AO Fluence Monitor

^^ Mission Equivalent Sun Hours (ESH) from Aegis Aerospace's "MISSE MSC UV Equivalent Sun Hours Calculation" Report (A. Goode, MEMO-MISSE-0004 Rev C03, August 17, 2022)

4.0 Polymers and Composites Experiment 1-4 (PCE 1-4) Overview

The MISSE-9 PCE-1 is a passive experiment with 138 samples that were flown in ram (39 samples), wake (52 samples) and zenith (47 samples) orientations as part of the MISSE-9 inaugural mission of MISSE-FF. The MISSE-10 PCE-2 is a passive experiment with 43 samples that were flown in ram (21 samples), zenith (10 samples), and nadir (12 samples) directions. The MISSE-12 PCE-3 is a passive experiment with 86 samples that were flown in ram (30 samples), wake (42 samples) and zenith (14 samples) directions. The MISSE-13 PCE-4 is a passive experiment with 98 samples that were flown in the wake (65 samples) and zenith (33 samples) directions. The PCE-3 wake MSC was never opened on-orbit during the MISSE-12 missions, therefore the 42 wake samples were re-flown as part of the MISSE-15 mission in the wake direction (thus, "MISSE-12/MISSE-15" naming convention).

The primary objective of the PCE-1, PCE-2 and PCE-3 is to determine the LEO AO erosion yield (E_y) of spacecraft polymers, composites, and coated samples as a function of solar irradiation and AO fluence. The PCE 1-3 also have numerous additional objectives including:

- Characterization of optical property degradation of spacecraft polymers and composites in LEO.
- Improving the understanding of AO scattering mechanisms for AO undercutting and erosion predictive models.
- Determining the functionality and durability of LEO exposed cosmic ray shielding and shape memory composite samples.

The PCE-1 also included a variety of Teflon fluorinated ethylene propylene (FEP) tensile samples that were flown in both the wake (38 samples) and zenith (24 samples) directions for radiation embrittlement studies.

The primary objectives of the PCE-4 are to determine optical and mechanical property degradation of spacecraft materials, and to assess the functionality of shape memory alloys (SMAs), shape memory polymer composites, melanin based composites and elastomer seal samples after radiation exposure in LEO. Twenty-four PCE-4 FEP and solar sail tensile samples were flown in the wake direction for radiation embrittlement studies. In addition, the AO E_y of various PCE-4 samples was also determined.

Each of the PCE 1-4 experiment included other unique samples such as AO Scattering Chambers, indium tin oxide (ITO) conductive coatings, specialty coatings (including Z307 black paint and Ball Infrared Black (BIRB) paint), potential space deployable structure materials, uncoated and coated docking seal samples, and cosmic ray shielding materials. Also as stated previously, each experiment included samples to determine the mission AO fluence and on-orbit molecular contamination in each flight orientation. Figures 6 to 9 provide pre-flight photographs of the PCE-1, PCE-2, PCE-3 and PCE-4 samples in the MSC flight decks, respectively.

Figure 6. Pre-flight photograph of the MISSE-9 PCE-1 samples loaded into the MSC MS flight decks, from left to right: R2 MSC 3 (ram), W3 MSC 8 (wake), and Z3 MSC 5 (zenith). The PCE-1 samples are outlined in red with the exception of the larger square samples in the R2 ram deck (4 samples) and the Z3 zenith deck (5 samples).

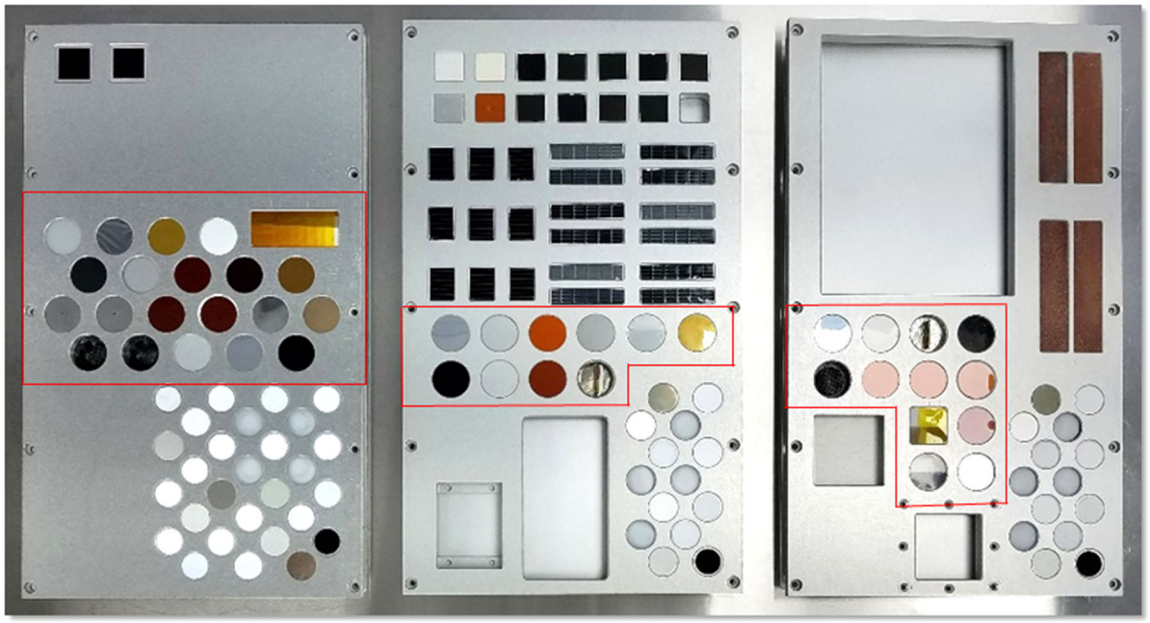

Figure 7. Pre-flight photograph of the MISSE-10 PCE-2 samples loaded into the MSC MS flight decks, from left to right: R1 MSC 11 (ram), Z2 MSC 10 (zenith), and N3 MSC 13 (wake). The PCE-2 samples are outlined in red.

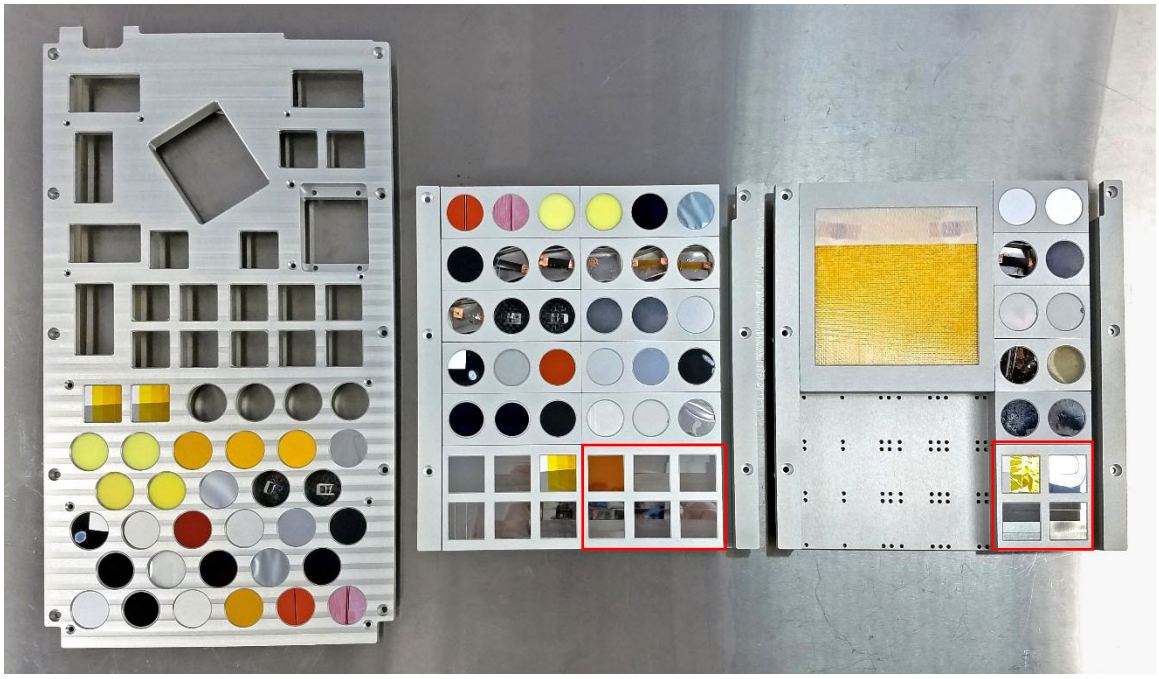

Figure 8. Pre-flight photograph of the MISSE-12 PCE-3 samples loaded into the MSC flight decks, from left to right: R2 MSC 4 SS (ram), W3 MSC 6 MS (wake) and Z1 MSC 18 MS (zenith). Samples in red boxes were moved to a different location on the deck prior to flight.

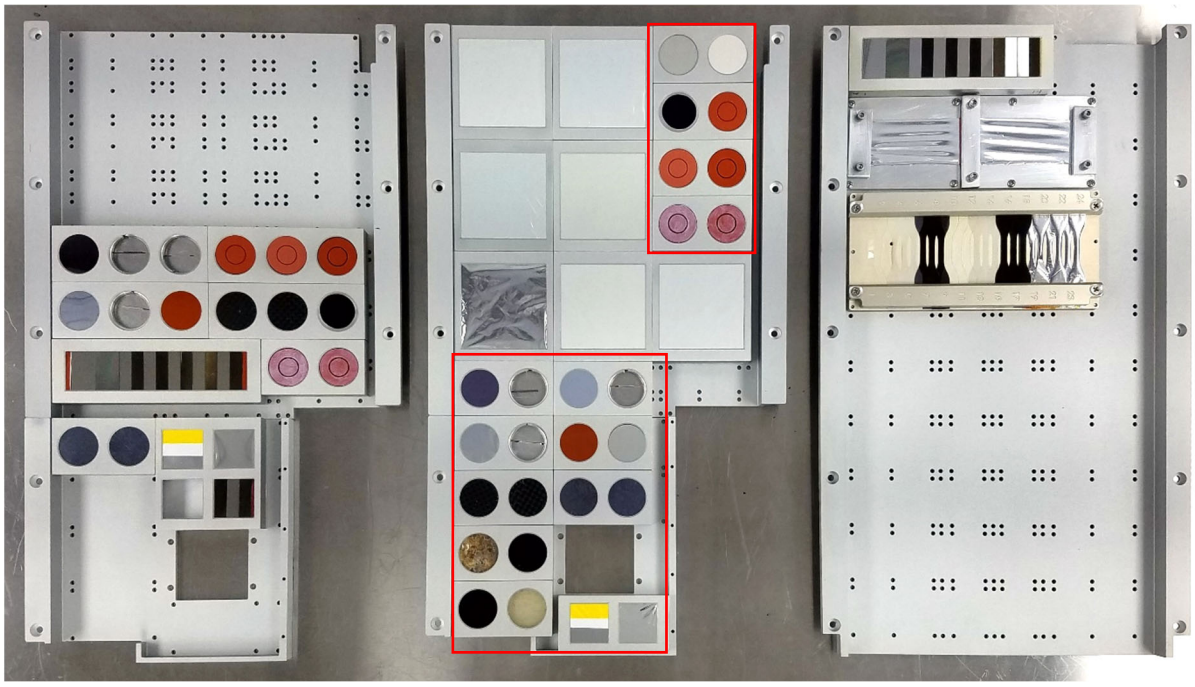

Figure 9. Pre-flight photograph of the MISSE-13 PCE-4 samples loaded into the MSC flight decks, from left to right: Z2 MSC 19 MS (zenith), W1 MSC 5 MS (wake) and W1 MSC 5 SS (wake). The PCE-4 samples in the wake MS deck are outlined in red.

As of February 2024, the PCE 1-4 experiments have 44 sample collaborators from 22 organizations including several NASA centers, academia, the Air Force Research Laboratory, and various commercial companies. Reference 8 by de Groh and Banks provides a detailed listing of all 365 PCE 1-4 flight samples, the sample objectives and includes lists of the sample collaborators for each experiment.

4.1 PCE 1-4 Contamination Samples

Table 2 provides a list of the 13 PCE 1-4 flight (F) contamination witness samples along with 12 corresponding non-flown "back-up" (B) control samples. A majority of the contamination samples were alumina (Al_2O_3, sapphire) slides as alumina does not erode with AO exposure and

Table 2. The PCE 1-4 Contamination Samples

MISSE Mission	Flight Orientation	Sample ID	Flight or Back-up	Material	Abbrev.	Thickness (inch)
MISSE-9	Ram	M9R-C6 F	Flight	Alumina slide	Al_2O_3	0.063
		M9R-C6 B	Back-up	Alumina slide	Al_2O_3	0.063
	Wake	M9W-C3 F	Flight	Alumina slide	Al_2O_3	0.063
		M9W-C3 B	Back-up	Alumina slide	Al_2O_3	0.063
	Zenith	M9Z-C3 F	Flight	Alumina slide	Al_2O_3	0.063
	Ram	M9R-C27 F	Flight	Magnesium Fluoride	MgF_2	0.108
		M9R-C27 B	Back-up	Magnesium Fluoride	MgF_2	0.108
	Zenith	M9Z-C18 F	Flight	Magnesium Fluoride	MgF_2	0.108
		M9Z-C18 B	Back-up	Magnesium Fluoride	MgF_2	0.108
MISSE-10	Ram	M10R-C4 F	Flight	Alumina slide	Al_2O_3	0.063
	Ram	M10R-C4 B	Back-up	Alumina slide	Al_2O_3	0.063
	Zenith	M10Z-C5 F	Flight	Alumina slide	Al_2O_3	0.063
	Zenith	M10Z-C5 B	Back-up	Alumina slide	Al_2O_3	0.063
	Nadir	M10N-C5 F	Flight	Alumina slide	Al_2O_3	0.063
	Nadir	M10N-C5 B	Back-up	Alumina slide	Al_2O_3	0.063
MISSE-12	Ram	M12R-C3 F	Flight	Alumina slide	Al_2O_3	0.063
	Ram	M12R-C3/ M12W-C3 B*	Back-up	Alumina slide	Al_2O_3	0.063
	Zenith	M12Z-S2 F^	Flight	Shape Memory Alloy	SMA NiTi	0.020
	Zenith	M12Z-S2 B^	Back-up	Shape Memory Alloy	SMA NiTi	0.020
MISSE-13	Wake	M13W-C4 F	Flight	Teflon FEP/Al	FEP/Al	0.005
	Wake	M13W-C4 B	Back-up	Teflon FEP/Al	FEP/Al	0.005
	Zenith	M13Z-C4 F	Flight	Teflon FEP/Al	FEP/Al	0.005
	Zenith	M13Z-C4 B	Back-up	Teflon FEP/Al	FEP/Al	0.005
MISSE-12/ MISSE-15	Wake	M12W-C3 F	Flight	Alumina slide	Al_2O_3	0.063
	Wake	M12R-C3/ M12W-C3 B*	Back-up	Alumina slide	Al_2O_3	0.063

*Shared control sample
^Two ½ x 1-inch rectangular binary NiTi pieces

silicone contamination can be easily detected. One of two binary NiTi SMA sample pieces was used for XPS analyses for the MISSE-12 zenith direction. Back-surface aluminized-Teflon fluorinated ethylene propylene (FEP/Al) samples were used for contamination detection for the MISSE-13 mission due to the low erosion yield of FEP and the easy detection of Si. All samples are 1-inch (2.43 cm) diameter circular (C) disks with the exception of the MISSE-12 zenith SMA samples (M12Z-S2 F and B). These samples are comprised of two ½ x 1-inch rectangular binary NiTi pieces.

The Sample ID provides the MISSE mission number (M#), the flight orientation (ram - R, wake - W, nadir - N, or zenith - Z), the sample's shape (circular - C or square - S), the ID number and the pre-flight sample designation of Flight (F) or Back-up (B). Therefore, M9R-C6 F was circular sample #6 flown on the MISSE-9 mission in the ram direction and was designated pre-flight as the flight sample. Optical properties were not obtained on the MISSE-12 zenith SMA sample due to the sample size.

5.0 Experimental Procedures

5.1 X-ray Photoelectron Spectroscopy (XPS) Analyses

X-ray Photoelectron Spectroscopy (XPS) is a surface sensitive technique that allows for the identification and quantification of elements and trace contaminants found on a surface. Analysis depth is between 3 to 5 nm (30 to 50 Å) and detection limits are parts per thousand. XPS is sensitive to the electronic environment of each atom, allowing for chemical state information to be obtained about any elements detected. It is also possible to evaluate deeper areas below a surface contamination layer using depth profiling. In this case, an argon ion gun is used to generate ions and information is obtained by alternating sputtering and measurement.

X-ray Photoelectron Spectroscopy measurements were performed on a PHI 5000 Versaprobe (ULVAC-PHI) using monochromatic microfocused Al x-rays (200 μm, 50 W) with a photoelectron takeoff angle of 45°. Survey scans using a 117.4 eV pass energy were initially taken to identify all components, followed by higher resolution individual region scans using a pass energy of 93.9 eV. Atomic concentrations were calculated based on the individual peaks. Sputtering was then done on each sample using a 3 kV Ar+ beam to remove 10 nm of material. For the control samples, this was done to remove any adventitious carbon that comes from normal air exposure. For the actual flight samples, sputtering was done in 1-minute increments (removing 10 nm) until a clean substrate surface was obtained. This way it was possible to determine the thickness of the contamination layer on the flight exposed surfaces.

5.2 Optical Properties

A Cary 5000 spectrophotometer, operating with a DRA 2500 integrating sphere, was used to obtain spectral total reflectance (TR_λ) and spectral total transmittance (TT_λ) from 250 to 2,500 nm wavelengths. A baseline and zero scan are used to calibrate the spectrophotometer prior to sample measurement. The baseline scan uses a 99% reflecting Spectralon standard that matches the lining

of the integrating sphere in order to calibrate the spectrophotometer for a perfect reflector. The zero scan represents a perfect absorbing material. For the baseline scan of TR_λ, a standard was placed in the integrating sphere reflectance sample port. For the zero scan, the standard was removed from the port and the beam was allowed to exit the integrating sphere into a blackbody absorbing cavity. For TR_λ, each sample was placed in the reflectance port for measurement which was located in the anterior of the sphere. To obtain the zero scans for TT_λ, a small piece of opaque material was inserted in the spectrophotometer entrance port to block the beam of light from passing through. The baseline was obtained in the same manner as for the TR_λ. After calibration, the flight or control sample was placed in the entrance port to the sphere for measurement of TT_λ and the standard was inserted into the reflectance port.

A NASA Glenn Research Center Cary 5000 Excel® Macro was used to compute the spectral absorptance (α_λ), which was determined using the equation $\alpha_\lambda = 1 - (TR_\lambda + TT_\lambda)$. The Excel® Macro was also used to integrate each spectral curve with respect to the air mass zero (AM0) solar spectrum (the spectrum of the solar radiation outside the Earth's atmosphere, see Figure 10) over the spectral range (250 to 2500 nm) to obtain the total AM0 integrated values for: total reflectance (TR), total transmittance (TT), and solar absorptance (α_s) for each flight and control sample.

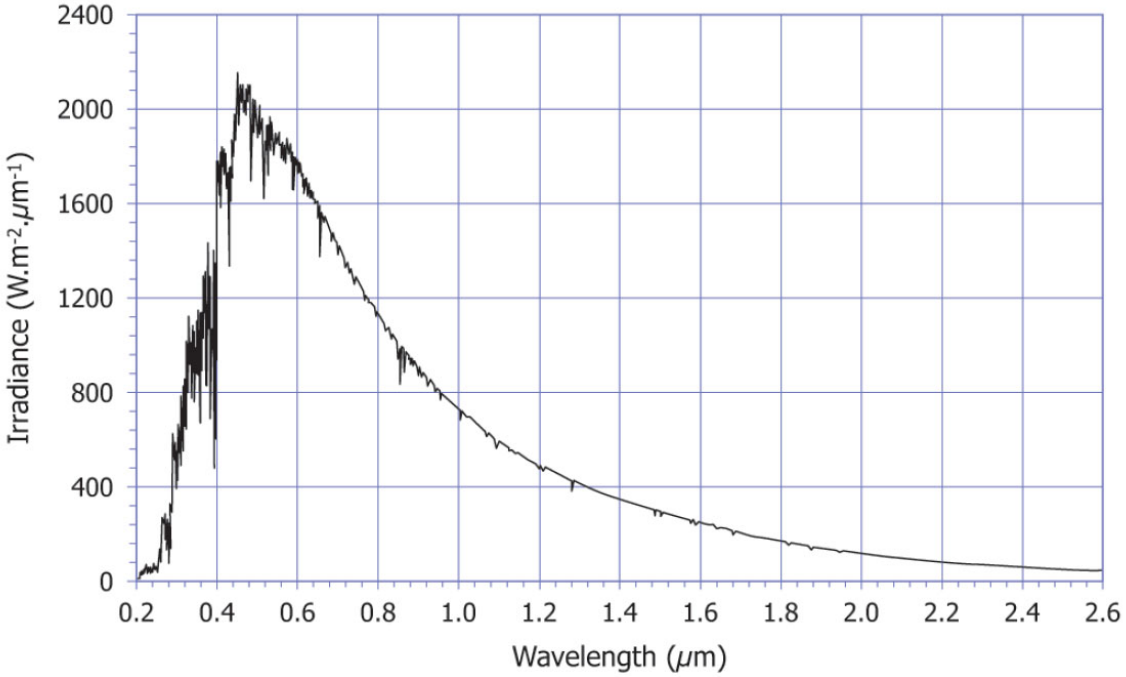

Figure 10. Air mass zero (AM0) solar spectrum irradiance.[11]

6.0 Post-Flight Results

6.1 Post-Flight Sample Images

6.1.1 MISSE-9 PCE-1 Samples

Figure 11 provides post-flight photographs of the alumina PCE-1 ram M9R-C6 F (flight) and M9R-C6 B (control) samples. Figure 11a shows the samples on a white background and Figure 11b shows the samples on a dark background. There was no visible color change of the flight sample. The only visible effect of the flight sample is holder marks at the perimeter. This is very noticeable in the image on the dark background (Figure 11b). The contamination samples were also examined, and imaged, with a 365 nm UV light source. The exposed area of the ram flight sample had a darker appearance than the protected area under the UV light, as shown in Figure 11c. This indicates a possible contaminant layer on the sample.

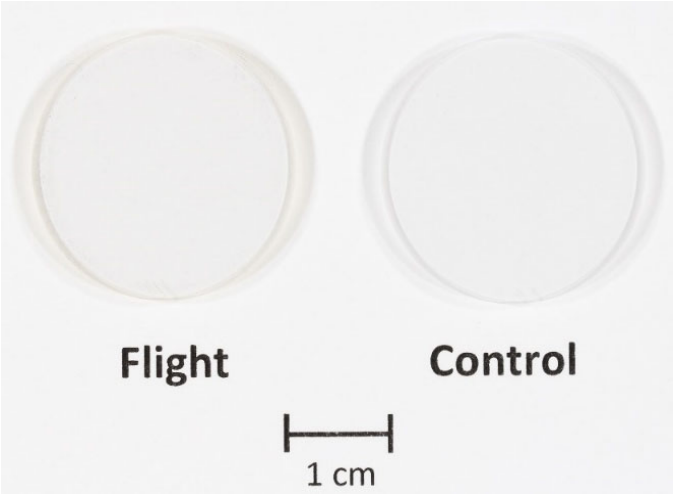

a.

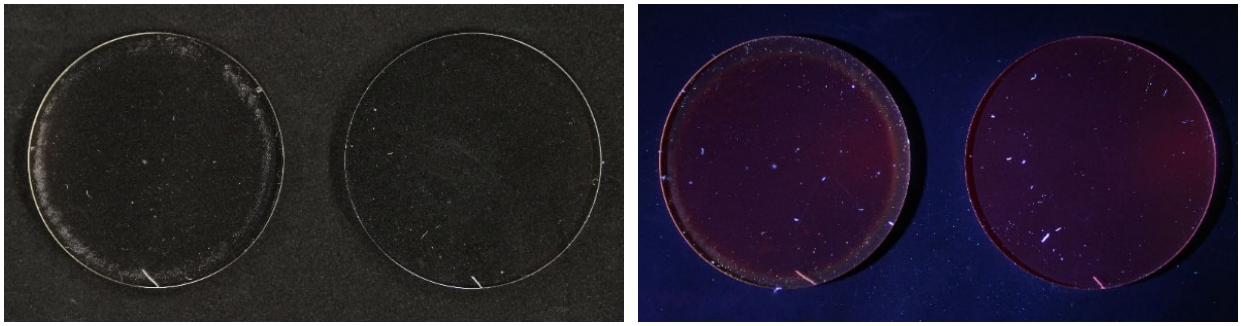

b. c.

Figure 11. Post-flight photographs of M9R-C6 F and M9R-C6 B (Al_2O_3): (a) Visible light image with a white background, (b) Visible light image with a dark background (F on the left and B on the right), and (c) UV light image (F on the left and B on the right).

Figure 12 provides post-flight photographs of the MgF_2 PCE-1 ram M9R-27 F (flight) and M9R-C27 B (control) samples. Figure 12a shows the samples on a white background and Figure 12b shows the samples on a dark background. There was no visible color change or holder marks in the flight sample as shown on either the white (Figure 12a) or dark backgrounds (Figure 12b). When imaged with a 365 nm UV light source, the exposed area of the ram flight sample had a slightly more fluorescing appearance than the protected area, especially when viewed close-up (Figure 12c). This fluorescence could indicate a possible contaminate layer on the sample.

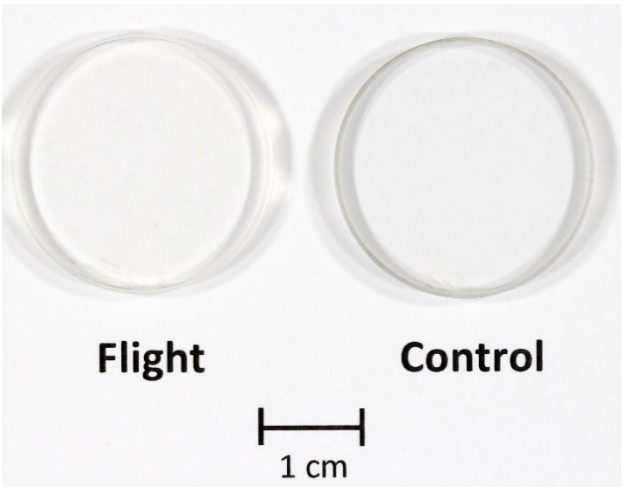

a.

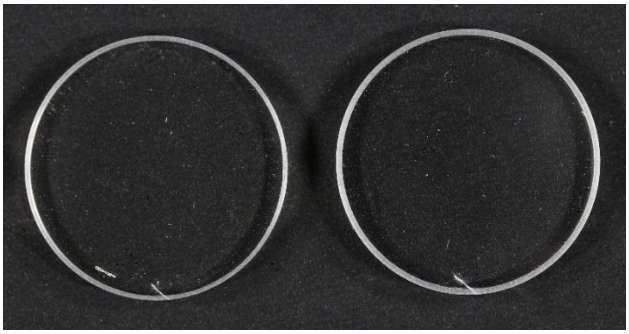

b.

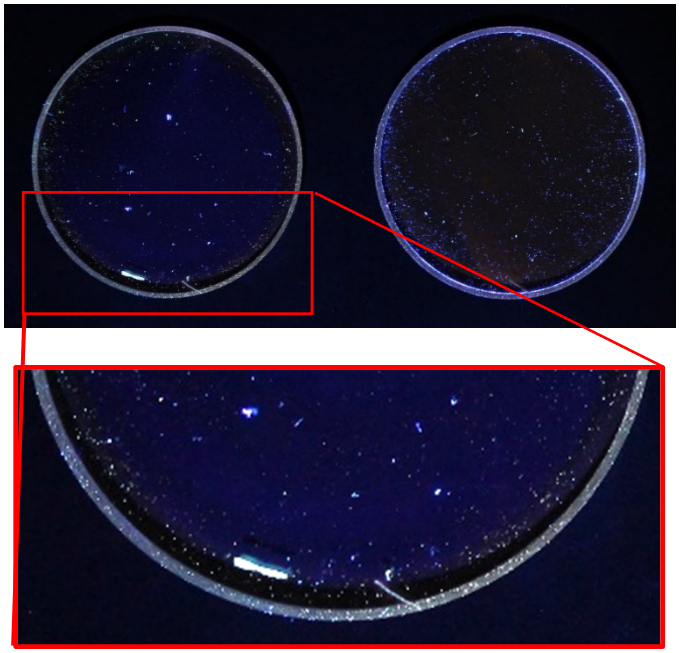

c.

Figure 12. Post-flight photographs of M9R-C27 F and M9R-C27 B (MgF_2): (a) Visible light image with a white background, (b) Visible light image with a dark background (F on left and B on right), and (c) UV light image (F on left and B on right).

Figure 13 provides post-flight photographs of the alumina PCE-1 wake M9W-C3 F (flight) and M9W-C3 B (control) samples. Figure 13a shows the samples on a white background and Figure 13b shows the samples on a dark background. There was no visible color change of the flight sample. The only visible effect of the flight sample is holder marks at the perimeter. This is very noticeable in the image on the dark background (Figure 13b). When imaged with a 365 nm UV light source, the exposed area of the wake flight sample had a darker appearance than the protected area, as shown in Figure 13c. This indicates a possible contaminate layer on the sample.

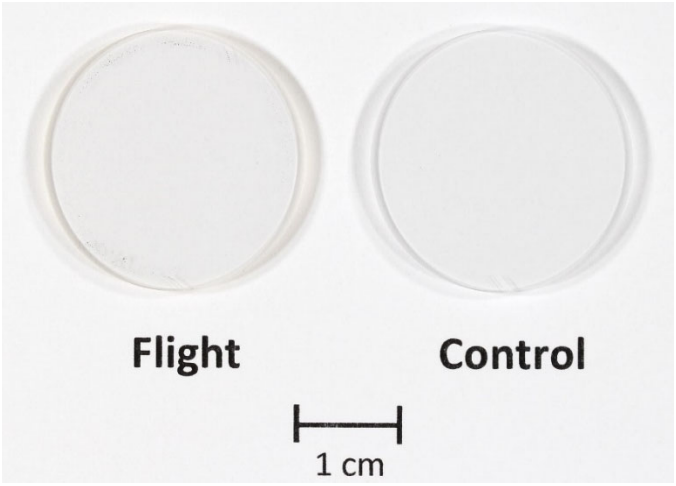

a.

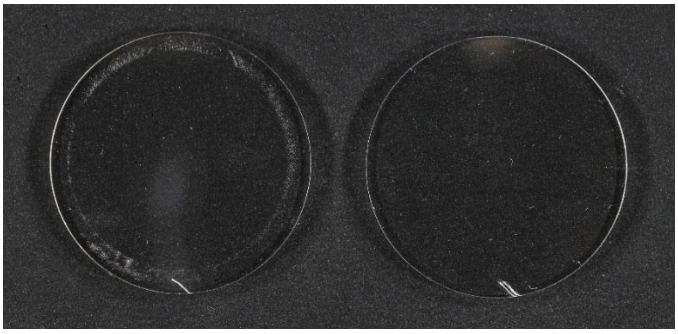

b.

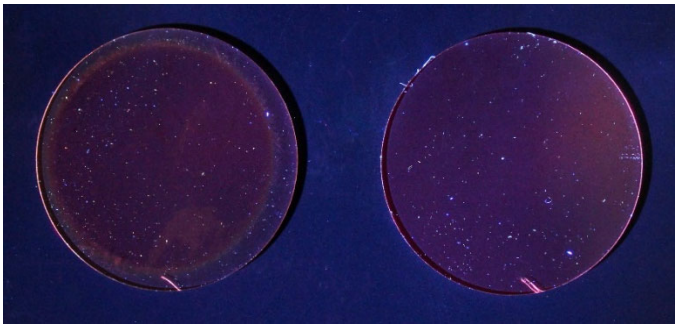

c.

Figure 13. Post-flight photographs of M9W-C3 F and M9W-C3 B (Al_2O_3): (a) Visible light image with a white background, (b) Visible light image with a dark background (F on left and B on right), and (c) UV light image (F on left and B on right).

Figure 14 provides post-flight photographs of the alumina PCE-1 zenith M9Z-C3 F (flight) and M12R-C3/M12W-C3 B (control) samples. Figure 14a shows the samples on a white background and Figure 14b shows the samples on a dark background. There was no visible color change of the flight sample. Like the other MISSE-9 alumina samples, the only visible effect of the flight sample is holder marks at the perimeter. This is noticeable in the image on the dark background (Figure 14b). When imaged with a 365 nm UV light source, the exposed area of the zenith flight sample had a darker appearance than the protected area, as shown in Figure 14c. Once again, this indicates a possible contaminate layer on the sample.

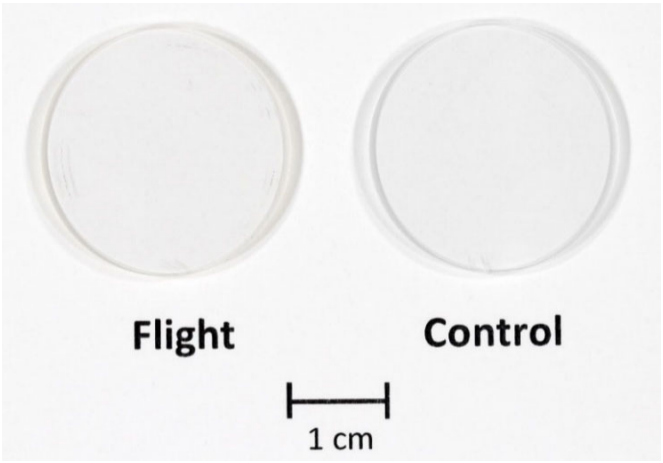

a.

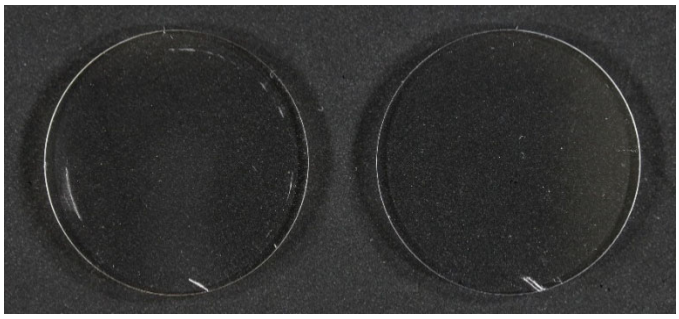

b.

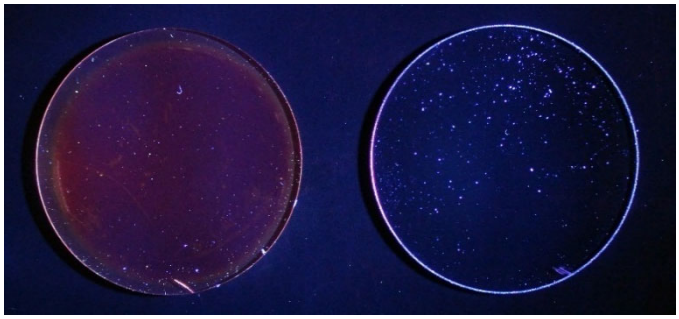

c.

Figure 14. Post-flight photographs of M9Z-C3 F and M12R-C3/M12W-C3 B (Al_2O_3): (a) Visible light image with a white background, (b) Visible light image with a dark background (F on left and B on right), and (c) UV light image (F on left and B on right).

Figure 15 provides post-flight photographs of the MgF_2 PCE-1 zenith M9Z-C18 F (flight) and M9Z-C18 B (control) samples. Figure 15a shows the samples on a white background and Figure 15b shows the samples on a dark background. There was no visible color change or holder marks in the flights samples as shown on either the white (Figure 15a) or dark backgrounds (Figure 15b). When imaged with a 365 nm UV light source, the exposed area of the zenith flight sample had a more fluorescing appearance than the protected area, especially when viewed close-up (Figure 15c). This fluorescence could indicate a possible contaminate layer on the sample.

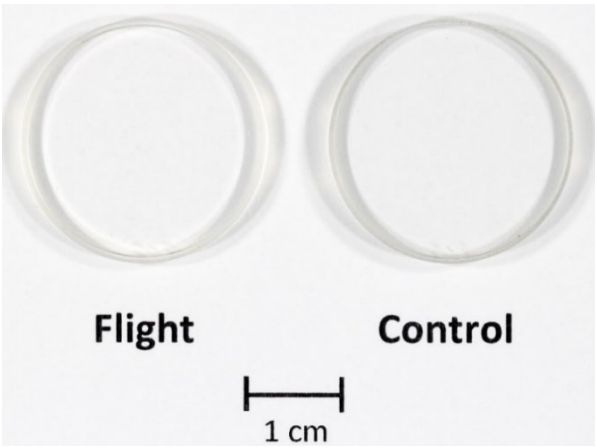

a.

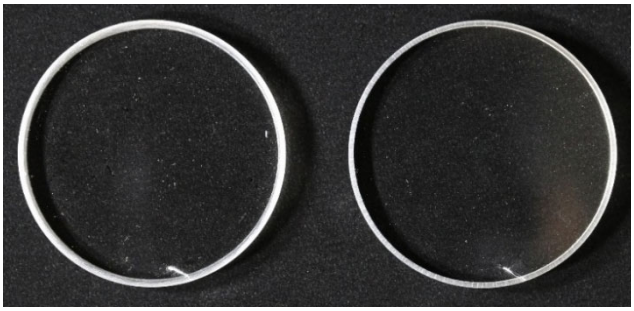

b.

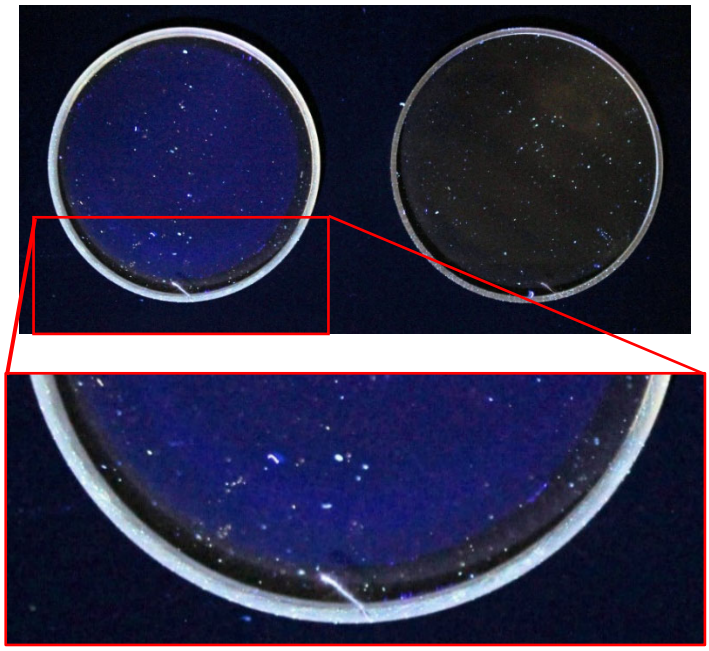

c.

Figure 15. Post-flight photographs of M9Z-C18 F and M9Z-C18 B (MgF_2): (a) Visible light image with a white background, (b) Visible light image with a dark background (F on left and B on right), and (c) UV light image (F on left and B on right).

6.1.2 MISSE-10 PCE-2 Samples

Figure 16 provides post-flight photographs of the alumina PCE-2 ram M10R-C4 F (flight) and M10R-C4 B (control) samples. Figure 16a shows the samples on a white background and Figure 16b shows the samples on a dark background. There was no visible color change of the flight sample. The only visible effects on the flight sample were faint holder marks at the perimeter. This is noticeable in the image on the dark background (Figure 16b). When imaged with a 365 nm UV light source, the exposed area of the MISSE-10 ram flight sample had a darker appearance than the protected area, as seen in Figure 16c.

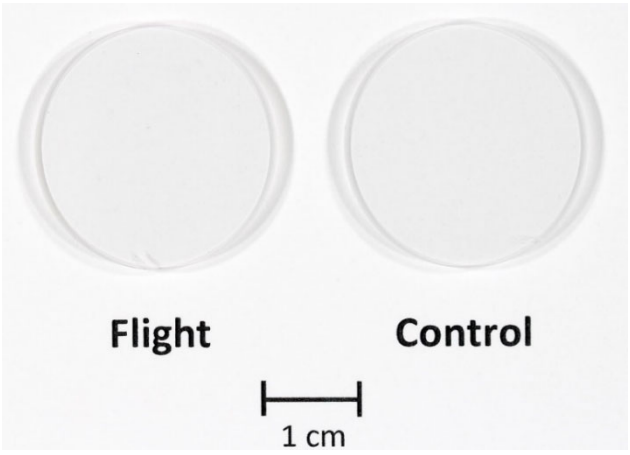

a.

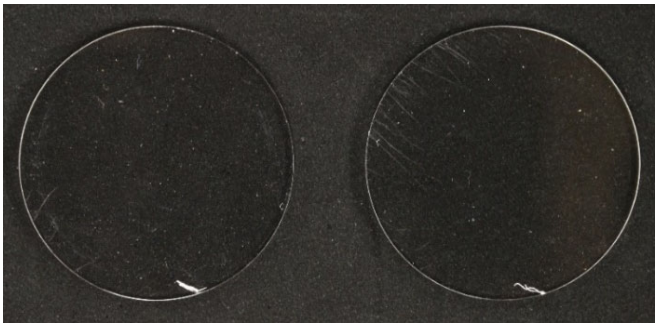

b.

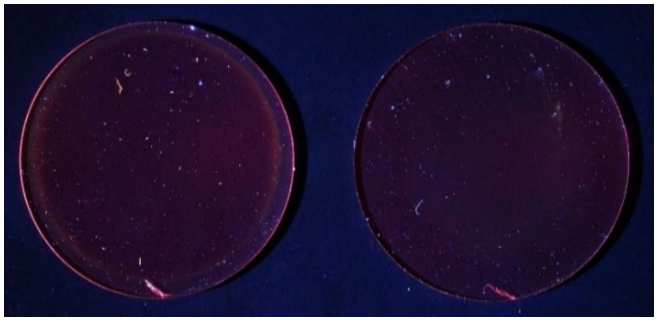

c.

Figure 16. Post-flight photographs of M10R-C4 F and M10R-C4 B (Al_2O_3): (a) Visible light image with a white background, (b) Visible light image with a dark background (F on left and B on right), and (c) UV light image (F on left and B on right).

Figure 17 provides post-flight photographs of the alumina PCE-2 zenith M10Z-C5 F (flight) and M10Z-C5 B (control) samples. Figure 17a shows the samples on a white background and Figure 17b shows the samples on a dark background. There was no visible color change of the flight sample. The only visible effects of the flight sample were slight holder marks at the perimeter and some scratch lines. These are noticeable in the image on the dark background (Figure 17b). When imaged with a 365 nm UV light source, the exposed area of the zenith flight sample had a darker appearance than the protected area, as shown in Figure 17c.

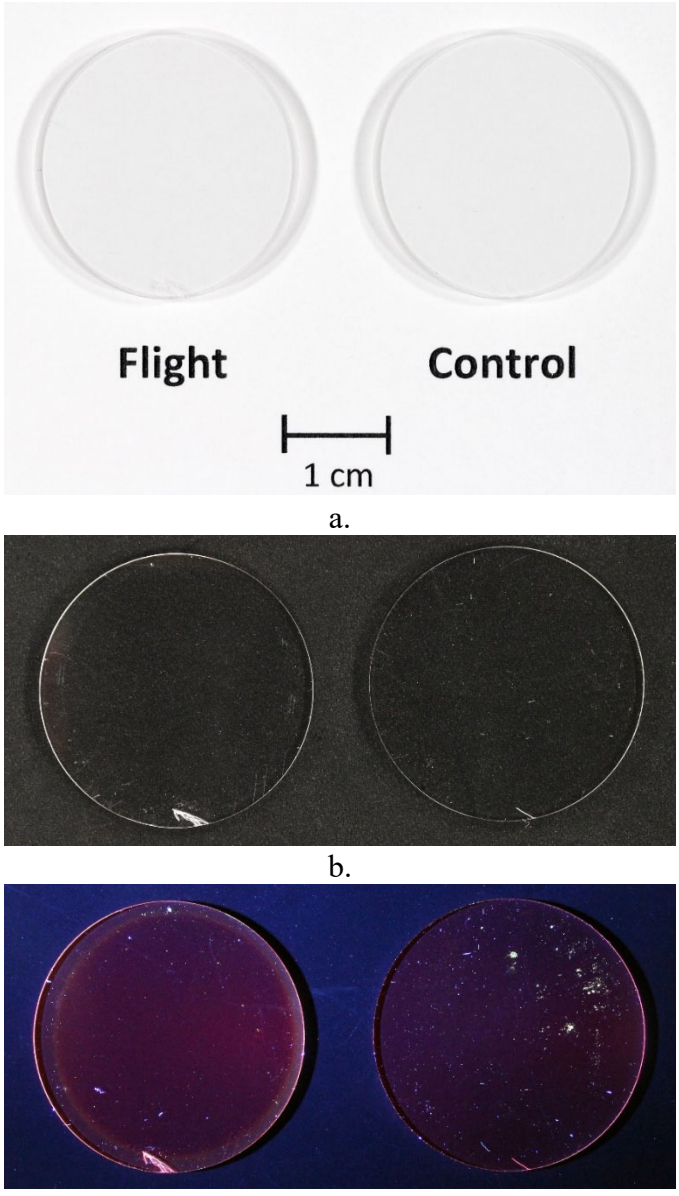

a.

b.

c.

Figure 17. Post-flight photographs of M10Z-C5 F and M10Z-C5 B (Al_2O_3): (a) Visible light image with a white background, (b) Visible light image with a dark background (F on left and B on right), and (c) UV light image (F on left and B on right).

Figure 18 provides post-flight photographs of the alumina PCE-2 nadir M10N-C5 F (flight) and M10N-C5 B (control) samples. Figure 18a shows the samples on a white background and Figure 18b shows the samples on a dark background. There was no visible color change of the flight sample. The only visible effects on the flight sample were the slight holder marks at the perimeter of the sample. These are noticeable in the image on the dark background (Figure 18b). When imaged with a 365 nm UV light source, the exposed area of the MISSE-10 nadir flight sample was barely discernable as compared to the protected area, as shown in Figure 18c. Based on the UV image it appears that this flight sample had less on-orbit contamination than the previously discussed flight samples.

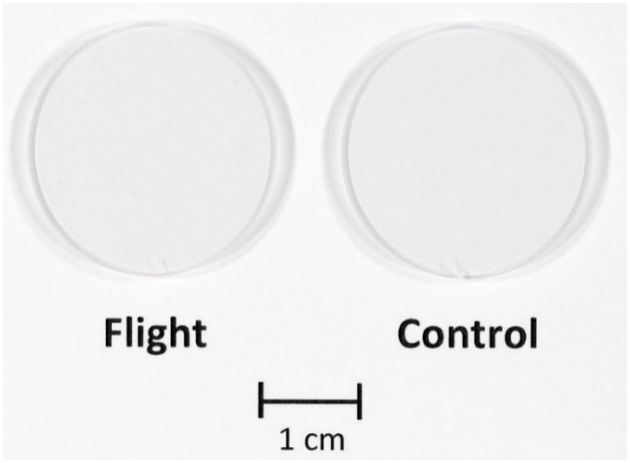

a.

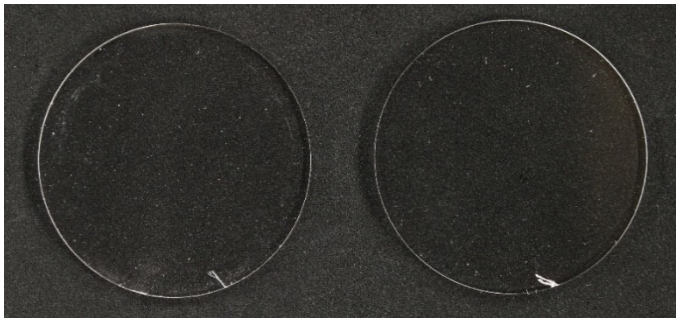

b.

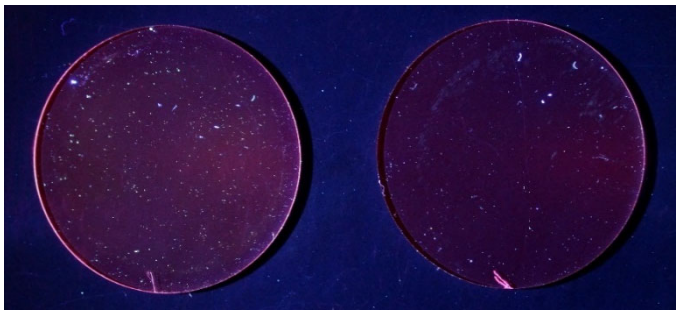

c.

Figure 18. Post-flight photographs of M10N-C5 F and M10N-C5 B (Al_2O_3): (a) Visible light image with a white background, (b) Visible light image with a dark background (F on left and B on right), and (c) UV light image (F on left and B on right).

6.1.3 MISSE-12 PCE-3 Samples

Figure 19 provides post-flight photographs of the alumina PCE-3 ram M12R-C3 F (flight) and M12R-C3/M12W-C3 B (control) samples. Figure 19a shows the samples on a white background and Figure 19b shows the samples on a dark background. There was no visible color change of the flight sample. The only visible effect of the flight sample is a few very faint holder marks at the perimeter noticeable in the image on the dark background at high magnification (Figure 19b). When imaged with a 365 nm UV light source, the exposed area of the MISSE-12 ram flight sample had a pronounced darker appearance than the protected area, as shown in Figure 19c. This pronounced darkened area, as imaged under the 365 nm UV light, seems to indicate that this MISSE-12 ram sample has a thicker contaminant layer than the MISSE-9 or MISSE-10 samples.

Figure 20 provides post-flight photographs of the SMA NiTi PCE-3 zenith M12Z-S2 F (flight) sample. A back-up/control sample was not available for imaging. Figure 20a shows the sample on a white background. The sample is comprised of two SMA pieces. They both have a polished finish, which reflects the lights and appears dark. There was no visible color change in either of the two flight sample pieces. The samples pieces did not fluoresce when imaged with a 365 nm UV light source and appear dark, as shown in Figure 20b. Thus, the UV image does not provide any insight to any on-orbit contamination.

Figure 21 provides post-flight photographs of the alumina PCE-3 wake M12W-C3 F (flight) and M12R-C3/M12W-C3 B (control) samples. The flight sample was exposed to the space environment during the MISSE-15 mission. Figure 21a shows the samples on a white background and Figure 21b shows the samples on a dark background. There was no visible color change of the flight sample. It should be noted that a small black mark was added to the edge of the back surface of the flight sample post-flight. This mark can be seen in Figure 21a. Besides this black mark, the only visible effect of the flight sample is a few very faint holder marks at the perimeter noticeable in the image on the dark background at high magnification (Figure 21b). When imaged with a 365 nm UV light source, the exposed area of the MISSE-12 wake flight sample had a pronounced darker appearance than the protected area, as shown in Figure 21c. Like the ram M12R-C3 F sample, this pronounced UV darkened area seems to indicate that this MISSE-12 wake sample has a thicker contaminant layer than the MISSE-9 or MISSE-10 samples.

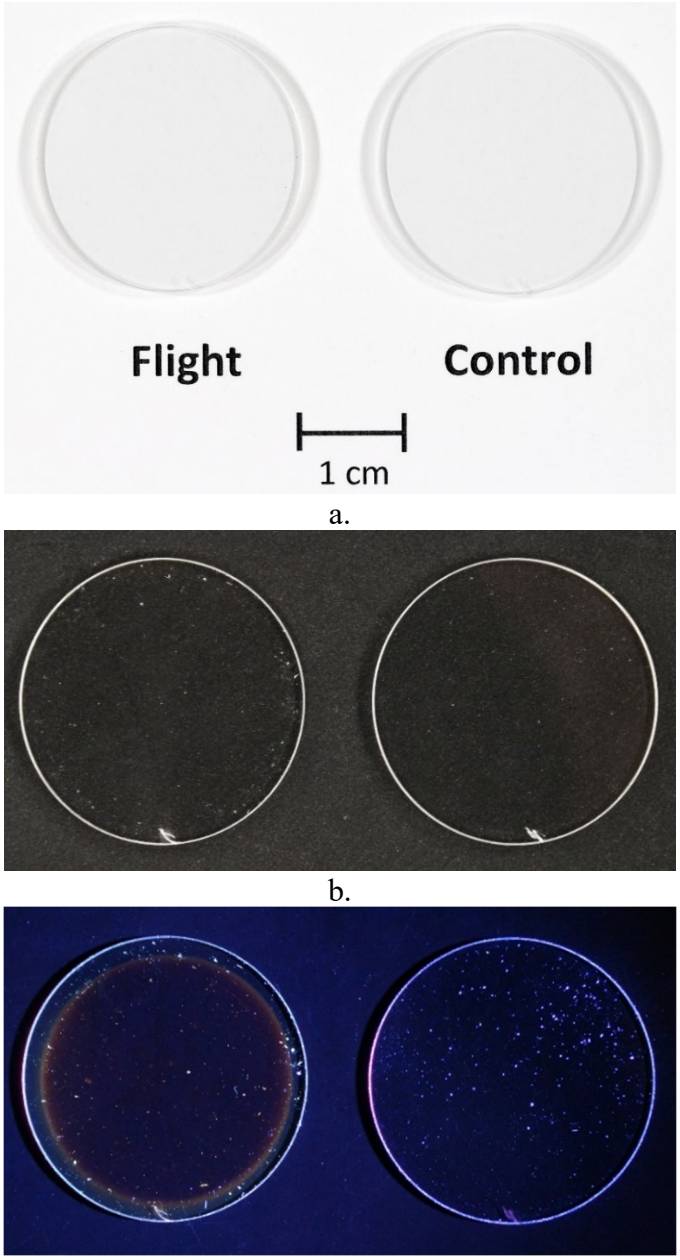

a.

b.

c.

Figure 19. Post-flight photographs of M12R-C3 F and M12R-C3/M12W-C3 B (Al_2O_3): (a) Visible light image with a white background, (b) Visible light image with a dark background (F on left and B on right), and (c) UV light image (F on left and B on right).

a.

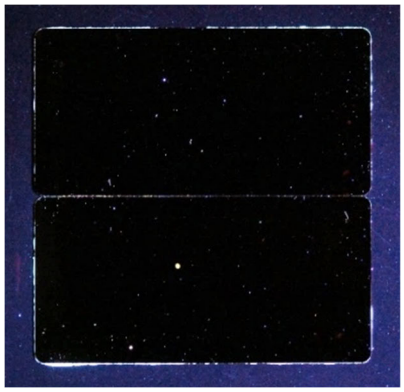

b.

Figure 20. Post-flight photographs of M12Z-S2 F (SMA NiTi): (a) Visible light image, and (b) UV light image.

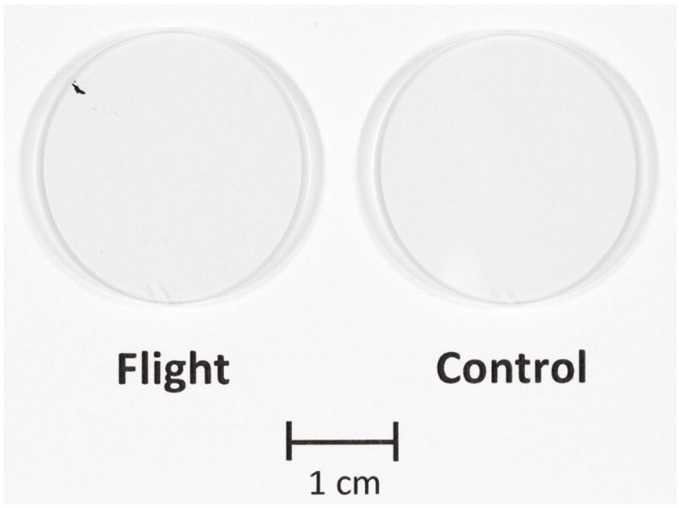

a.

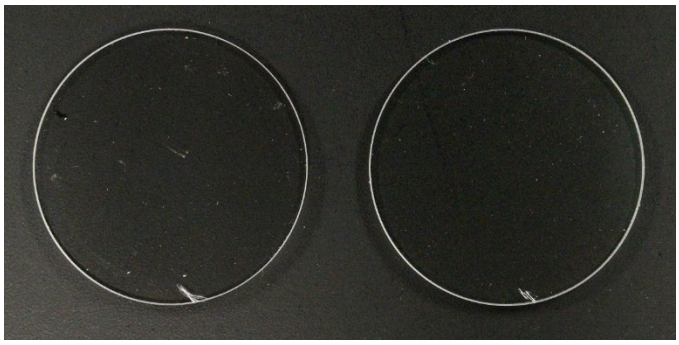

b.

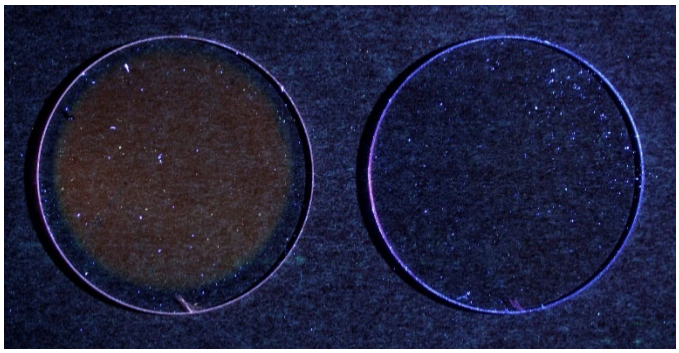

c.

Figure 21. Post-flight photographs of M12W-C3 F and M12R-C3/M12W-C3 B (Al_2O_3): (a) Visible light image with a white background, (b) Visible light image with a dark background (F on left and B on right), and (c) UV light image (F on left and B on right).

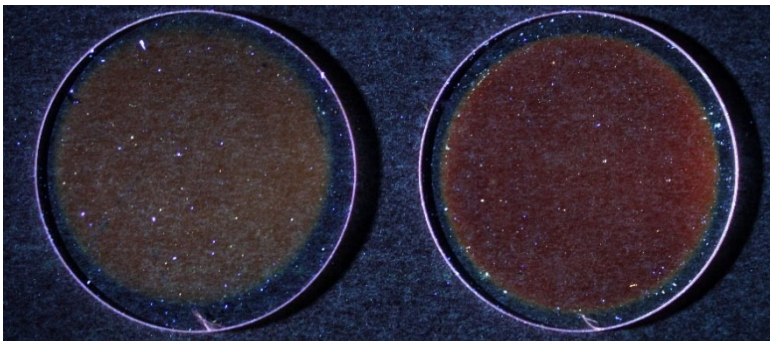

Figure 22. Post-flight UV light (365 nm) photograph of flight samples M12W-C3 F (wake, left) and M12R-C3 F (ram, right).

Because the M12W-C3 F sample was re-flown as part of the MISSE-15 mission, the post-flight images were taken later and with a different black background material than the M12R-C3 F samples. Thus, to compare the level of UV fluorescence of these two samples, a UV light image was taken of both the wake (M12W-C3 F) and ram (M12R-C3 F) flight samples together, as shown in Figure 22. As can be seen in Figure 22, the MISSE-12 ram sample (right) appears to have a darker, more pronounced exposed area than the wake sample (left). This could be due to a thicker contaminant layer on the ram sample, or perhaps a contaminant layer with a different chemistry than the wake sample.

6.1.4 MISSE-13 PCE-4 Samples

Figure 23 provides post-flight photographs of the back-surface aluminized Teflon PCE-4 wake M13W-C4 F (flight) and M13W-C4 B (control) samples. Figure 23a shows the samples on a white background and Figure 23b shows the samples on a dark background. There was no visible color change of the flight sample. The only visible effects on the flight sample were holder marks at the perimeter. These are noticeable in both the white and dark background images (Figure 23a and Figure 23b, respectively). When imaged with a 365 nm UV light source, the exposed area of the wake Teflon sample fluoresced as compared to the unexposed area of the flight sample, and the control sample, as shown in Figure 23c. This fluorescence occurs with space exposure of Teflon FEP and does not necessarily indicate a contaminant layer.

Figure 24 provides post-flight photographs of the back-surface aluminized Teflon PCE-4 zenith M13Z-C4 F (flight) and M13Z-C4 B (control) samples. Figure 24a shows the samples on a white background and Figure 24b shows the samples on a dark background. There was no visible color change of the flight sample. The only visible effects on the flight sample were holder marks at the perimeter. These are noticeable in both the white and dark background images (Figure 24a and Figure 24b, respectively). When imaged with a 365 nm UV light source, the exposed area of the wake Teflon sample fluoresced as compared to the unexposed area of the flight sample, and the control sample, as shown in Figure 24c. As stated for M13W-C4 F, fluorescence occurs with space exposure of Teflon FEP and does not necessarily indicate a contaminant layer. The level of fluorescence of the MISSE-13 wake and zenith Teflon FEP samples appears similar, which would indicate a similar solar exposure for these two flight samples.

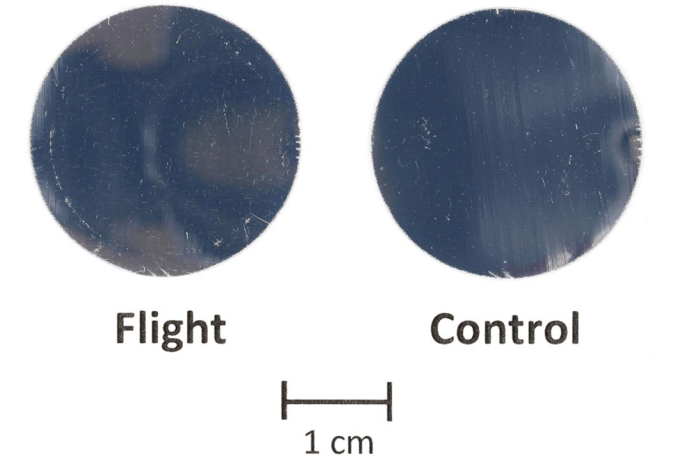

a.

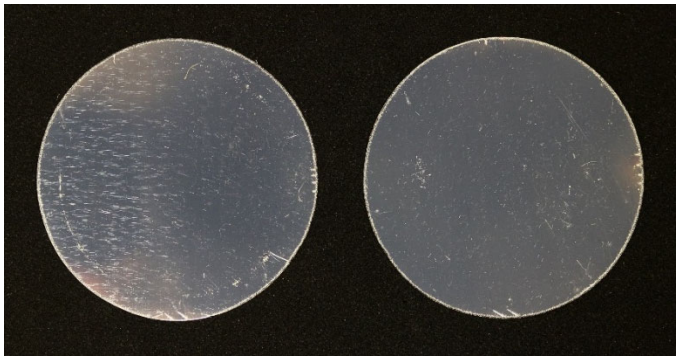

b.

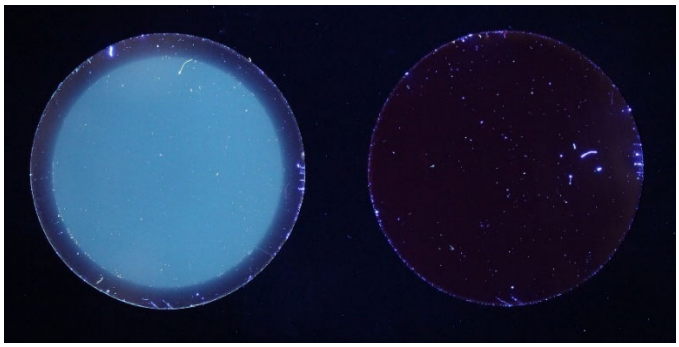

c.

Figure 23. Post-flight photographs of M13W-C4 F and M13W-C4 B (FEP/Al): (a) Visible light image with a white background, (b) Visible light image with a dark background (F on left and B on right), and (c) UV light image (F on left and B on right).

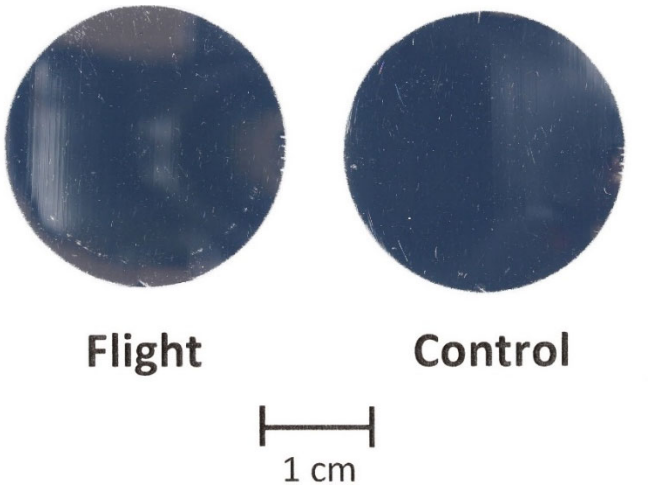

a.

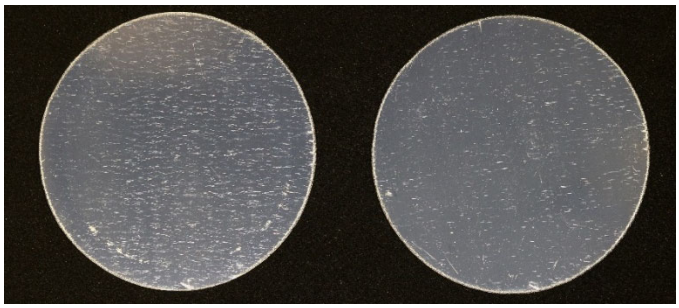

b.

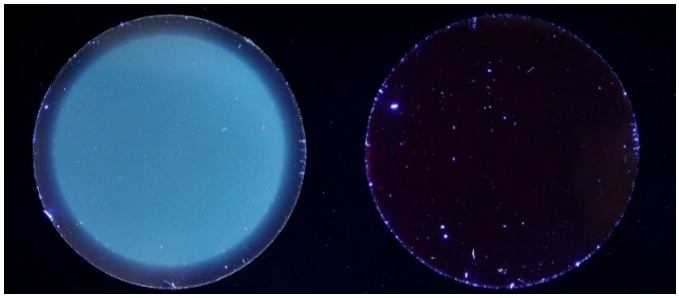

c.

Figure 24. Post-flight photographs of M13Z-C4 F and M13Z-C4 B (FEP/Al): (a) Visible light image with a white background, (b) Visible light image with a dark background (F on left and B on right), and (c) UV light image (F on left and B on right).

6.2 X-ray Photoelectron Spectroscopy (XPS) Results

6.2.1 XPS Survey Spectra Comparing Control and Flight Surfaces

The following section contains the XPS survey spectrum from each space flight exposed sample ("After Flight Exposure") overlaid with its corresponding control surface ("Control Sample", no space exposure) spectrum. The actual surface atomic concentrations for all the samples are provided in XPS tables later in the report. Since most surfaces on Earth generally become coated with a monolayer of contamination referred to as adventitious carbon, the control spectra used in the overlays were obtained after the surface had been lightly sputter etched (≤10 nm) to remove the adventitious carbon that had built up on the surface during its storage. An overlay of one of the alumina control samples (M9R-C6 B) before and after sputtering is shown in Figure 25, demonstrating that only carbon has been removed. Elements with higher atomic concentrations that were detected on the flight exposed surfaces (other than carbon) that were not present on the control sample surfaces have been circled and highlighted in red in the following spectra (Figures 26 to 36). Most of these contaminant layers were thin (≤10 nm); however, some did not reduce until 2 minutes of sputtering, suggesting a thickness of ≤20 nm or more. From the XPS results, it was not possible to determine if the layers were continuous, or present as islands.

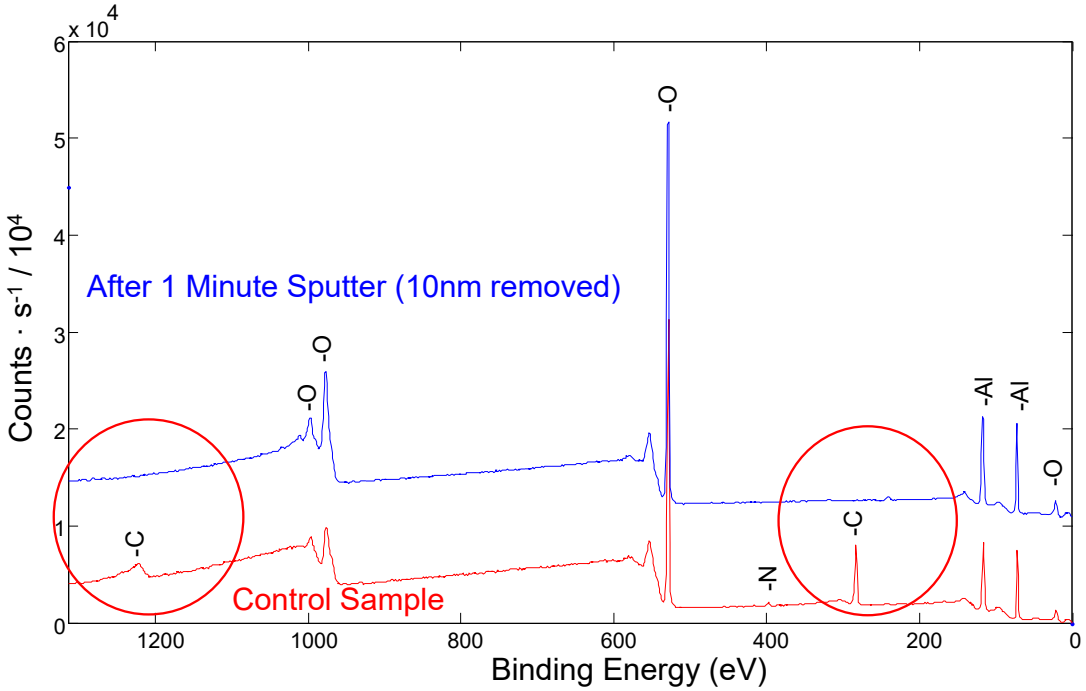

Figure 25. The XPS binding energy data for the MISSE-9 ram alumina control (M9R-C6 B) sample before and after sputtering to remove the adventitious carbon.

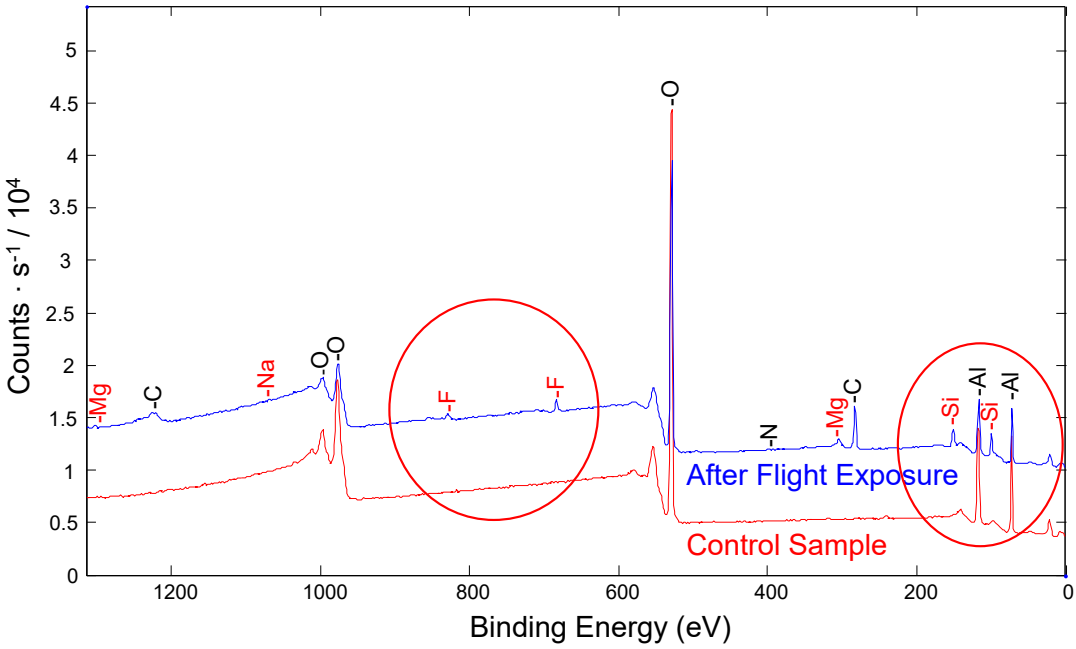

Figure 26. The XPS binding energy data for the MISSE-9 ram alumina flight (M9R-C6 F) and control (M9R-C6 B) samples indicating a contamination layer containing Si, F, and Mg ≤20 nm (trace amount of N was present on both samples).

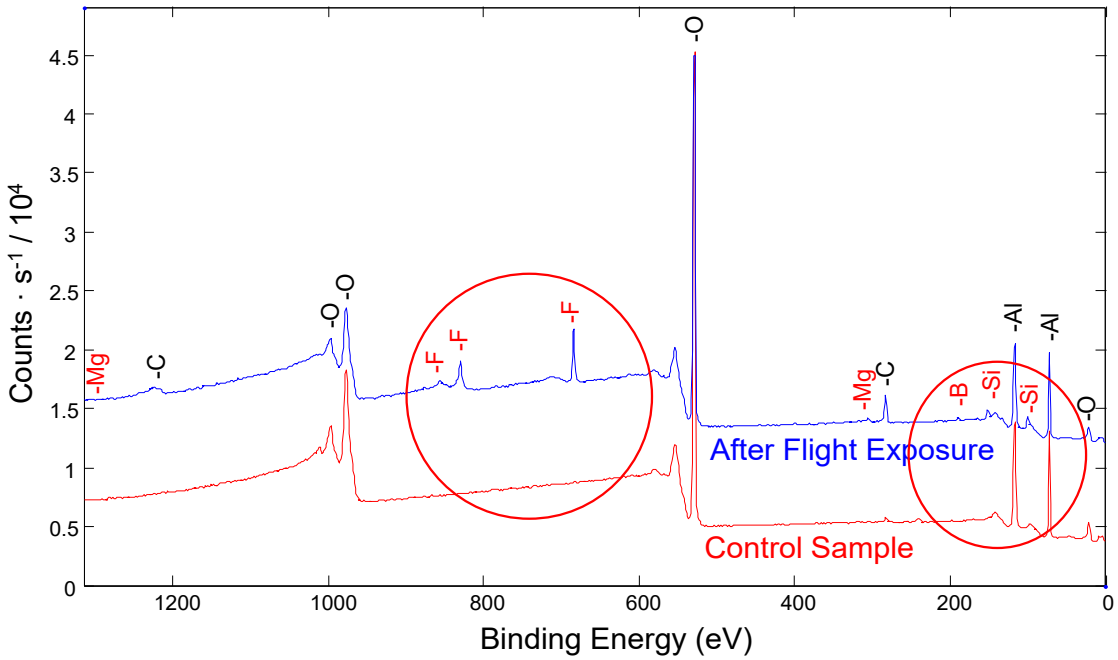

Figure 27. The XPS binding energy data for the MISSE-9 wake alumina flight (M9W-C3 F) and control (M9W-C3 B) samples showing Si, F, Mg and B present on the surface ≤10 nm.

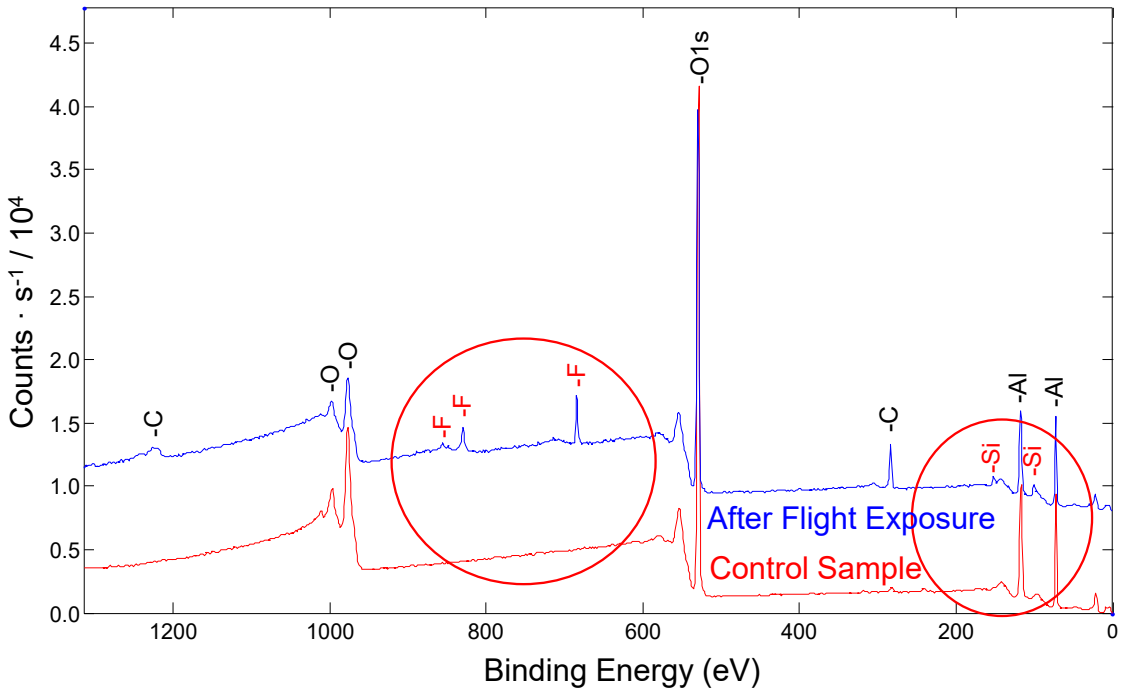

Figure 28. The XPS binding energy data for the MISSE-9 zenith alumina flight (M9Z-C3 F) and control (M9Z-C3 B) samples indicating a Si and F contamination layer ≤10 nm.

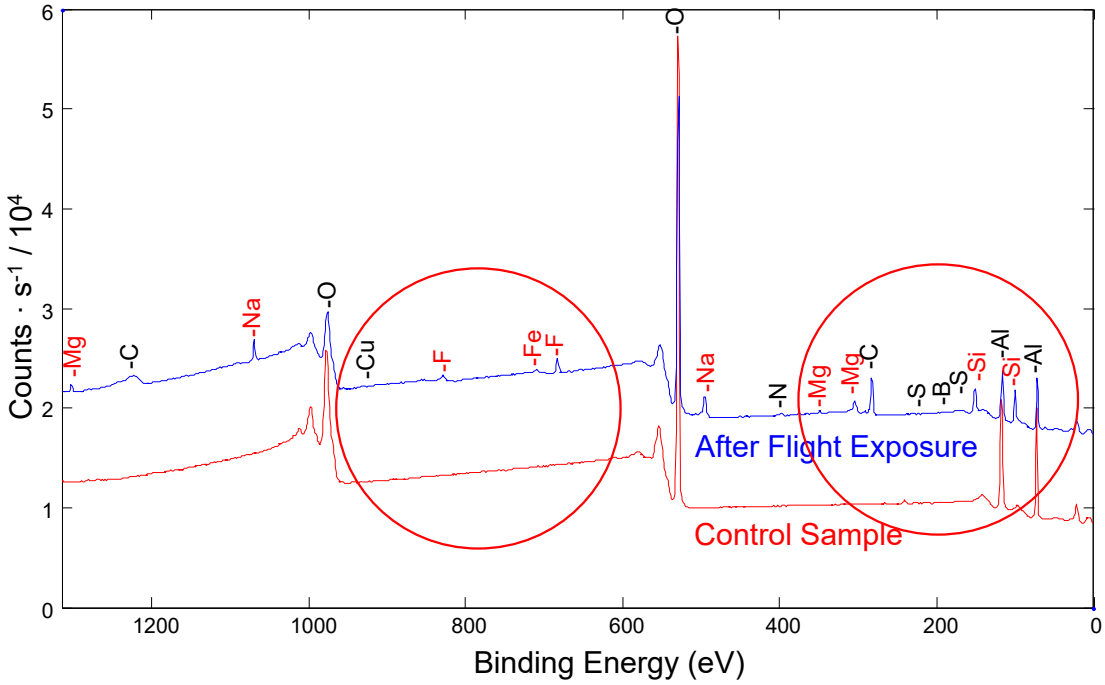

Figure 29. The XPS binding energy data for the MISSE-10 ram alumina flight (M10R-C4 F) and control (M10R-C4 B) samples. Silicon along with trace amounts of Na and Fe were identified on the surface. A thicker layer (≤20 nm) of Mg and F was also detected on the flight sample. Trace amounts of N, B, and Cu were present on both samples.

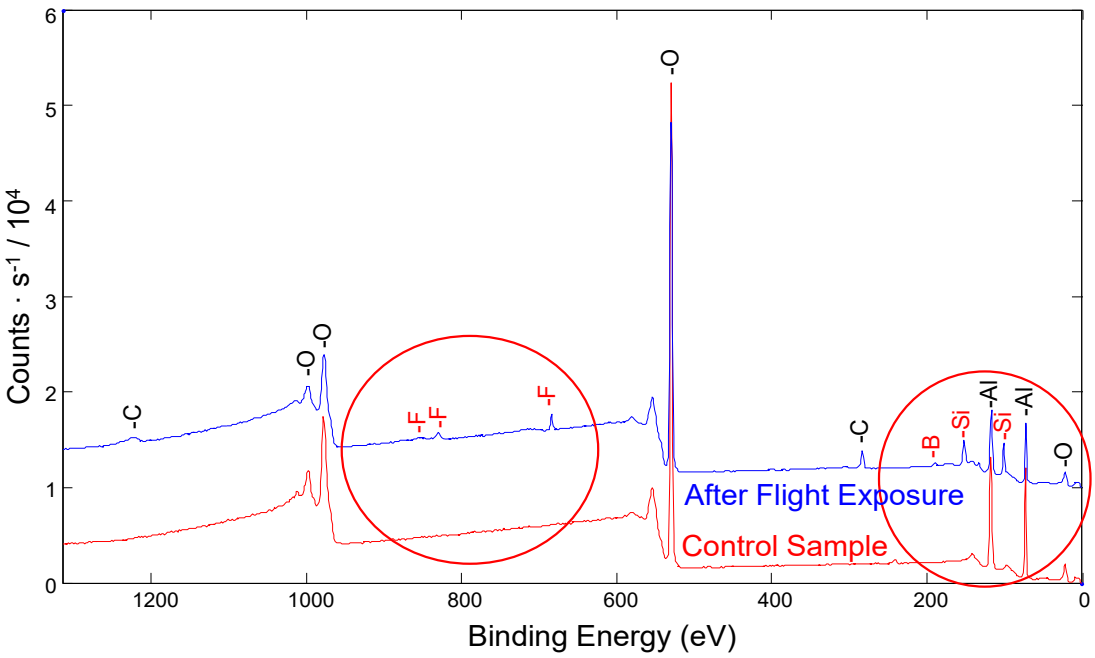

Figure 30. The XPS binding energy data for the MISSE-10 nadir alumina flight (M10N-C5 F) and control (M10N-C5 B) samples showing the presence of Si and F ≤10 nm thick on the flight sample. Boron and nitrogen were identified on both samples.

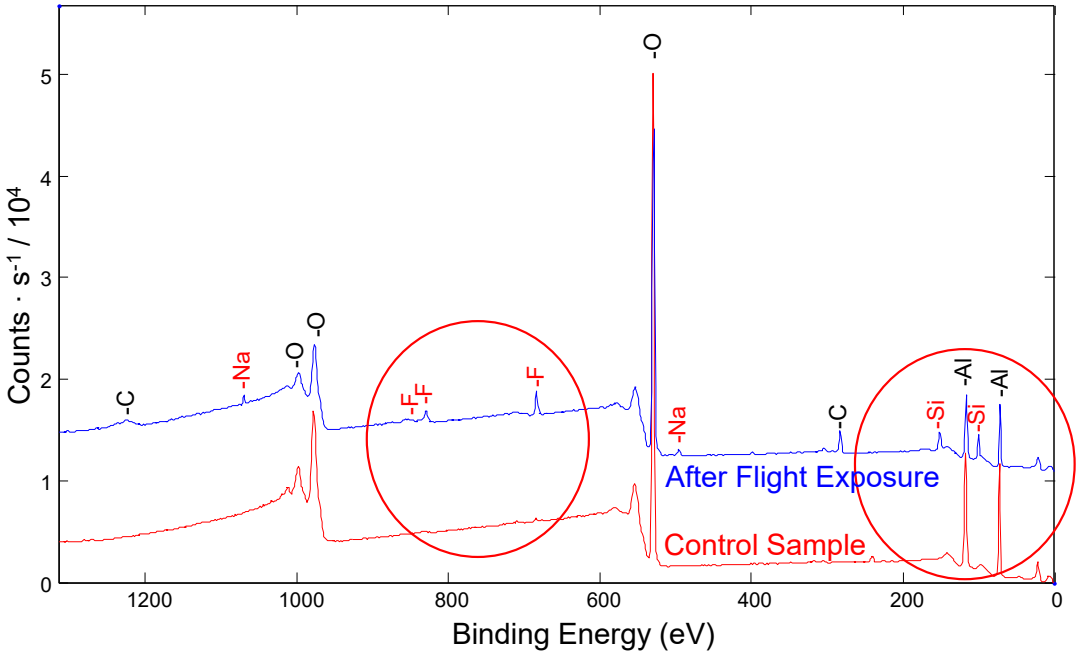

Figure 31. The XPS binding energy data for the MISSE-10 zenith alumina flight (M10Z-C5 F) and control (M10Z-C5 B) samples. Trace amounts of Na and F were present on both surfaces, although the flight sample also showed Si, Mg, N and F up to 20 nm thick.

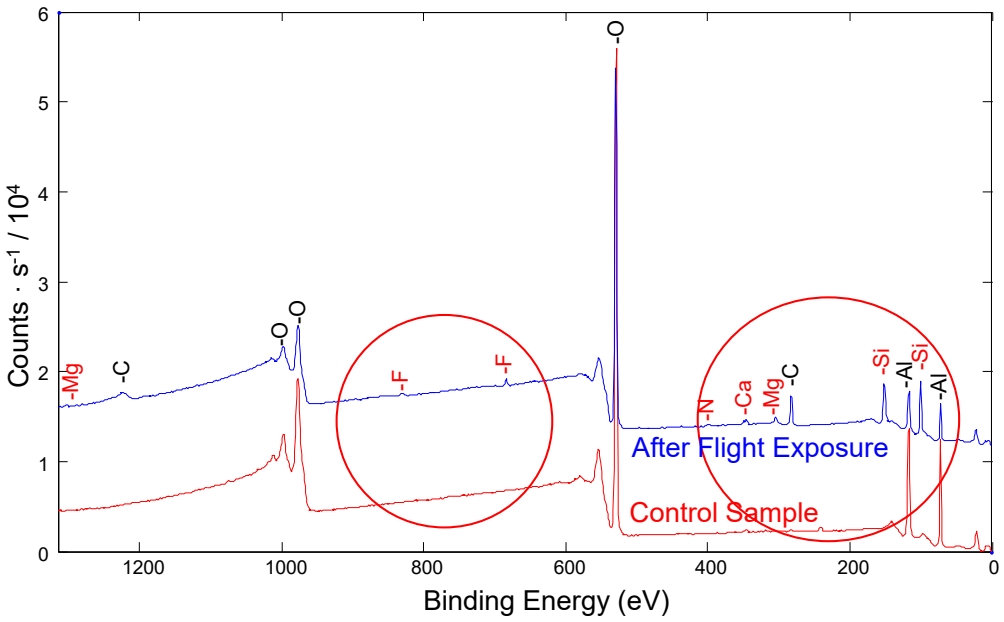

Figure 32. The XPS binding energy data for the MISSE-12 ram alumina flight (M12R-C3 F) and control (M12R-C3/M12W-C3 B) samples. Trace amounts of Ca, Mg, and N were found on both surfaces; however, a high concentration of Si (15.1 at.%) along with a smaller amount of F (0.8 at.%) were present up to 20 nm on the flight sample.

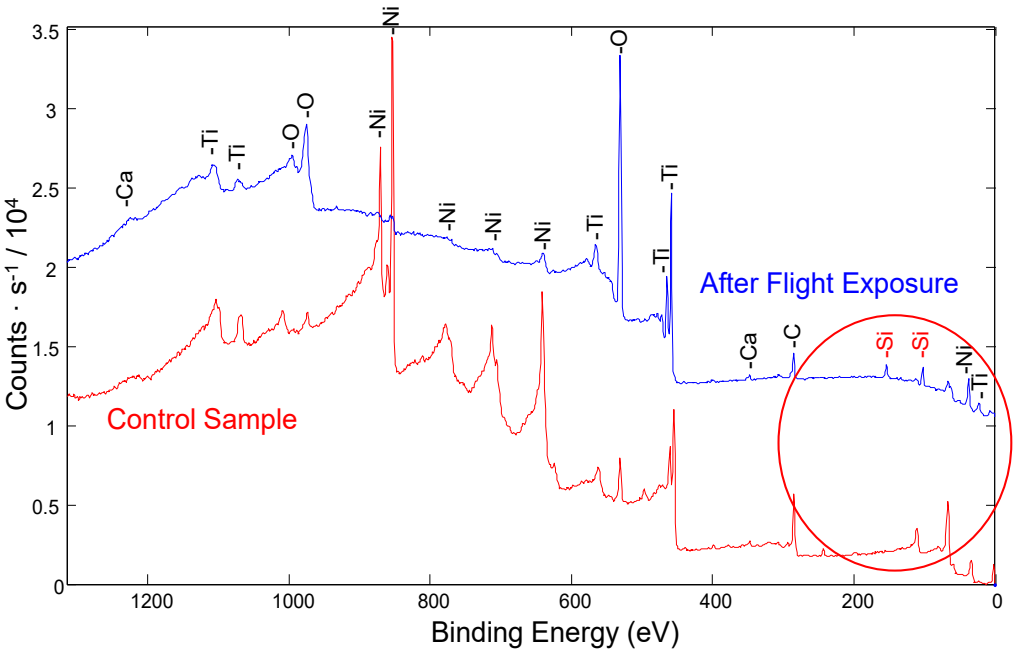

Figure 33. The XPS binding energy data for the MISSE-12 zenith SMA NiTi flight (M12Z-S2 F) and control (M12Z-S2 B) samples. A silicon layer ≤10 nm thick was identified on the flight sample.

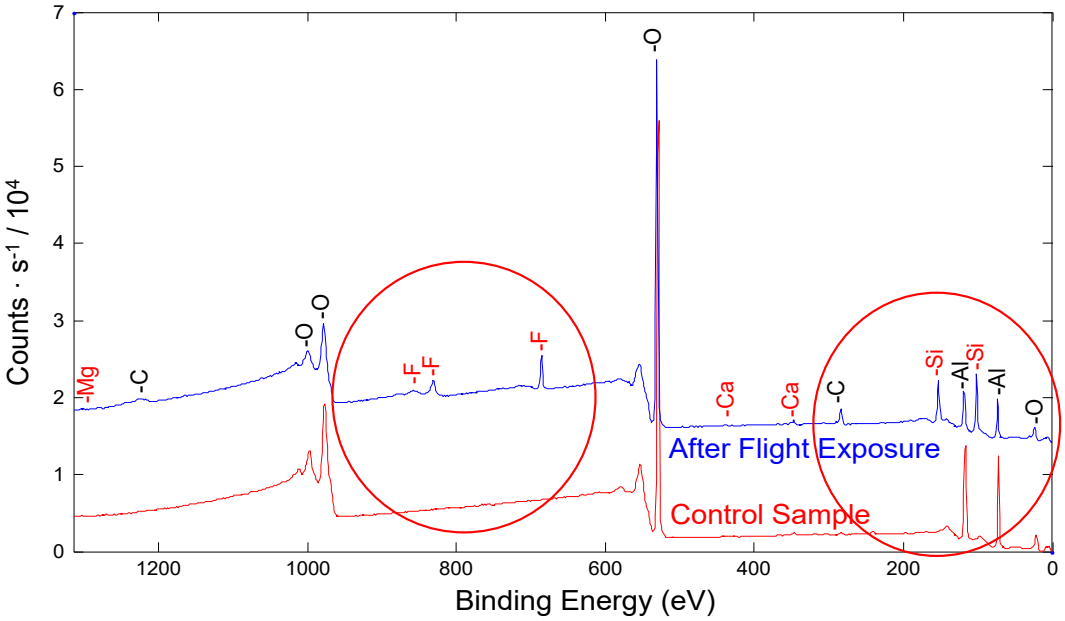

Figure 34. The XPS binding energy data for the MISSE-12/MISSE-15 wake alumina flight (M12W-C3 F) and control (M12W-C3/M12W-C3 B) samples. Trace amounts of Ca and Mg were found on both surfaces; however, a high concentration of Si (15.1 at.%) along with a smaller amount of F (5.0 at.%) were present up to 20 nm on the flight sample.

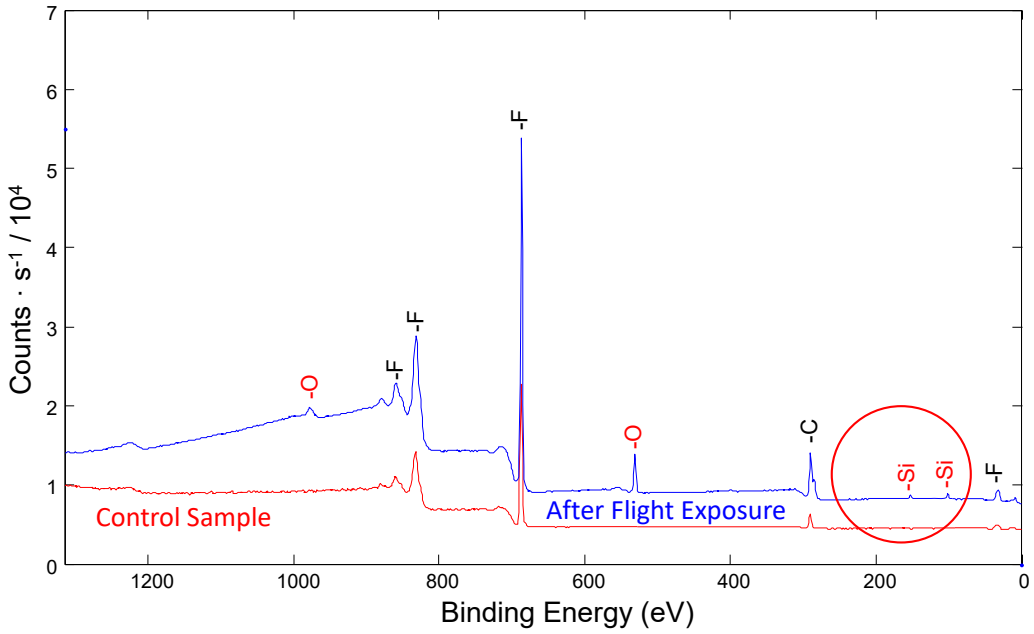

Figure 35. The XPS binding energy data for the MISSE-13 wake FEP/Al flight (M13W-C4 F) and control (M13W-C4 B) samples. A Si and O containing layer ≤20 nm thick was found on the flight sample.

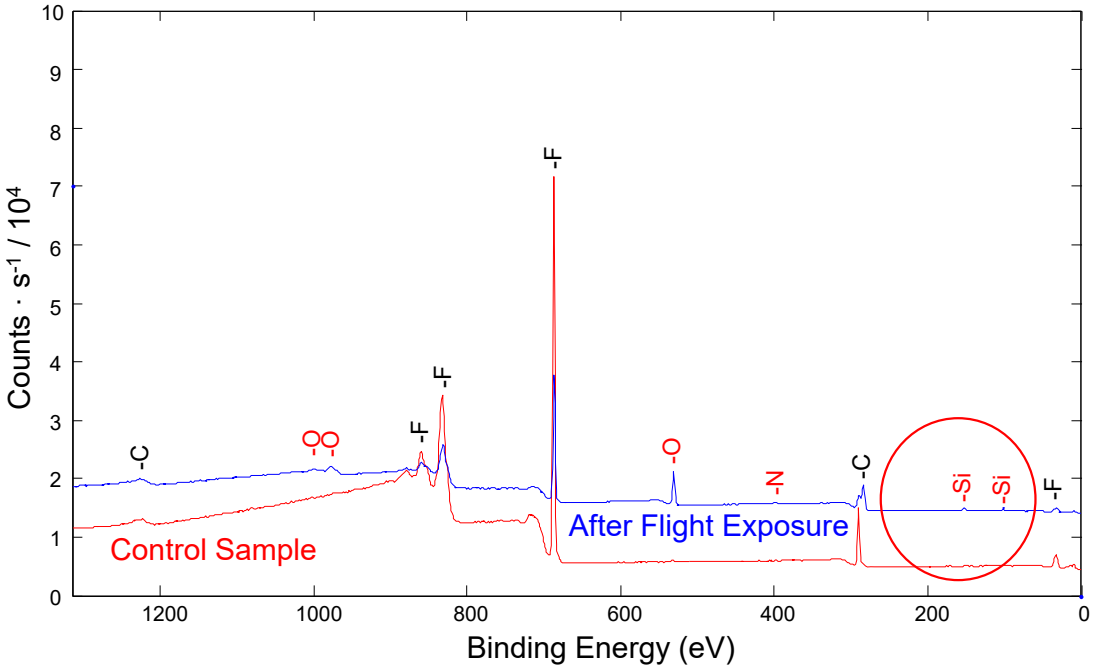

Figure 36. The XPS binding energy data for the MISSE-13 zenith FEP/Al flight (M13Z-C4 F) and control (M13Z-C4 B) samples. A thin layer (≤10 nm) containing of Si, O, and N was detected on the flight sample.

6.2.2 XPS Atomic Concentrations for Control and Flight Surfaces

Tables 3 to 7 provide the XPS atomic concentrations (at.%) data for the MISSE-9 PCE-1, MISSE-10 PCE-2, MISSE-12 PCE-3 ram and zenith, MISSE-12/MISSE-15 PCE-3 wake and MISSE-13 PCE-4 contamination samples, respectively. Data is provided for the surface layer (unsputtered for both the flight and control), and then after sputtering for up to 3 minutes (30 nm) depending on the thickness of the contamination layer. The surface Si atomic concentration varied from 1.5 to 15.1 at.%. None of the corresponding control samples had any detectable Si, with the exception of M10N-C5 B (Al_2O_3) which had <0.1 at.% Si. The higher levels of Si contamination could certainly impact the erosion and other properties of the MISSE spaceflight samples. The MISSE-12 and MISSE-12/MISSE-15 missions appear to have received significant amounts of Si (15.1% for both ram and wake directions). This is consistent with the darker UV light appearance for the MISSE-12 ram and MISSE-12/MISSE-15 wake alumina samples as compared to other alumina samples under UV light.

Table 3. XPS Results of the MISSE-9 PCE-1 Contamination Witness Samples

MISSE-9	Flight Orientation	Material	Atomic Concentrations (at.%)									
			C	O	Al	N	Si	F	Mg	Na	B	S
M9R-C6-B Back up		Al_2O_3	22.8	51.4	25.3	0.5						
Sputtered 1 min (10 nm)				66.6	33.4							
M9R-C6-F Flight	Ram	Al_2O_3	18.1	53.3	20.2	0.5	6	1.6	0.2	0.1		
Sputtered 1 min (10 nm)			0.1	65	30.5		2.3	1.6	0.6			
Sputtered 2 min (20 nm)			<0.1	65.8	33.2		0.3	0.5	0.1			
M9W-C3-B Back up		Al_2O_3	29.3	47.2	23.5							
Sputtered 1 min (10 nm)			1.3	66.1	32.6							
M9W-C3-F Flight	Wake	Al_2O_3	8.9	55.6	26.1	0.2	1.7	6.1	0.1		1.3	
Sputtered 1 min (10 nm)			0.1	65.8	33.8			0.1			0.2	
M9Z-C3-F Flight	Zenith	Al_2O_3	14.9	53.3	25.2		1.5	4.9	0.2			
Sputtered 1 min (10 nm)			1	66.1	32.9							
***M9R-C27-B Back up**		MgF_2	64.1	22.2				12.2	0.8	0.3		0.5
Sputtered 2 min (20 nm)			30.1	3.2				50.4	15.3	0.9		
Sputtered 5 min (50 nm)			4.6	1.7				59	34.7			
M9R-C27-F Flight	Ram	MgF_2	41.1	31.3			4.4	16	6.2			1
Sputtered 1 min (10 nm)			3.8	20.2			2.8	36.2	37			
Sputtered 2 min (20 nm)			2.7	10.5			1.1	45.8	39.9			
****M9Z-C18 B Back up**		MgF_2	68.6	25.3			1.7	2.9	0.9			0.7
Sputtered 2 min (20 nm)			23.7	4.4				51.5	20.5			
Sputtered 5 min (50 nm)			2.3	0.2				60.3	37.2			
M9Z-C18 F Flight	Zenith	MgF_2	14.7	8.4			1.8	55.4	19.7			0.1
Sputtered 1 min (10 nm)			2.2	0.3				56.6	40.8			

*Back of M9R-C27 F Flight sample

**Back of M9Z-C18 F Flight sample

Table 4. XPS Results of the MISSE-10 PCE-2 Contamination Witness Samples

MISSE-10	Flight Orientation	Material	Atomic Concentrations (at.%)											
			C	O	Al	N	Si	F	Mg	Na	B	S	Fe	Cu
M10R-C4-B Back up		Al_2O_3	18.4	53.5	24.1	1.5		0.3			2	0.1		0.2
Sputtered 1 min (10 nm)				66.7	33.3									
M10R-C4 F Flight	Ram	Al_2O_3	13	55.5	17.1	0.5	8.4	1.8	0.7	2.1	0.7		0.2	<0.1
Sputtered 1 min (10 nm)				65.3	29.8			1.5	0.8	0.3				
Sputtered 2 min (20 nm)				66.2	33			0.5	0.3					
M10Z-C5 B Back up		Al_2O_3	23.1	49.9	23.7			2.6		0.7				
Sputtered 1 min (10 nm)				66.3	33.2			0.4						
M10Z-C5 F Flight	Zenith	Al_2O_3	8.5	59	21.4	0.6	6.6	2.9	0.2	0.8				
Sputtered 1 min (10 nm)				65.1	30.7	0.4	1.4	2	0.4					
Sputtered 2 min (20 nm)				65.8	33.3		0.1	0.6	0.2					
M10N-C5 B Back up		Al_2O_3	24.8	47.8	25.1	0.6	<0.1				1.4	0.1		0.1
Sputtered 1 min (10 nm)				66.2	33.8									
M10N-C5 F Flight	Nadir	Al_2O_3	7.2	60.5	19.5	0.5	8.1	1.8			2.3			
Sputtered 1 min (10 nm)				66.2	32.9		0.4	0.4						

Table 5. XPS Results of the MISSE-12 PCE-3 Ram and Zenith Contamination Witness Samples

MISSE-12	Flight Orientation	Material	Atomic Concentrations (at.%)									
			C	O	Al	N	Si	Ca	Mg	Na	F	S
M12R-C3/M12W-C3 B Back up*		Al_2O_3	36.4	41.1	20.5	0.7		0.6	0.1			0.8
Sputtered 1 min (10 nm)			0.5	67.4	32.1							
M12R-C3 F Flight	Ram	Al_2O_3	11	58.8	13.4	0.4	15.1	0.5	0.1		0.8	
Sputtered 1 min (10 nm)				66	31.6		1.1	0.2	0.5		0.5	
Sputtered 2 min (20 nm)				66.1	33.9							
MISSE-12	**Flight Orientation**	**Material**	**C**	**O**	**Ni**	**Ti**	**Ca**	**N**	**Na**	**Cl**	**K**	**Si**
M12Z-S2 B Back up		SMA NiTi	84.9	12.8	0.1	0.5	0.8	0.8	0.2			
Sputtered 1 min (10 nm)			57.1	14	16	9.6	0.2	1.4	0.4	1.1	0.2	
Sputtered 2 min (20 nm)			42.4	13.3	25.8	15.5	0.6	1	0.6	0.5	0.1	
Sputtered 3 min (30 nm)			31.1	9.6	37	22			0.3			
M12Z-S2 F Flight	Zenith	SMA NiTi	15.3	61.5	1.3	14.3	0.5	1				6.2
Sputtered 1 min (10 nm)					67.4	32.6						

*M12R-C3 & M12W-C3 shared back-up sample

Table 6. XPS Results of the MISSE-12/MISSE-15 PCE-3 Wake Contamination Witness Samples

MISSE-15	Flight Orientation	Material	Atomic Concentrations (at.%)									
			C	O	Al	N	Si	Ca	Mg	Na	F	S
M12R-C3/M12W-C3 B Back up*		Al_2O_3	36.4	41.1	20.5	0.7		0.6	0.1			0.8
Sputtered 1 min (10 nm)			0.5	67.4	32.1							
M12W-C3 F Flight	Wake	Al_2O_3	7.2	58.7	13.3		15.1	0.6	<0.1		5	
Sputtered 1 min (10 nm)			0.5	62.2	26.1		5.8	0.8	0.1		4.4	
Sputtered 2 min (20 nm)			0.5	65.2	32.2		0.7	0.3	0.1		0.9	

*M12R-C3 & M12W-C3 shared back-up sample

Table 7. XPS Results of the MISSE-13 PCE-4 Contamination Witness Samples

MISSE-13	Flight Orientation	Material	Atomic Concentrations (at.%)				
			C	O	F	Si	N
M13W-C4-B Back up		FEP/Al	28.7		71.3		
Sputtered 1 min (10 nm)			34.7		65.3		
M13W-C4 F Flight	Wake	FEP/Al	37.1	7.6	53.3	1.6	0.4
Sputtered 1 min (10 nm)			39.1	3.7	55.7	1.4	0.1
Sputtered 2 min (20 nm)			42.5	1.9	54.9	0.7	
M13Z-C4-B Back up		FEP/Al	36.1	0.5	63.4		
Sputtered 1 min (10 nm)			34.7		65.3		
M13Z-C4 F Flight	Zenith	FEP/Al	51.2	14	31.4	2.2	1.2
Sputtered 1 min (10 nm)			58	2	39.9		

In summary, the XPS binding energy data and associated atomic concentrations provided in Tables 3 to 7 provide the following contamination data for the MISSE-9 to MISSE-15 samples:

- The MISSE-9 ram alumina flight sample (M9R-C6 F) had a contamination layer ≤20 nm thick containing Si (6 at.%), F (1.6 at.%) and Mg (0.2 at.%).
- The MISSE-9 wake alumina flight sample (M9W-C3 F) had a contamination layer ≤10 nm thick containing Si (1.7 at.%), F (6.1 at.%), Mg (0.1 at.%) and B (1.3 at.%).
- The MISSE-9 zenith alumina flight sample (M9Z-C3 F) had a contamination layer ≤10 nm thick containing Si (1.5 at.%), F (4.9 at.%) and Mg (0.2 at.%).
- The MISSE-10 ram alumina flight sample (M10R-C4 F) had a surface contamination layer containing Si (8.4 at.%), Na (2.1 at.%) and Fe (0.2 at.%). A thicker layer (≤20 nm) of Mg (0.7 at.%) and F (1.8 at.%) was also detected on the flight sample. N, B, and Cu were detected on both samples.

- The MISSE-10 nadir alumina flight sample (M10N-C5 F) had a contamination layer ≤10 nm thick containing Si (8.1 at.%) and F (1.8 at.%). B was present on control sample but increased in concentration on the flight sample (1.4 to 2.3 at.%).
- The MISSE-10 zenith alumina flight sample (M10Z-C5 F) had a contamination layer ≤20 nm thick containing Si (6.6 at.%), Mg (0.2 at.%), N (0.6 at.%) and F (2.9 at.%).
- The MISSE-12 ram alumina flight sample (M12R-C3 F) had a contamination layer up to 20 nm thick with a high concentration of Si (15.1 at.%) along with a smaller amount of F (0.8 at.%).
- The MISSE-12 zenith SMA NiTi flight sample (M12Z-S2 F) had a contamination layer ≤10 nm thick containing Si (6.2 at.%).
- The MISSE-12/MISSE-15 wake alumina flight sample (M12W-C3 F) had a contamination layer up to 20 nm thick with a high concentration of Si (15.1 at.%) along with a smaller amount of F (5.0 at.%).
- The MISSE-13 wake FEP/Al flight sample (M13W-C4 F) had a contamination layer ≤20 nm thick containing Si (1.6 at.%) and O (7.6 at.%).
- The MISSE-13 zenith FEP/Al flight sample (M13Z-C4 F) had a thin contamination layer (≤10 nm) containing Si (2.2 at.%), O (14 at.%) and N (1.2 at.%).

All of the flight samples had some level of Si contamination and all the alumina samples also contained some level of F. The levels of Si varied from 1.5 to 15.1 at.%., with the MISSE-12 ram and MISSE-12/MISSE-15 wake mission samples having the highest level (15.1 at.% Si). The F level varied from 0.8 to 5.0 at.%, with the highest level on the MISSE-12/MISSE-15 wake sample. All three ram samples (MISSE-9, MISSE-10 and MISSE-12) had a thick contaminant layer (≤20 nm). The other samples with a thicker layer (≤20 nm) included the MISSE-10 zenith sample, the MISSE-12/MISSE-15 wake sample and the MISSE-13 wake sample. Carbon was not considered in this study since it is an identifiable contaminant on Earth.

7.0 Optical Property Results

Tables 8-12 provide the integrated optical properties for the MISSE-9 PCE-1, MISSE-10 PCE-2, MISSE-12 PCE-3 ram, MISSE-12/MISSE-15 PCE-3 wake and MISSE-13 PCE-4 contamination flight and corresponding control samples, respectively. Each table includes the AM0 integrated total reflectance (TR), total transmittance (TT) and solar absorptance (SA). Changes in optical data for the flight samples as compared to the control (back-up) samples are also provided. The corresponding absorptance spectra for each of the contamination flight and corresponding control samples are provided in Figures 37 to 48. Optical properties of the MISSE-12 zenith SMA flight sample (M12Z-S2 F) were not obtained due to the sample size.

The change in the alumina flight sample's AM0 solar absorptance as compared to the control samples was small and ranged from -0.001 to 0.005. The change in the MgF_2 flight sample's AM0 solar absorptance was also very small (0.001 to 0.002). As can be seen in the corresponding absorptance spectra, these small changes are mostly within the UV region of the spectra.

Enlarged UV ranges are provided for the following three samples: M10N-C5 F versus B (Figure 44b), M12R-C3 F versus B (Figure 45b) and M12W-C3 F versus B (Figure 46b). The M10N-C5 F sample had no change in AM0 integrated solar absorptance and the UV section shows a small increase in absorptance in the 250 to 300 nm range with a 0.015 absorptance at 250 nm. Whereas the MISSE-12 ram and MISSE-12/MISSE-15 wake samples, which had the largest Si at.% shows greater solar absorptance in the UV range, as shown in Figure 45b and 46b, respectively. The MISSE ram alumina sample (M12R-C3 F) had an increase in the integrated AM0 of only 0.002, but the absorptance increased in the 250 to 700 nm range with an absorptance of 0.035 at 250 nm. While the MISSE-12/MISSE-15 wake alumina sample (M12W-C3 F) had no increase in the integrated AM0 as compared to the control sample, but the absorptance increased in the 250 to 400 nm range with an absorptance of 0.030 at 250 nm. Thus, the MISSE ram sample has greater absorptance in the UV section as compared to the MISSE-12 wake sample, which is consistent with the post-flight UV light images shown in Figure 22.

The two samples with a significant change in solar absorptance are the two MISSE-13 back-surface aluminized Teflon FEP (FEP/Al) samples. The MISSE-13 wake sample (M13W-C4 F) had a 0.012 increase in AM0 integrated solar absorptance and the MISSE-13 zenith sample (M13Z-C4 F) had a 0.016 increase in AM0 integrated solar absorptance, as shown in Figures 47 and 48, respectively. Metallized Teflon FEP often undergoes changes in optical properties with space radiation exposure, and is not necessarily an indication of contamination by itself.

Table 8. Optical Properties for the MISSE-9 PEC-1 Contamination Samples

MISSE Mission	Flight Orientation	Sample ID	Sample Type	Material	Optical Property	Optical Data	Flight vs. Back-up
MISSE-9	Ram	M9R-C6 F	**Flight**	Alumina slide	AM0 TR	0.141	0.000
					AM0 TT	0.856	-0.005
					AM0 SA	0.003	**0.005**
		M9R-C6 B	Back-up	Alumina slide	AM0 TR	0.141	N/A
					AM0 TT	0.861	N/A
					AM0 SA	-0.002	N/A
	Wake	M9W-C3 F	**Flight**	Alumina slide	AM0 TR	0.140	-0.001
					AM0 TT	0.858	-0.002
					AM0 SA	0.002	**0.003**
		M9W-C3 B	Back-up	Alumina slide	AM0 TR	0.141	N/A
					AM0 TT	0.860	N/A
					AM0 SA	-0.001	N/A
	Zenith	M9Z-C3 F	**Flight**	Alumina slide	AM0 TR	0.140	0.000
					AM0 TT	0.857	-0.001
					AM0 SA	0.003	**0.001**
		M9W-C3 B	Back-up	Alumina slide	AM0 TR	0.141	N/A
					AM0 TT	0.860	N/A
					AM0 SA	-0.001	N/A
	Ram	M9R-C27 F	**Flight**	Magnesium Fluoride	AM0 TR	0.053	-0.036
					AM0 TT	0.942	0.035
					AM0 SA	0.006	**0.002**
		M9R-C27 B	Back-up	Magnesium Fluoride	AM0 TR	0.089	N/A
					AM0 TT	0.907	N/A
					AM0 SA	0.004	N/A
	Zenith	M9Z-C18 F	**Flight**	Magnesium Fluoride	AM0 TR	0.053	-0.037
					AM0 TT	0.942	0.036
					AM0 SA	0.005	**0.001**
		M9Z-C18 B	Back-up	Magnesium Fluoride	AM0 TR	0.090	N/A
					AM0 TT	0.906	N/A
					AM0 SA	0.004	N/A

Table 9. Optical Properties for the MISSE-10 PEC-2 Contamination Samples

MISSE Mission	Flight Orientation	Sample ID	Sample Type	Material	Optical Property	Optical Data	Flight vs. Back-up
MISSE-10	Ram	M10R-C4 F	**Flight**	Alumina slide	AM0 TR	0.142	0.001
					AM0 TT	0.857	-0.001
					AM0 SA	0.000	**-0.001**
		M10R-C4 B	Back-up	Alumina slide	AM0 TR	0.141	N/A
					AM0 TT	0.858	N/A
					AM0 SA	0.001	N/A
	Zenith	M10Z-C5 F	**Flight**	Alumina slide	AM0 TR	0.140	-0.001
					AM0 TT	0.856	-0.002
					AM0 SA	0.004	**0.003**
		M10Z-C5 B	Back-up	Alumina slide	AM0 TR	0.141	N/A
					AM0 TT	0.858	N/A
					AM0 SA	0.001	N/A
	Nadir	M10N-C5 F	**Flight**	Alumina slide	AM0 TR	0.142	0.000
					AM0 TT	0.858	-0.001
					AM0 SA	0.000	**0.000**
		M10N-C5 B	Back-up	Alumina slide	AM0 TR	0.142	N/A
					AM0 TT	0.859	N/A
					AM0 SA	0.000	N/A

Table 10. Optical Properties for the MISSE-12 PEC-3 Ram Contamination Samples

MISSE Mission	Flight Orientation	Sample ID	Sample Type	Material	Optical Property	Optical Data	Flight vs. Back-up
MISSE-12	Ram	M12R-C3 F	**Flight**	Alumina slide	AM0 TR	0.141	0.000
					AM0 TT	0.855	-0.003
					AM0 SA	0.003	**0.002**
		M12R-C3 / M12W-C3 B*	Back-up	Alumina slide	AM0 TR	0.141	N/A
					AM0 TT	0.858	N/A
					AM0 SA	0.001	N/A

*Shared back-up with M12W-C3 F

Table 11. Optical Properties for the MISSE-12/MISSE-15 PEC-3 Wake Contamination Samples

MISSE Mission	Flight Orientation	Sample ID	Sample Type	Material	Optical Property	Optical Data	Flight vs. Back-up
MISSE-12/ MISSE15	Wake	M12W-C3 F	**Flight**	Alumina slide	AM0 TR	0.143	0.002
					AM0 TT	0.856	-0.002
					AM0 SA	0.001	**0.000**
		M12R-C3 / M12W-C3 B*	Back-up	Alumina slide	AM0 TR	0.141	N/A
					AM0 TT	0.858	N/A
					AM0 SA	0.001	N/A

*Shared back-up with M12R-C3 F

Table 12. Optical Properties for the MISSE-13 PEC-4 Contamination Samples

MISSE Mission	Flight Orientation	Sample ID	Sample Type	Material	Optical Property	Optical Data	Flight vs. Back-up
MISSE-13	Wake	M13W-C4 F	**Flight**	Aluminized-Teflon FEP	AM0 TR	0.851	-0.010
					AM0 TT	0.004	-0.002
					AM0 SA	0.145	**0.012**
		M13W-C4 B	Back-up	Aluminized-Teflon FEP	AM0 TR	0.861	N/A
					AM0 TT	0.006	N/A
					AM0 SA	0.133	N/A
	Zenith	M13Z-C4 F	**Flight**	Aluminized-Teflon FEP	AM0 TR	0.846	-0.015
					AM0 TT	0.003	0.000
					AM0 SA	0.151	**0.016**
		M13Z-C4 B	Back-up	Aluminized-Teflon FEP	AM0 TR	0.861	N/A
					AM0 TT	0.003	N/A
					AM0 SA	0.135	N/A

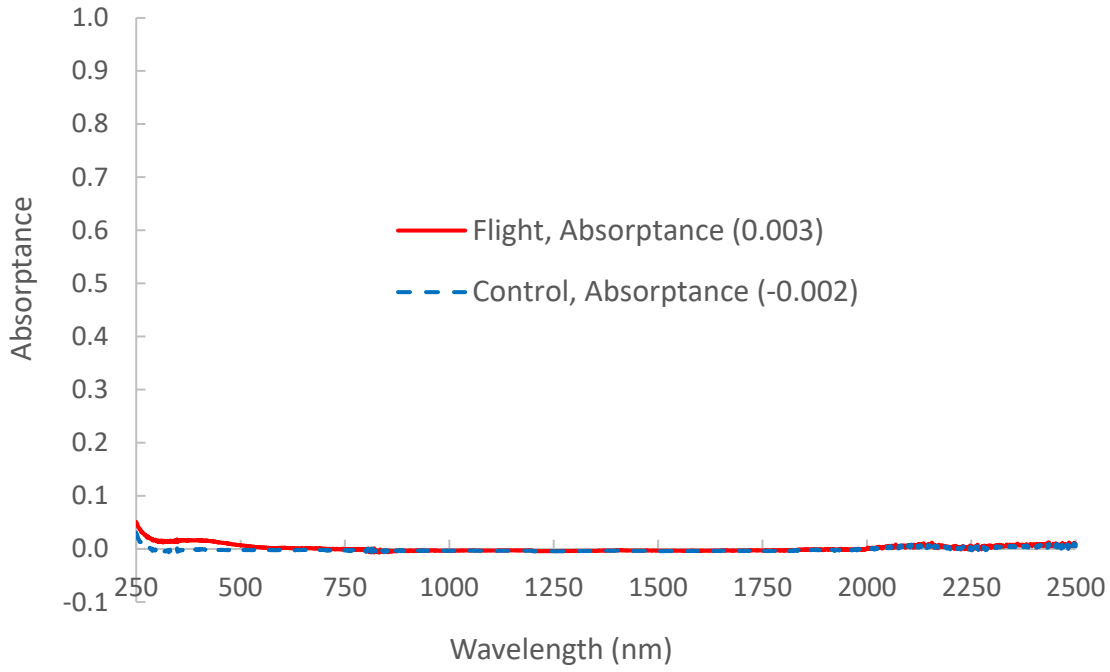

Figure 37. Solar absorptance curves and integrated AM0 values for the MISSE-9 ram alumina flight (M9R-C6 F) and control (M9R-C6 B) samples. See Figures A1a and A1b in the Appendix for total reflectance and total transmittance data.

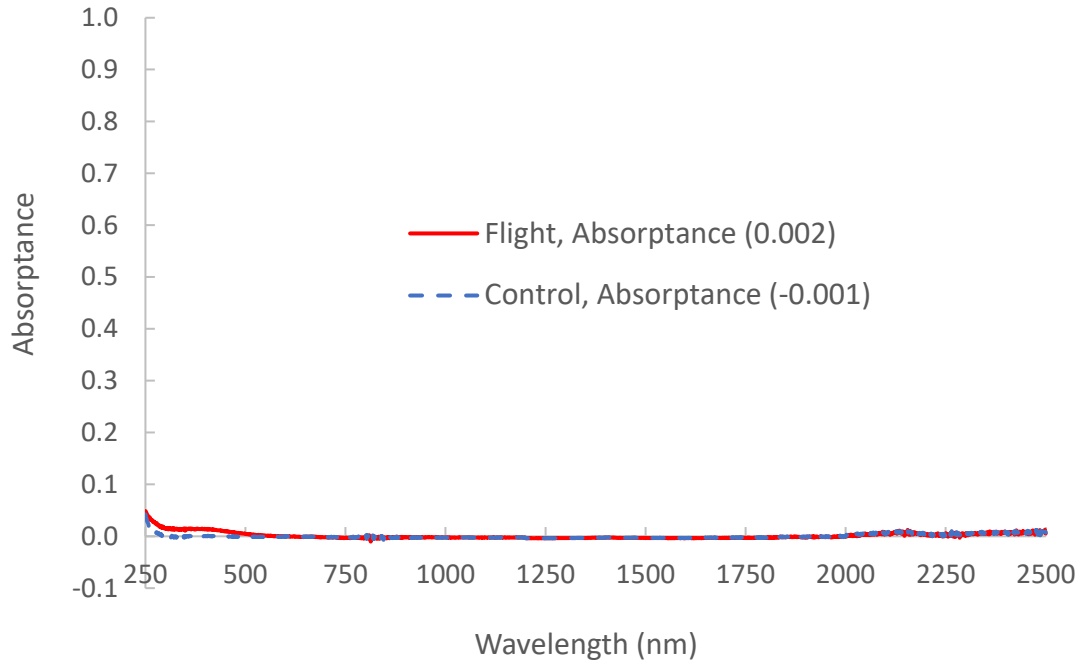

Figure 38. Solar absorptance curves and integrated AM0 values for the MISSE-9 wake alumina flight (M9W-C3 F) and control (M9W-C3 B) samples. See Figures A2a and A2b in the Appendix for total reflectance and total transmittance data.

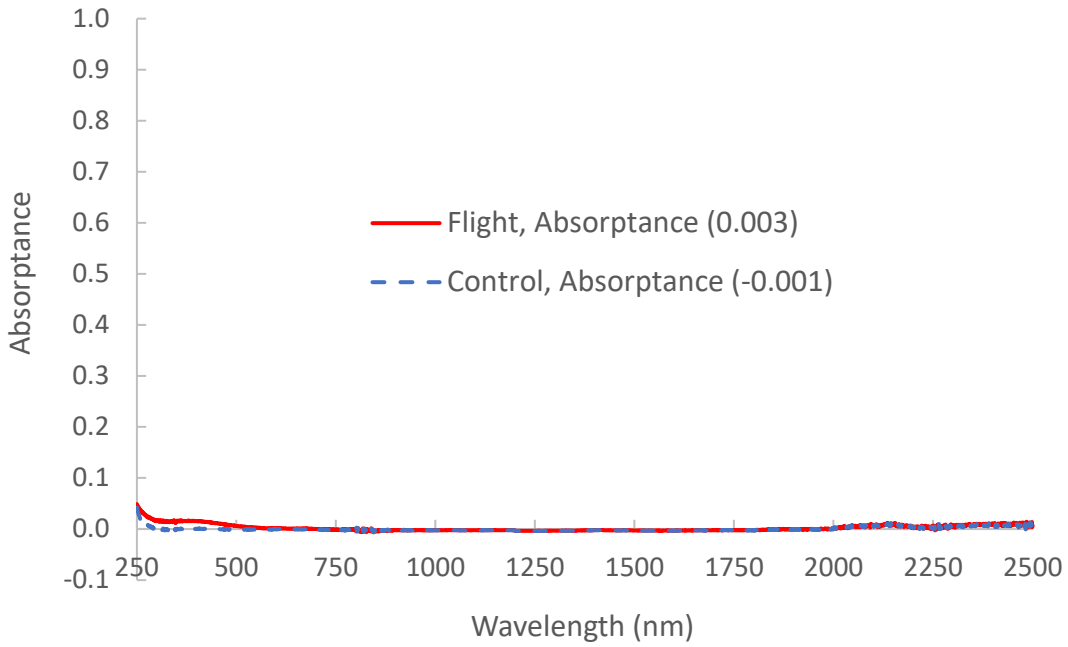

Figure 39. Solar absorptance curves and integrated AM0 values for the MISSE-9 zenith alumina flight (M9Z-C3 F) and control (M9W-C3 B) samples. See Figures A3a and A3b in the Appendix for total reflectance and total transmittance data.

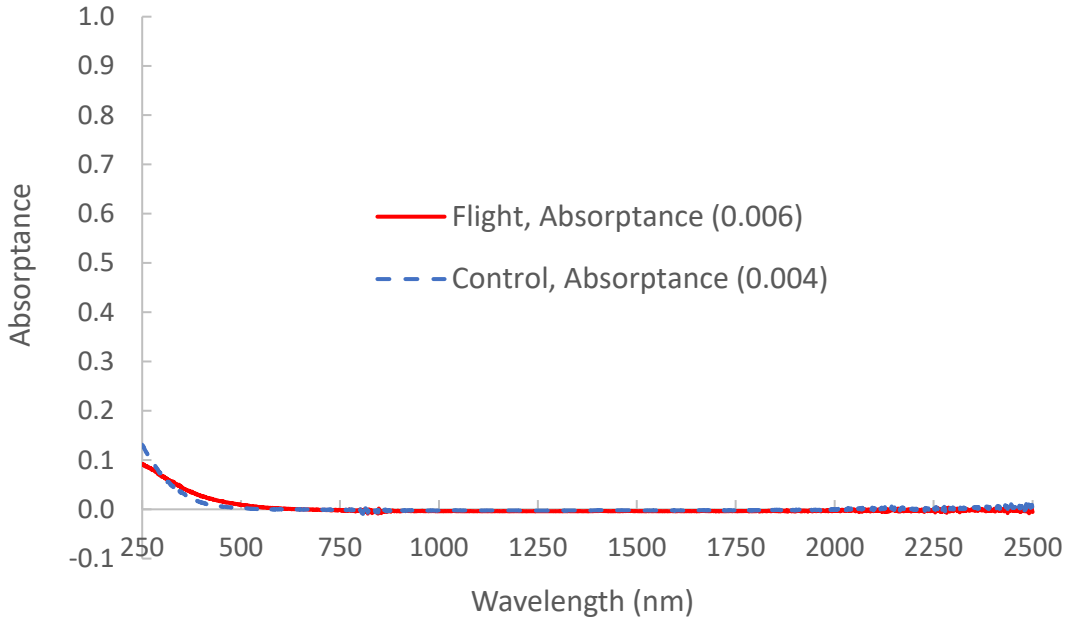

Figure 40. Solar absorptance curves and integrated AM0 values for the MISSE-9 ram magnesium fluoride flight (M9R-C27 F) and control (M9R-C27 B) samples. See Figures A4a and A4b in the Appendix for total reflectance and total transmittance data.

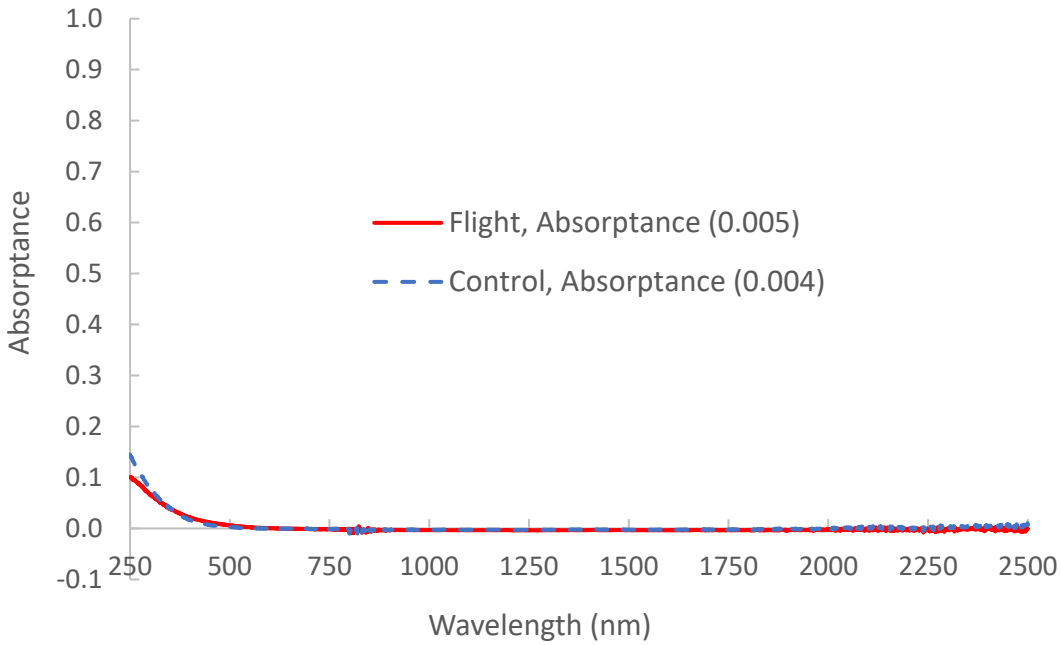

Figure 41. Solar absorptance curves and integrated AM0 values for the MISSE-9 zenith magnesium fluoride flight (M9Z-C18 F) and control (M9Z-C18 B) samples. See Figures A5a and A5b in the Appendix for total reflectance and total transmittance data.

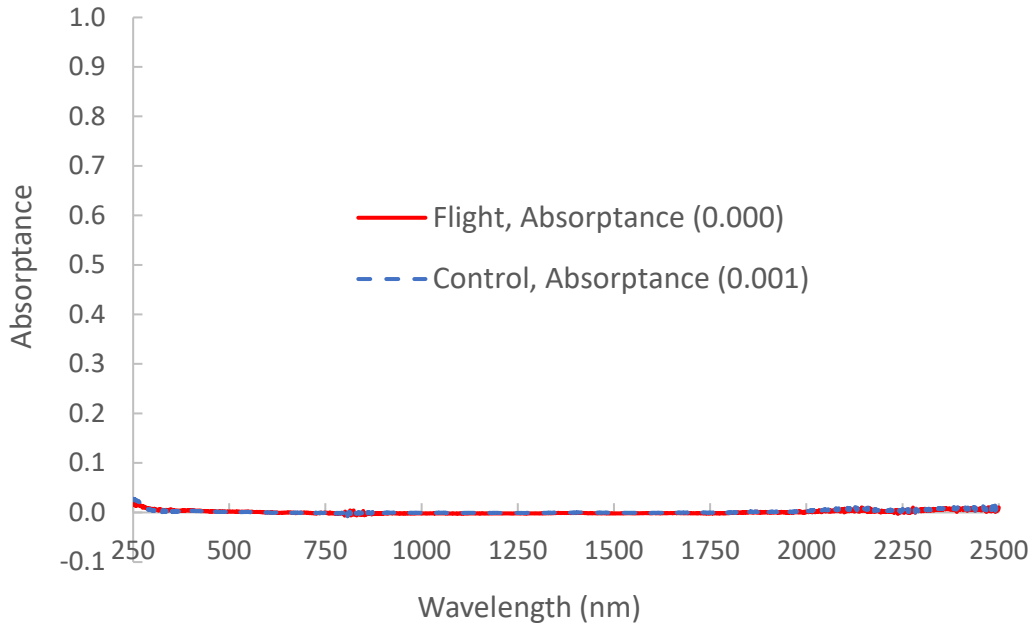

Figure 42. Solar absorptance curves and integrated AM0 values for the MISSE-10 ram alumina flight (M10R-C4 F) and control (M10R-C4 B) samples. See Figures A6a and A6b in the Appendix for total reflectance and total transmittance data.

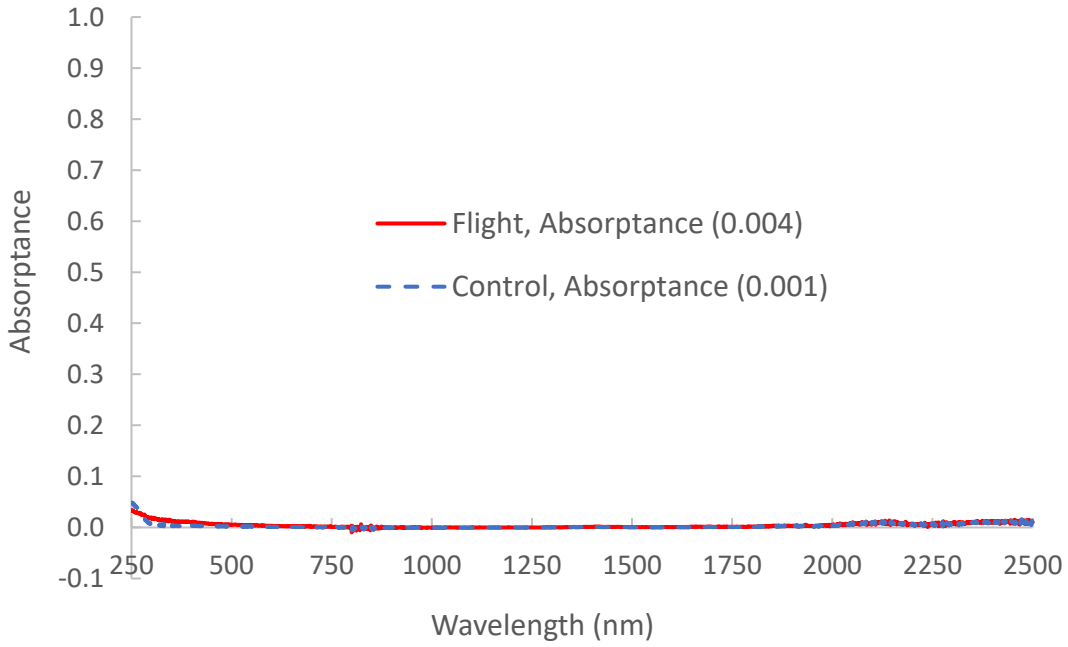

Figure 43. Solar absorptance curves and integrated AM0 values for the MISSE-10 zenith alumina flight (M10Z-C5 F) and control (M10Z-C5 B) samples. See Figures A7a and A7b in the Appendix for total reflectance and total transmittance data.

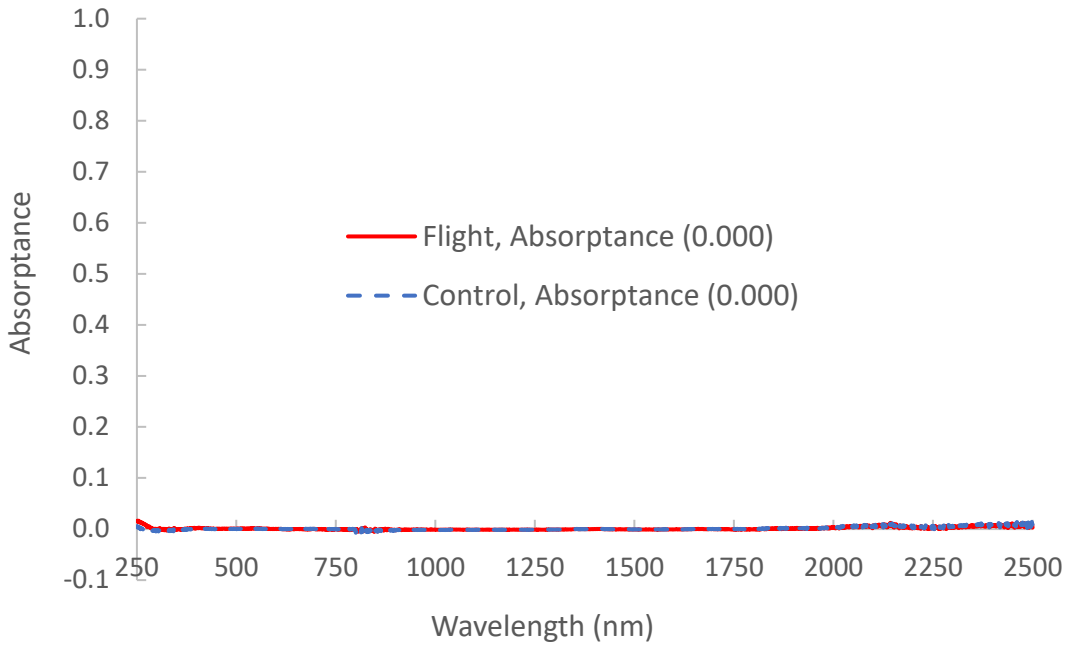

a.

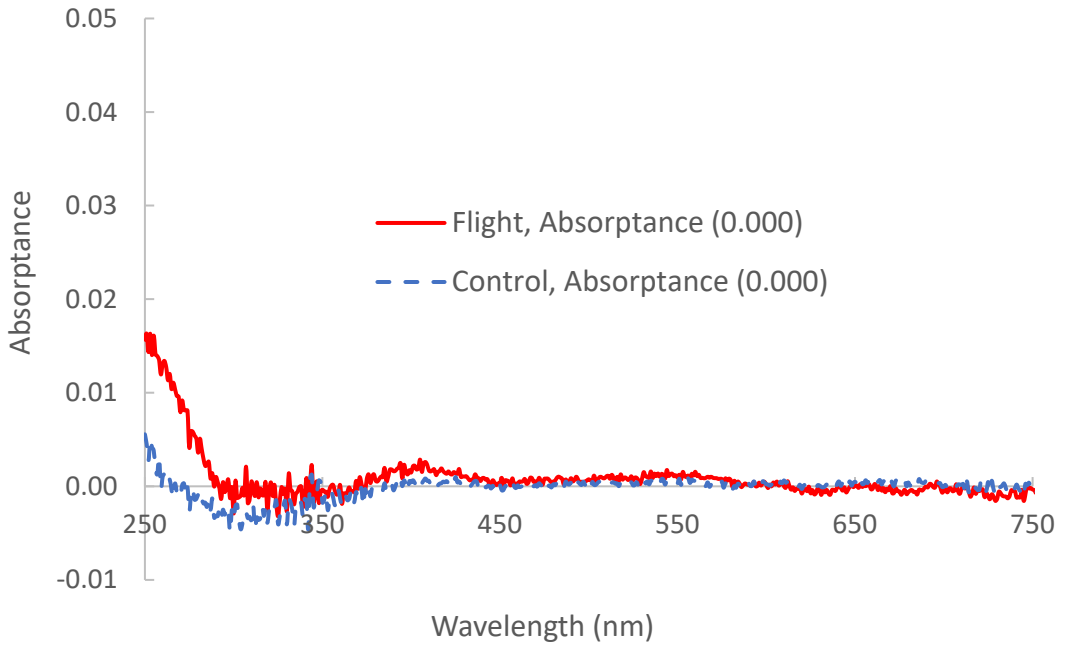

b.

Figure 44. Solar absorptance curves and integrated AM0 values for the MISSE-10 nadir alumina flight (M10N-C5 F) and control (M10N-C5 B) samples (see Figures A8a and A8b in the Appendix for total reflectance and total transmittance data): (a) Full scale graph, and (b) Enlarged UV section of graph.

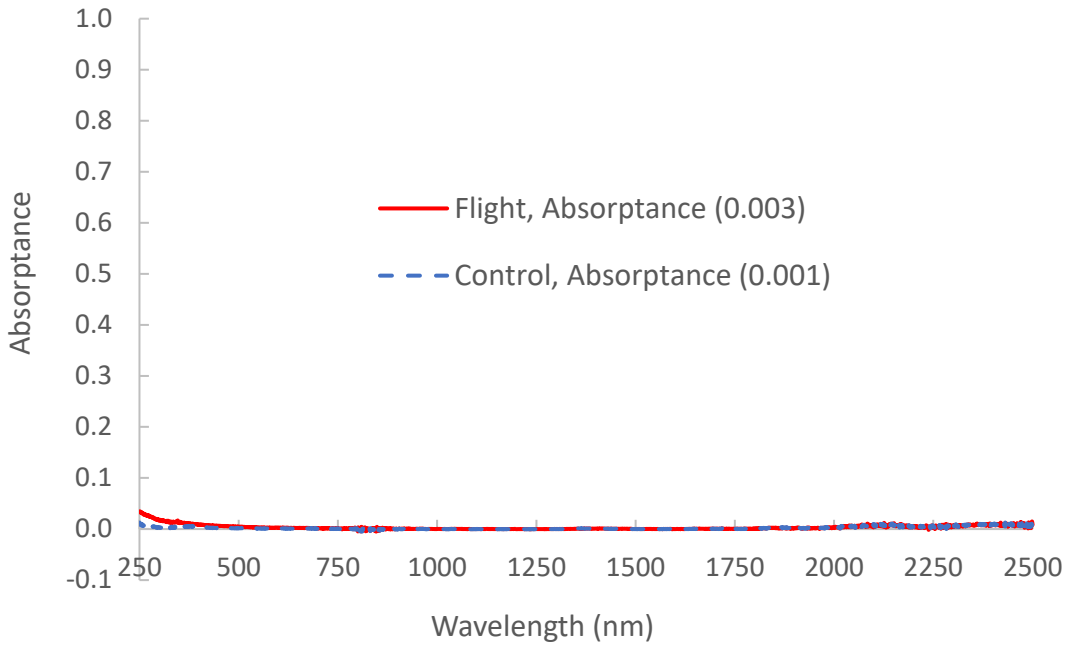

a.

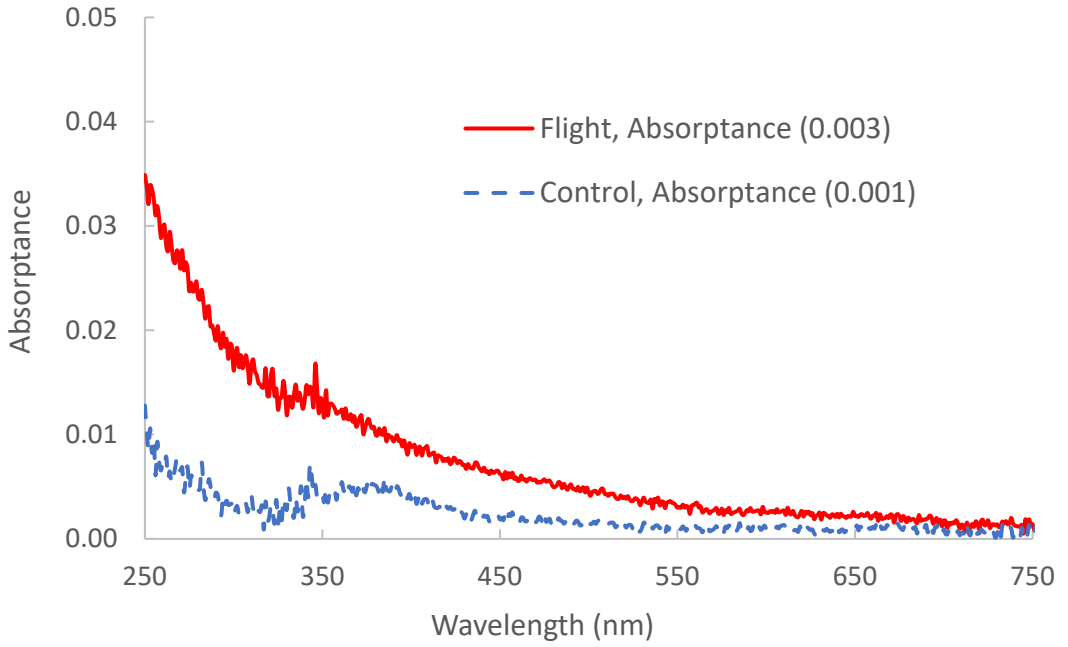

b.

Figure 45. Solar absorptance curves and integrated AM0 values for the MISSE-12 ram alumina flight (M12R-C3 F) and control (M12R-C3/M12W-C3 B) samples (see Figures A9a and A9b in the Appendix for total reflectance and total transmittance data): (a) Full scale graph, and (b) Enlarged UV section of graph.

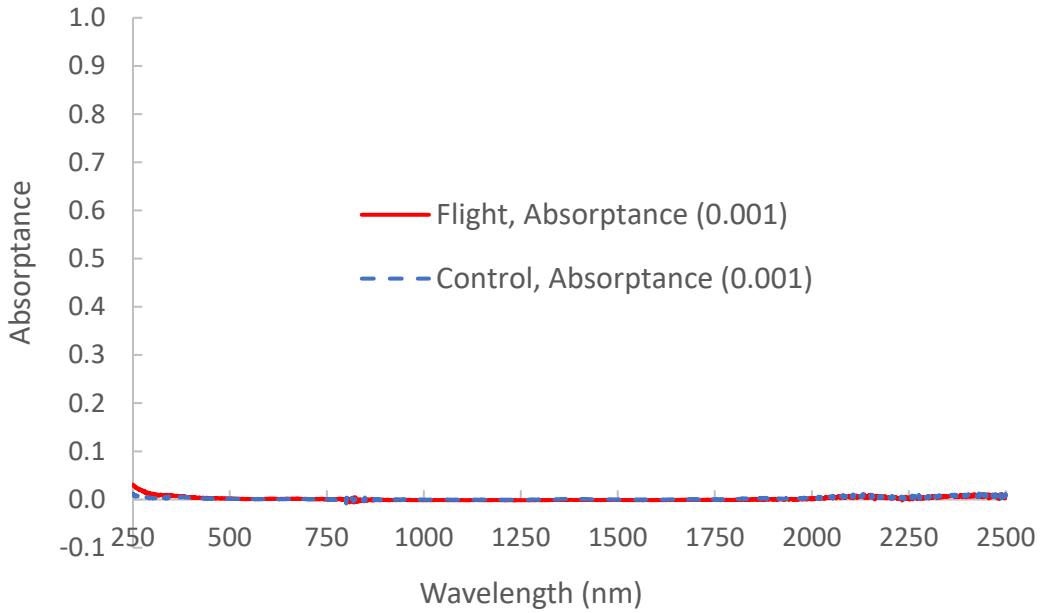

a.

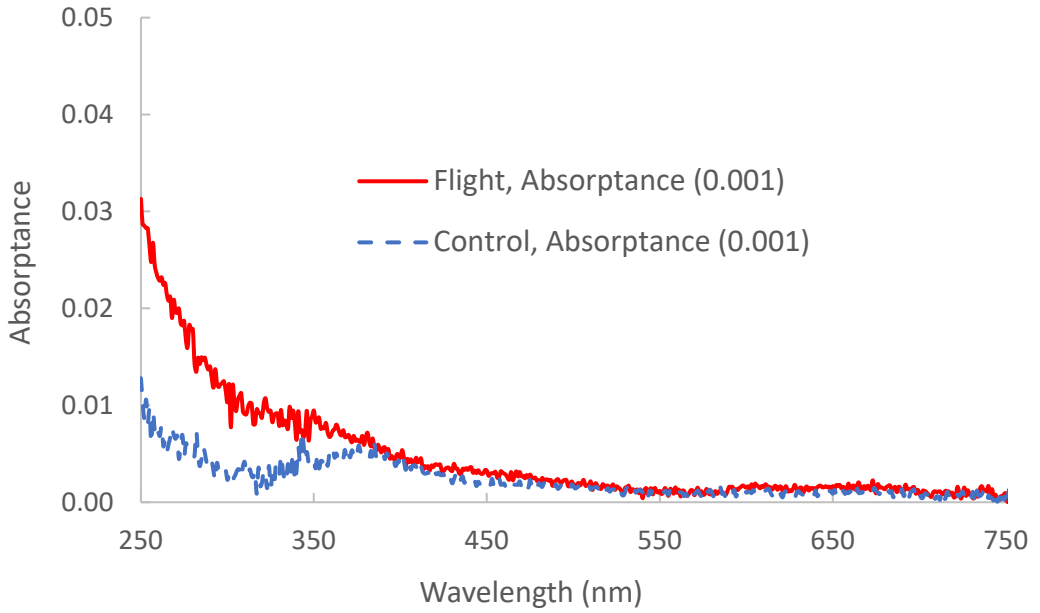

b.

Figure 46. Solar absorptance curves and integrated AM0 values for the MISSE-12 wake alumina flight (M12W-C3 F) and control (M12R-C3/M12W-C3 B) samples (see Figures A10a and A10b in the Appendix for total reflectance and total transmittance data): (a) Full scale graph, and (b) Enlarged UV section of graph.

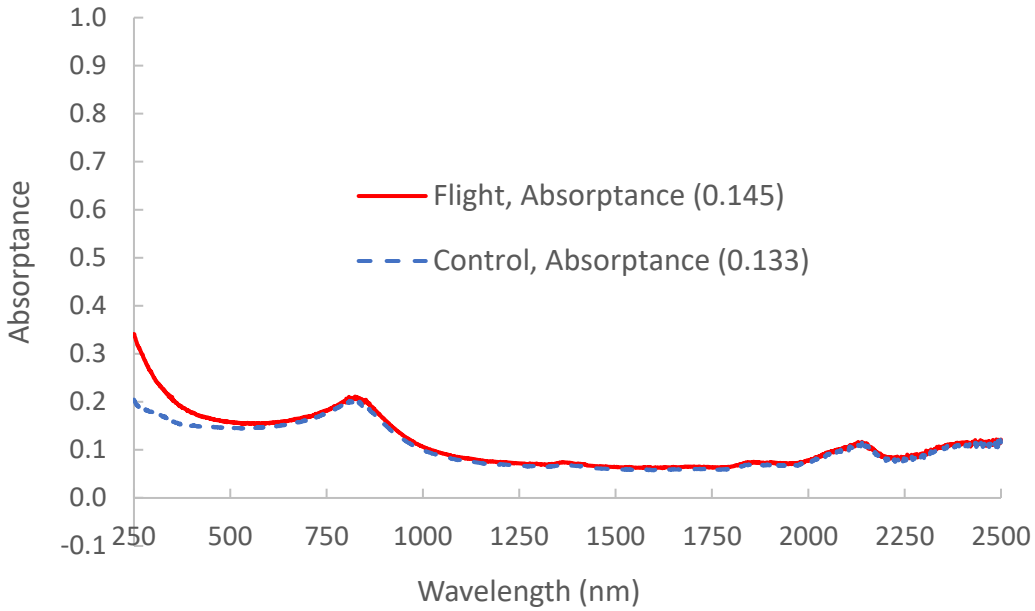

Figure 47. Solar absorptance curves and integrated AM0 values for the MISSE-13 ram aluminized-Teflon FEP flight (M13W-C4 F) and control (M13W-C4 B) samples. See Figures A11a and A11b in the Appendix for total reflectance and total transmittance data.

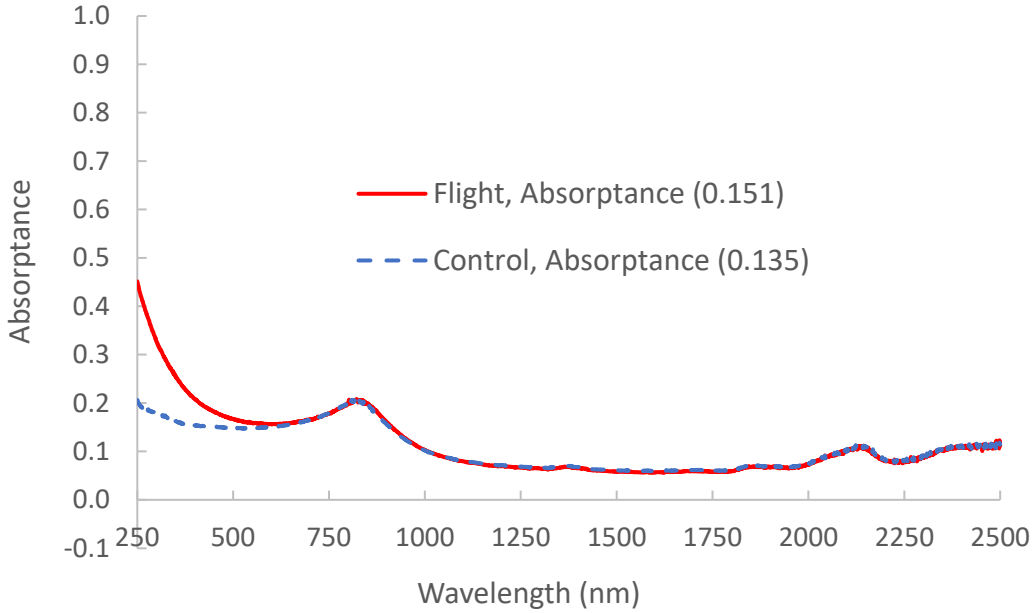

Figure 48. Solar absorptance curves and integrated AM0 values for the MISSE-13 zenith aluminized-Teflon FEP flight (M13Z-C4 F) and control (M13Z-C4 B) samples. See Figures A12a and A12b in the Appendix for total reflectance and total transmittance data.

Discussion

Silicone contamination is one of the greatest on-orbit contamination concerns. Table 13 provides a summary of the Si atomic concentrations for the PCE 1-4 contamination samples. Included in the table are Si atomic concentration per year (at.%/year). The MISSE-9 mission ram average Si atomic concentration per year is 6.8 at.%. This is twice the contamination that occurred in the MISSE-9 wake (3.1 at.% per year) or zenith (3.1 average Si at.% per year) directions. For the MISSE-10 mission, the ISS facing nadir direction had substantially more Si (16.9 at.% per year) than the ram (7.2 at.% per year) or zenith (9.6 at.% per year) directions. The MISSE-12 and MISSE-12/MISSE-15 mission samples received significantly more Si contamination than the other mission samples. The MISSE-12 ram sample received 17.0 Si at.% per year, the MISSE-12 zenith sample received 13.8 Si at.% per year, while the re-flown MISSE-12/MISSE-12 wake sample received 34.3 Si at.% per year. Finally, the MISSE-13 wake sample received 3.6 Si at.% per year and the MISSE-13 zenith sample received 4.8 Si at.% per year. These levels of Si contamination, especially for the MISSE-10 nadir, MISSE-12 and MISSE-12/MISSE-15 missions, are significant.

Table 13. PCE 1-4 Contamination Samples Si Atomic Concentrations

MISSE-FF Flight Sample ID	Flight Orientation	Material	Time on MISSE-FF (years)	Direct Space Exposure Duration (years)	Si Atomic Concentration (at.%)	Si Atomic Concentration per year (at.%/year)
MISSE-9						
M9R-C6 F	Ram	Al_2O_3	1.57	0.77	6.0	7.8
M9R-C27 F	Ram	MgF_2	1.57	0.77	4.4	5.7
M9W-C3 F	Wake	Al_2O_3	1.02	0.54	1.7	3.1
M9Z-C3 F	Zenith	Al_2O_3	1.02	0.54	1.5	2.8
M9Z-C18 F	Zenith	MgF_2	1.02	0.54	1.8	3.3
MISSE-10						
M10R-C4 F	Ram	Al_2O_3	1.9	1.17	8.4	7.2
M10N-C5 F	Nadir	Al_2O_3	1.2	0.48	8.1	16.9
M10Z-C5 F	Zenith	Al_2O_3	1.2	0.69	6.6	9.6
MISSE-12						
M12R-C3 F	Ram	Al_2O_3	1.04	0.89	15.1	17.0
M12W-C3 F	Wake	Al_2O_3	1.05	0**	N/A	N/A
M12Z-S2 F	Zenith	SMA NiTi	1.05	0.45	6.2	13.8
MISSE-13						
M13W-C4 F	Wake	FEP/Al	0.7	0.44	1.6	3.6
M13Z-C4 F	Zenith	FEP/Al	0.7	0.46	2.2	4.8
MISSE-12 & MISSE-15 Re-flight**						
M12W-C3 F	Wake	Al_2O_3	1.05 + 0.6	0.44	15.1	34.3

The Stratospheric Aerosol and Gas Experiment (SAGE) III is a solar and lunar occultation instrument mounted externally on the ISS.[13] It measures Earth's stratospheric ozone, aerosols, water vapor and other trace gases.[13] The SAGE III payload is located on ISS's ELC-4 and has two Contamination Monitoring Packages (CMP1 and CMP2) to monitor environmental conditions.[13] The CMP1 and CMP2 have multiple sensors containing quartz crystals that vibrate at frequencies dependent on the amount of contamination deposited onto them.[13] After more than four years of collecting and studying CMP data, the SAGE III team determined that the ram surface had large amounts of accumulated contamination, as shown in Figure 49.[13] The SAGE III team determined that visiting vehicles have been the largest source of on-orbit contamination.[13] They found that Cargo Dragon vehicles consistently had the highest rates of contamination on the CMP sensors that could not be burned off and removed, also known as chemisorption.[13] Although the SAGE III is located in a different location than the MISSE-FF, the CMP sensor data indicates accumulated on-orbit contamination is a concern on ISS.

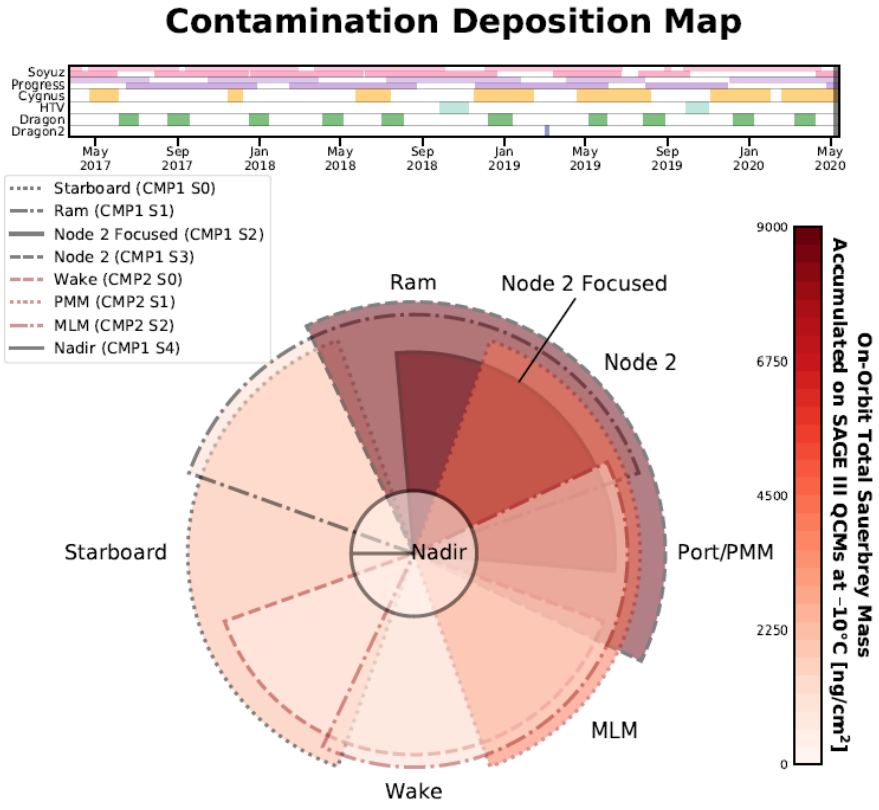

Figure 49. Contamination Deposition Map of the SAGE III Sensors from Reference 13.

Table 14. Average Ram AO Fluence per Year for the MISSE-9, -10 and -12 missions.[9]

MISSE-FF Expt.	Space Exposure Duration	Direct Space Exposure Duration (Years)	AO Fluence (atoms/cm^2)	AO Fluence/ Exposure Duration (atoms/cm^2/year)	Si Atomic Concentration (at.%)	Solar Cycle
MISSE-9 Ram	4/19/2018 to 10/2/2019	0.77	3.44E+20	4.46E+20	6.0	Solar min
MISSE-10 Ram	4/26/2019 to 11/25/2020	1.17	3.93E+20	3.36E+20	8.4	Solar min & increasing
MISSE-12 Ram	12/3/2019 to 11/25/2020	0.89	2.97E+20	3.34E+20	15.1	Solar min & increasing

One potential impact of PCE 1-4 on-orbit contamination is the effect on the AO erosion of Kapton H AO fluence witness and AO erosion yield samples. The AO ram fluence for the MISSE-FF missions was found to be low as compared to the MISSE 1-8 missions of equivalent space exposure duration.[9,14] The average ram AO fluence per year for the MISSE 2-8 missions ranges from 1.36 to 2.83 x 10^{21} atoms/cm^2, while the average ram AO fluence per year for the MISSE-9, -10 and -12 missions ranges from 3.34 to 4.46 x 10^{20} atoms/cm^2, as shown in Table 14.[9,14] Thus, the MISSE 2-8 missions received 3.0 to 8.5X the ram AO fluence for an equivalent exposure duration as the MISSE 9-12 missions.

One of the significant contributing factors to the AO fluence is the variation in AO flux with the 11-year solar cycle. As discussed by de Groh and Banks in Reference 9, the solar cycle would account for a good portion of the difference in AO fluence for the MISSE 2-8 missions as compared to the MISSE 9-12 missions. Other factors could be differences in the ISS location for some of the MISSE missions and a very small contribution from the MISSE-FF 8 degrees "pitch up" rotation.[9] Another contributor to a lower AO fluence for the MISSE-FF missions could be the on-orbit contamination effects. Table 14 lists the XPS atomic concentration of Si for the MISSE-9, -10 and -12 ram missions along with the mission AO fluence. A notable observation for the MISSE-9, MISSE-10 and MISSE-12 missions is that the higher the Si at.%, the lower the average ram AO fluence per year. This data indicates that Si contamination can affect the AO fluence. Dever reported XPS analyses for sapphire (Al_2O_3) contamination witness slides for the MISSE-2 mission.[12] The ram samples had 5.4 to 5.5 at.% of Si on the surface. Thus, the MISSE-2 mission had somewhat lower Si contamination than the MISSE-9, MISSE-10 and MISSE-12 missions.

8.0 Summary and Conclusions

Four Glenn experiments with 365 flight samples were flown on ISS's MISSE-Flight Facility (MISSE-FF). These experiments are the Polymers and Composites Experiment-1 (PCE-1) flown as part of the MISSE-9 mission, the PCE-2 flown as part of the MISSE-10 mission, the PCE-3 flown as part of the MISSE-12 and MISSE-15 missions, and the PCE-4 flown as part of the MISSE-13 mission. The experiment samples were flown in either ram, wake, nadir or zenith orientations and were directly exposed to the space environment from 0.44 to 1.17 years depending on the flight mission and orientation.

Each of these experiments included passive contamination witness samples in each flight direction for post-flight molecular contamination analyses. A total of 13 contamination flight samples were flown. The majority of contamination samples were alumina (Al_2O_3, sapphire) slides as alumina does not erode with AO exposure and silicone contamination can be easily detected. One of two binary NiTi SMA samples was used for XPS analyses for the MISSE-12 zenith direction. Back-surface aluminized-Teflon FEP samples (FEP/Al) were used for contamination detection for the MISSE-13 mission due to the low erosion yield of FEP and the easy detection of Si. Post-flight images of flight and control samples were taken with visible and UV light. Post-flight analyses of the PCE 1-4 contamination samples and corresponding control samples (also called back-up samples) included XPS analyses (surface and ion sputter depth analyses) and optical properties (total reflectance, total transmittance, and solar absorptance).

Minimal changes occurred in the optical properties of the flight samples. The integrated AM0 solar absorptance of the alumina flight samples changed from -0.001 to 0.005 as compared to the control samples. Small increases in absorptance were typically observed in the UV wavelengths. The FEP/Al samples had larger integrated AM0 solar absorptance changes (0.012 to 0.016), but these optical changes often occur to metallized FEP in space and do not necessarily indicate contamination. Visible light images did not show significant changes in the flight samples as compared to the control samples. Although the UV (365 nm) light images showed significant changes in numerous flight samples in the space exposed regions. The XPS analyses indicated varying levels of molecular contamination with Si atomic concentrations from 1.5 to 15.5 at.%. The MISSE-12 ram and MISSE-12/MISSE-15 wake samples experienced the highest levels of silicone contamination at 15.1 at.%. Knowledge of on-orbit contamination is important for flight data interpretation.

Appendix A.—Reflectance and Transmittance of PCE 1-4 Contamination Samples

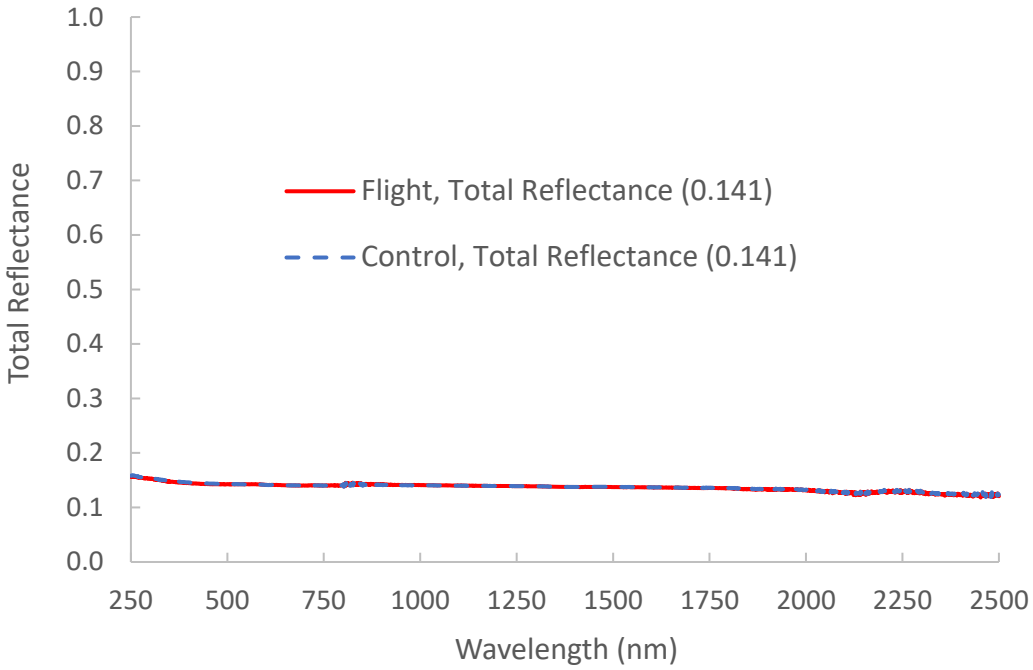

Fig. A1a. Total reflectance curves and integrated AM0 values for the MISSE-9 ram alumina flight (M9R-C6 F) and control (M9R-C6 B) samples.

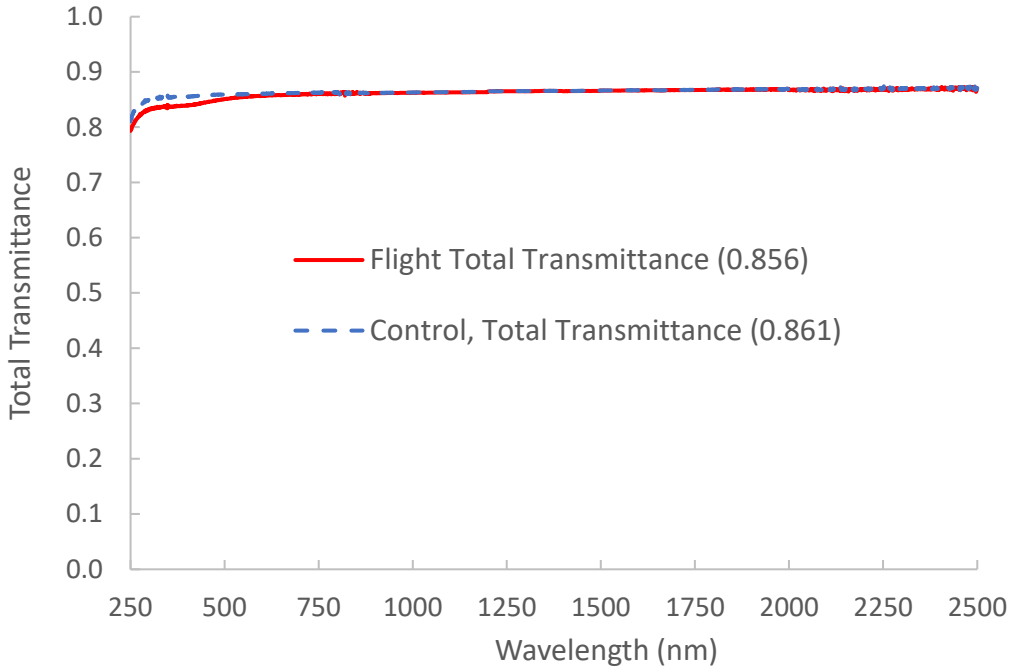

Fig. A1b. Total transmittance curves and integrated AM0 values for the MISSE-9 ram alumina flight (M9R-C6 F) and control (M9R-C6 B) samples.

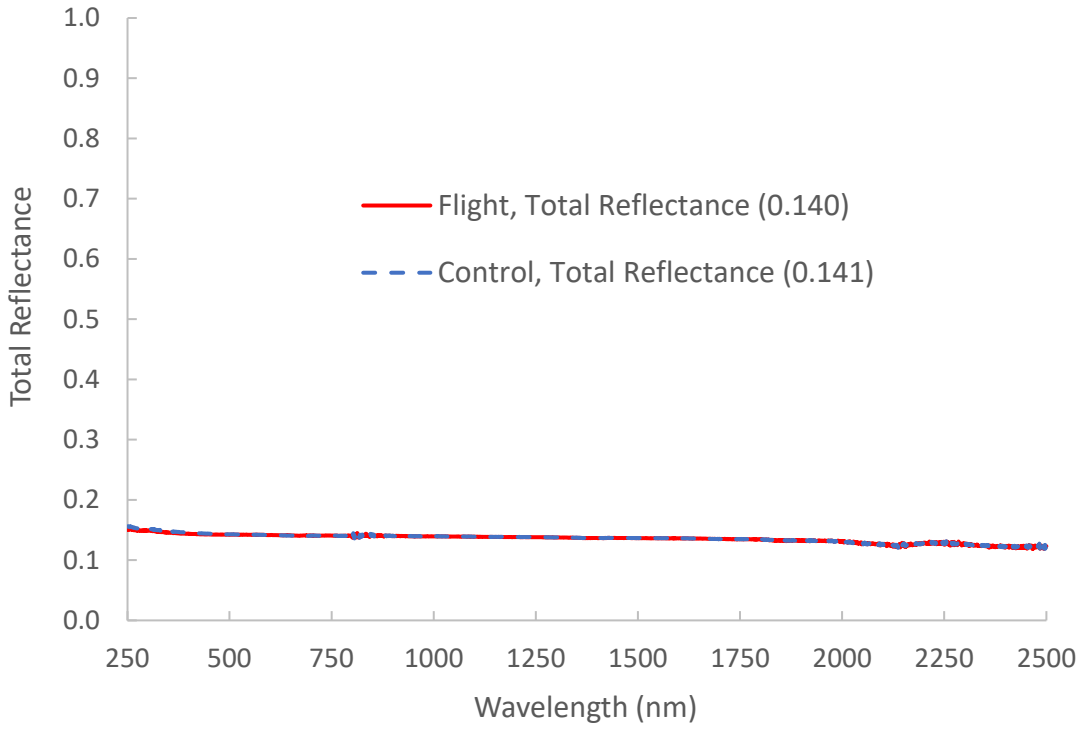

Fig. A2a. Total reflectance curves and integrated AM0 values for the MISSE-9 wake alumina flight (M9W-C3 F) and control (M9W-C3 B) samples.

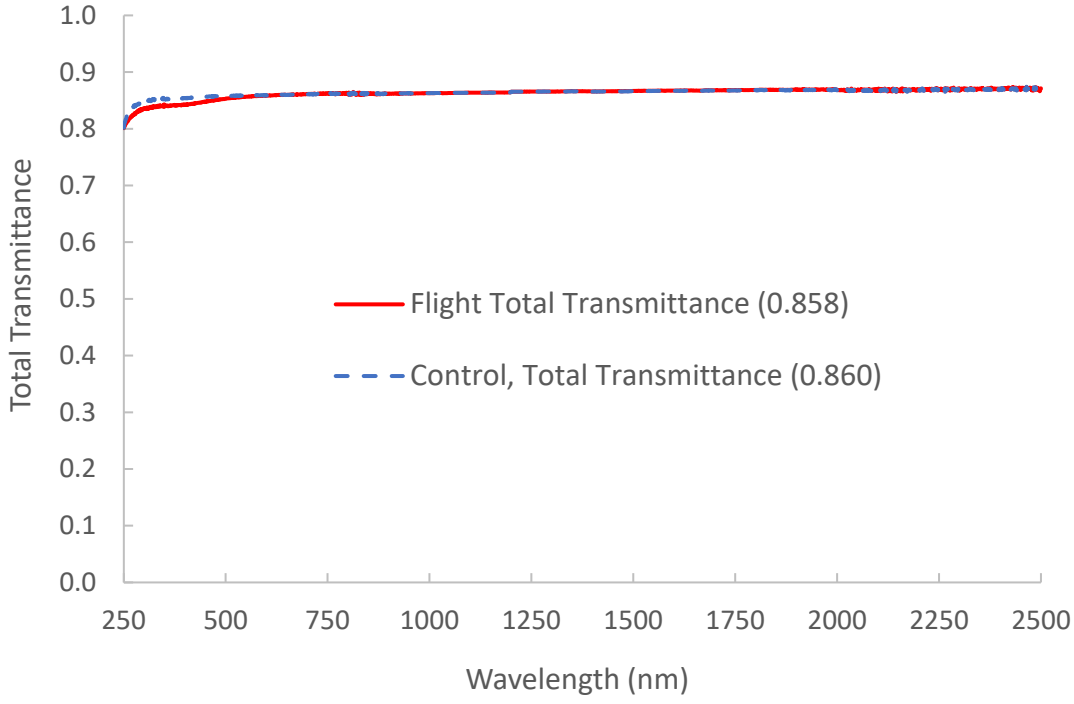

Fig. A2b. Total transmittance curves and integrated AM0 values for the MISSE-9 wake alumina flight (M9W-C3 F) and control (M9W-C3 B) samples.

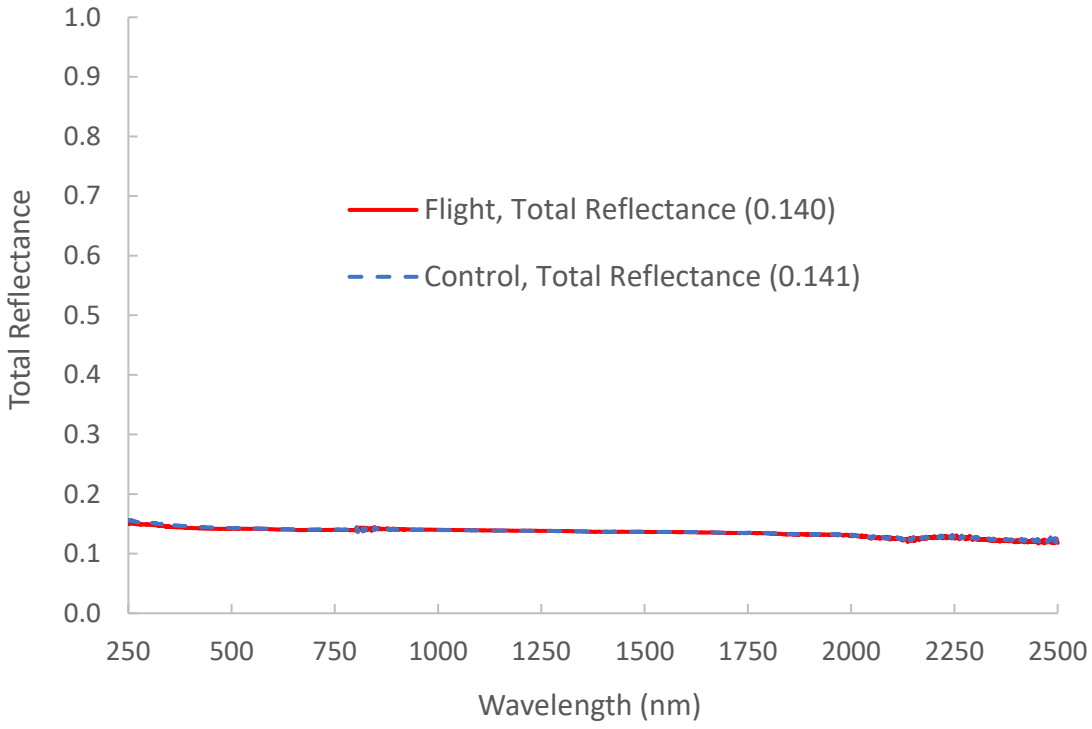

Fig. A3a. Total reflectance curves and integrated AM0 values for the MISSE-9 zenith alumina flight (M9Z-C3 F) and control (M9W-C3 B) samples.

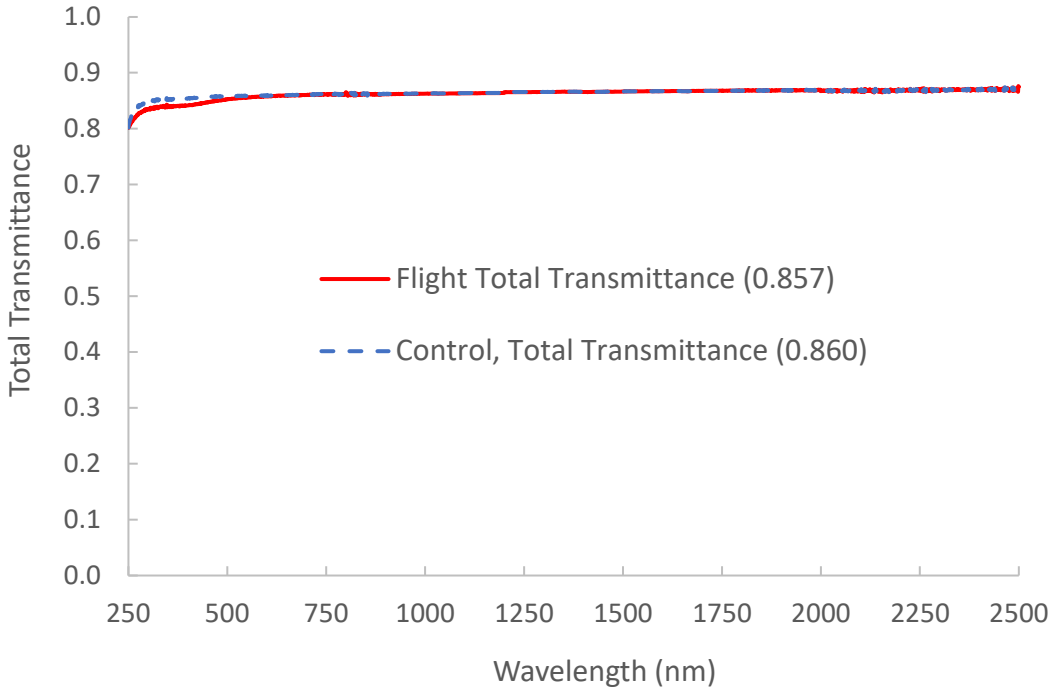

Fig. A3b. Total transmittance curves and integrated AM0 values for the MISSE-9 zenith alumina flight (M9Z-C3 F) and control (M9W-C3 B) samples.

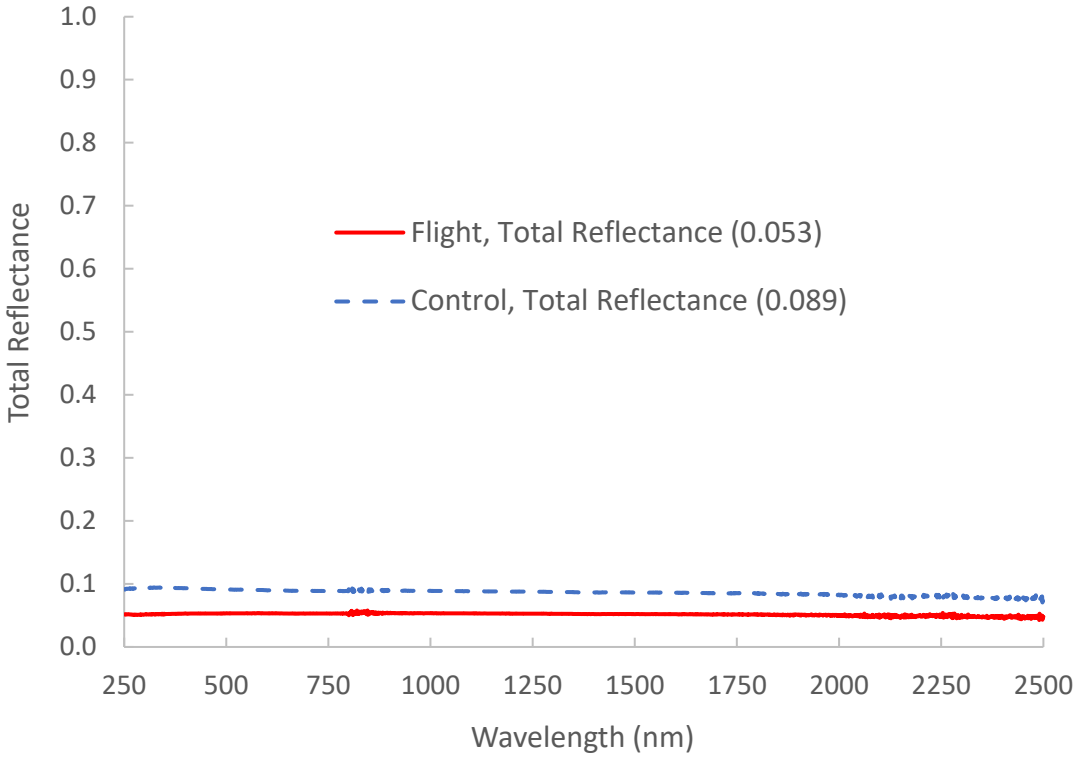

Fig. A4a. Total reflectance curves and integrated AM0 values for the MISSE-9 ram magnesium fluoride flight (M9R-C27 F) and control (M9R-C27 B) samples.

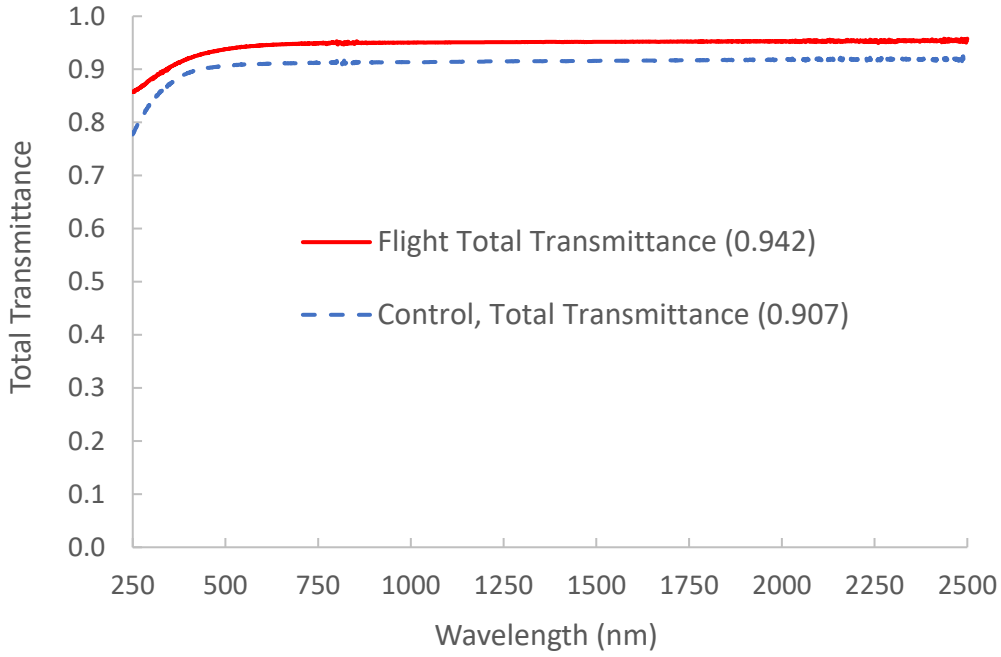

Fig. A4b. Total transmittance curves and integrated AM0 values for the MISSE-9 ram magnesium fluoride flight (M9R-C27 F) and control (M9R-C27 B) samples.

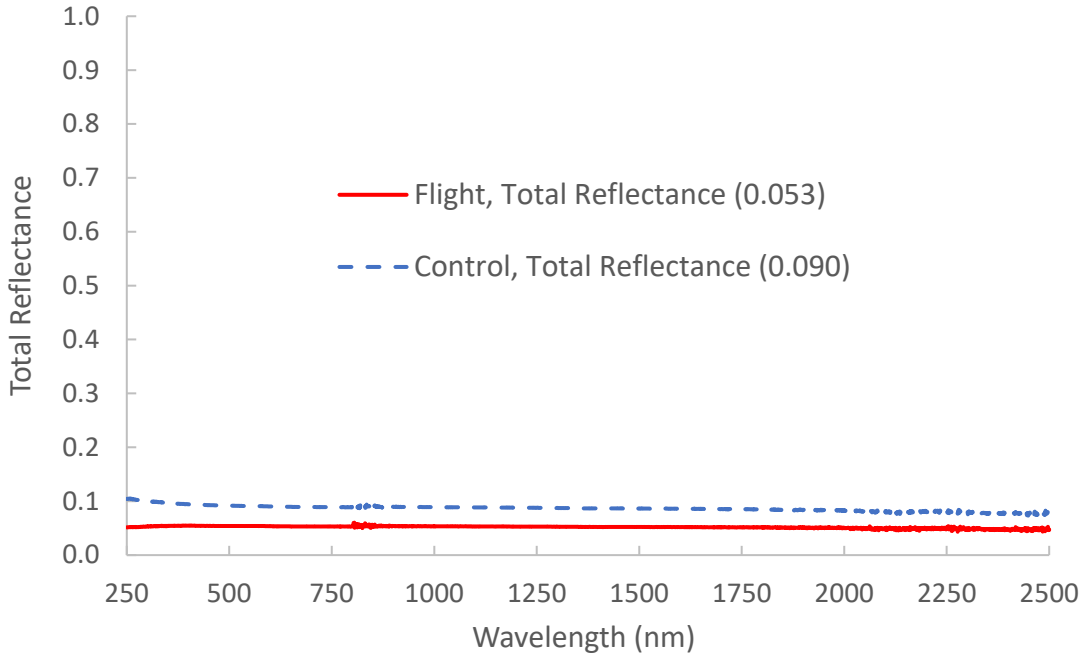

Fig. A5a. Total reflectance curves and integrated AM0 values for the MISSE-9 zenith magnesium fluoride flight (M9Z-C18 F) and control (M9Z-C18 B) samples.

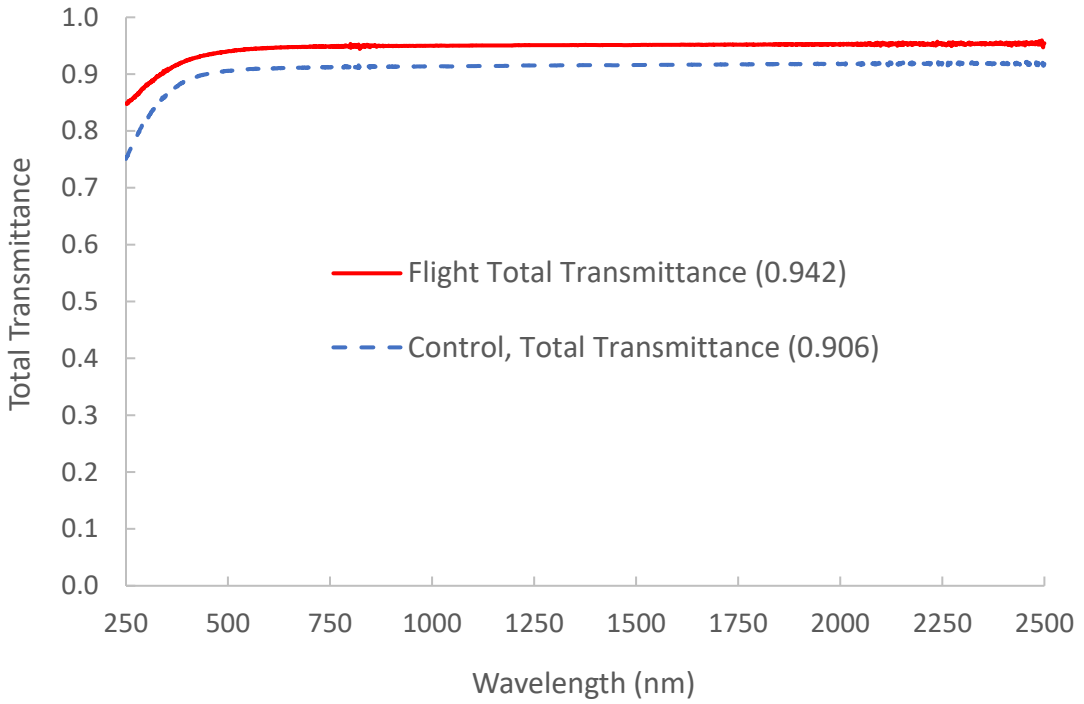

Fig. A5b. Total transmittance curves and integrated AM0 values for the MISSE-9 zenith magnesium fluoride flight (M9Z-C18 F) and control (M9Z-C18 B) samples.

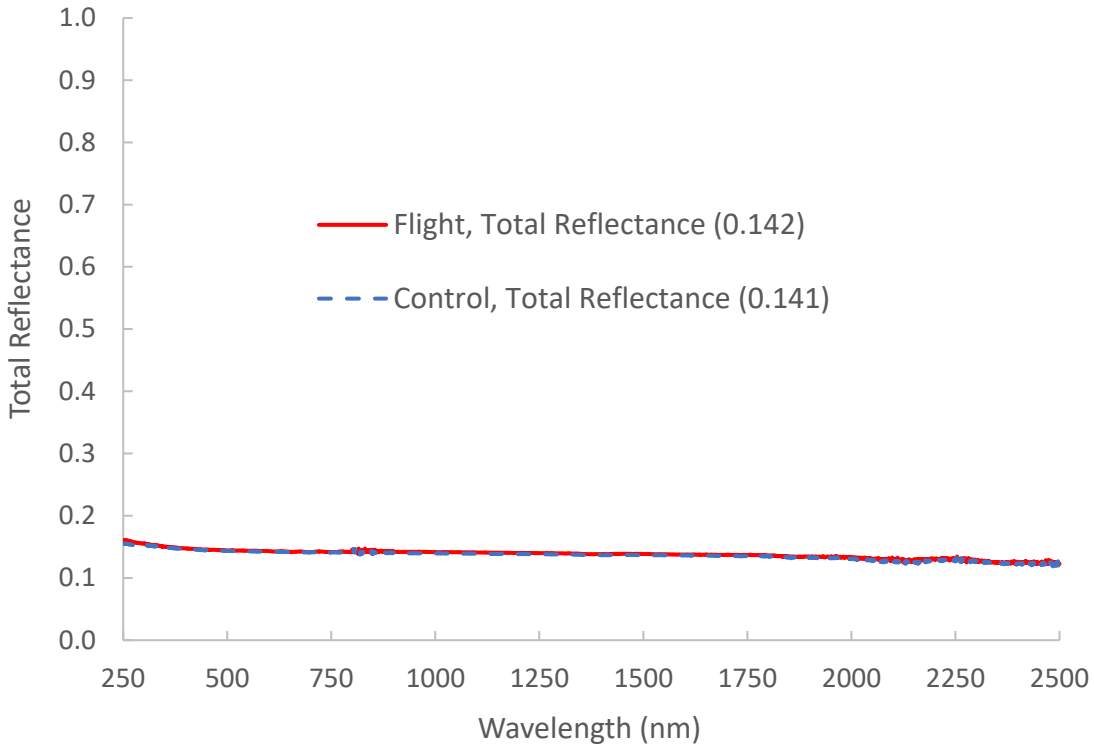

Fig. A6a. Total reflectance curves and integrated AM0 values for the MISSE-10 ram alumina flight (M10R-C4 F) and control (M10R-C4 B) samples.

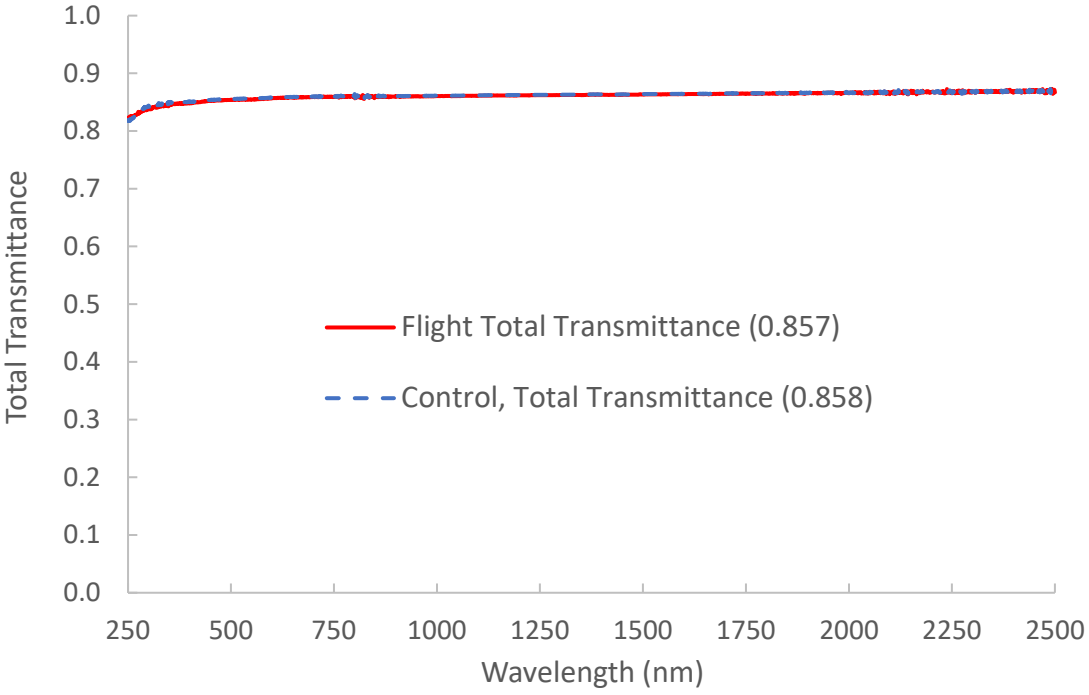

Fig. A6b. Total transmittance curves and integrated AM0 values for the MISSE-10 ram alumina flight (M10R-C4 F) and control (M10R-C4 B) samples.

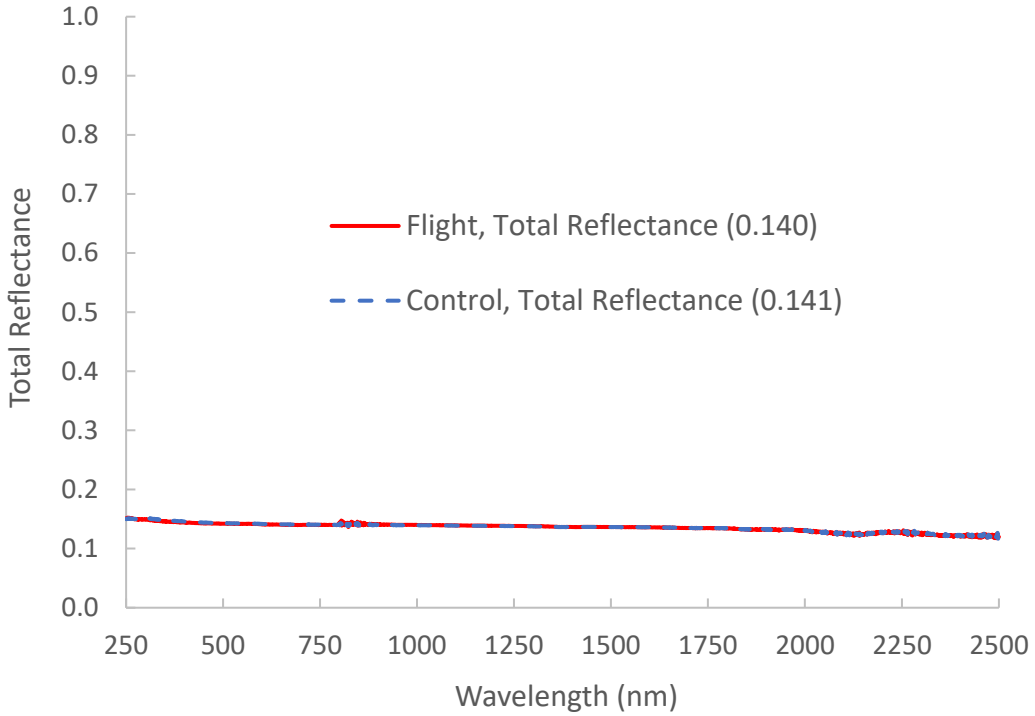

Fig. A7a. Total reflectance curves and integrated AM0 values for the MISSE-10 zenith alumina flight (M10Z-C5 F) and control (M10Z-C5 B) samples.

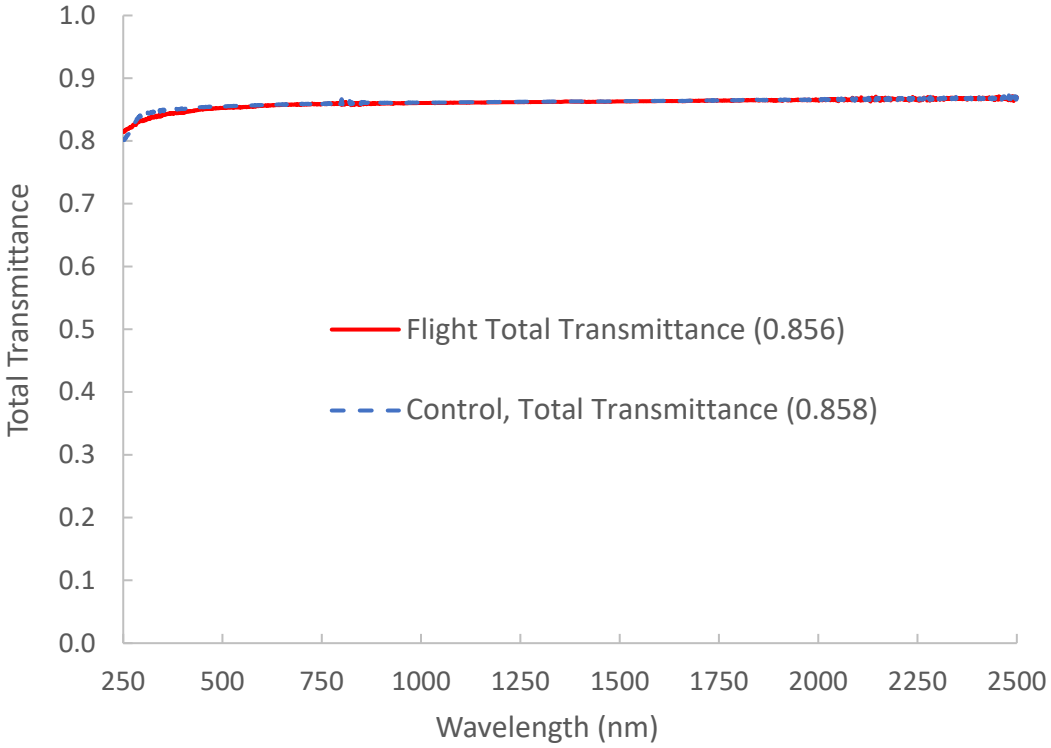

Fig. A7b. Total transmittance curves and integrated AM0 values for the MISSE-10 zenith alumina flight (M10Z-C5 F) and control (M10Z-C5 B) samples.

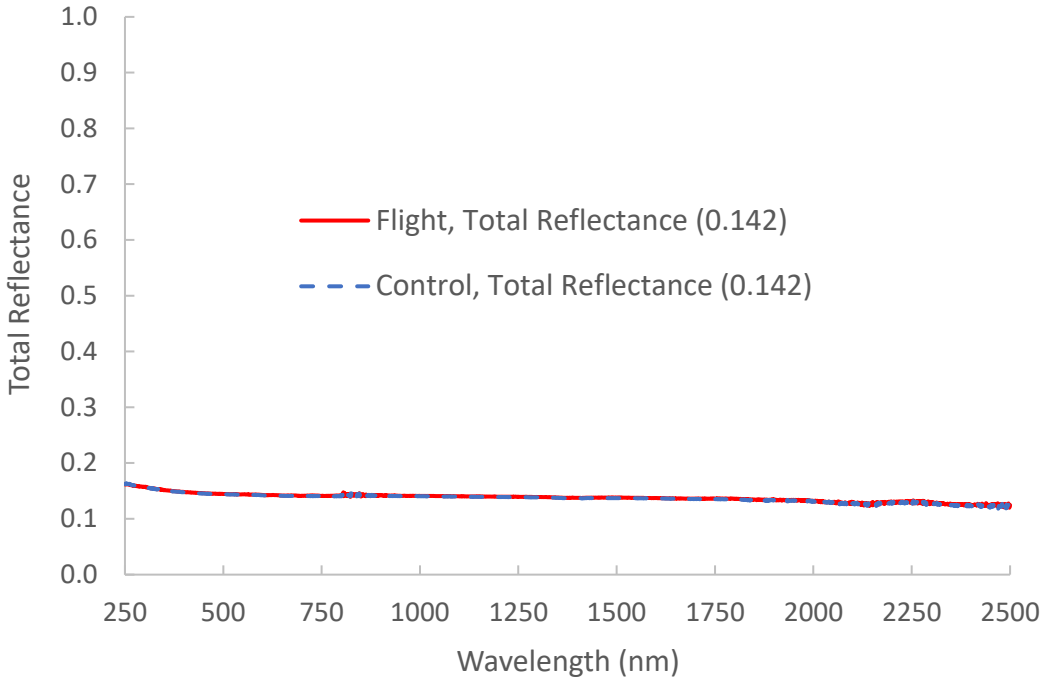

Fig. A8a. Total reflectance curves and integrated AM0 values for the MISSE-10 nadir alumina flight (M10N-C5 F) and control (M10N-C5 B) samples.

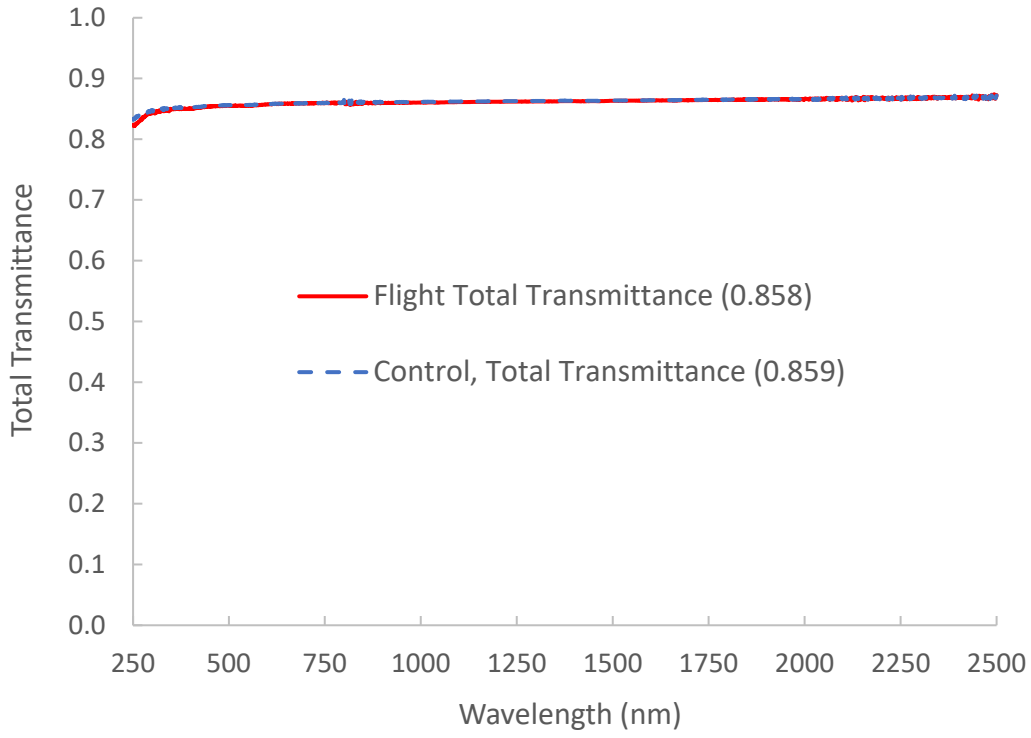

Fig. A8b. Total transmittance curves and integrated AM0 values for the MISSE-10 nadir alumina flight (M10N-C5 F) and control (M10N-C5 B) samples.

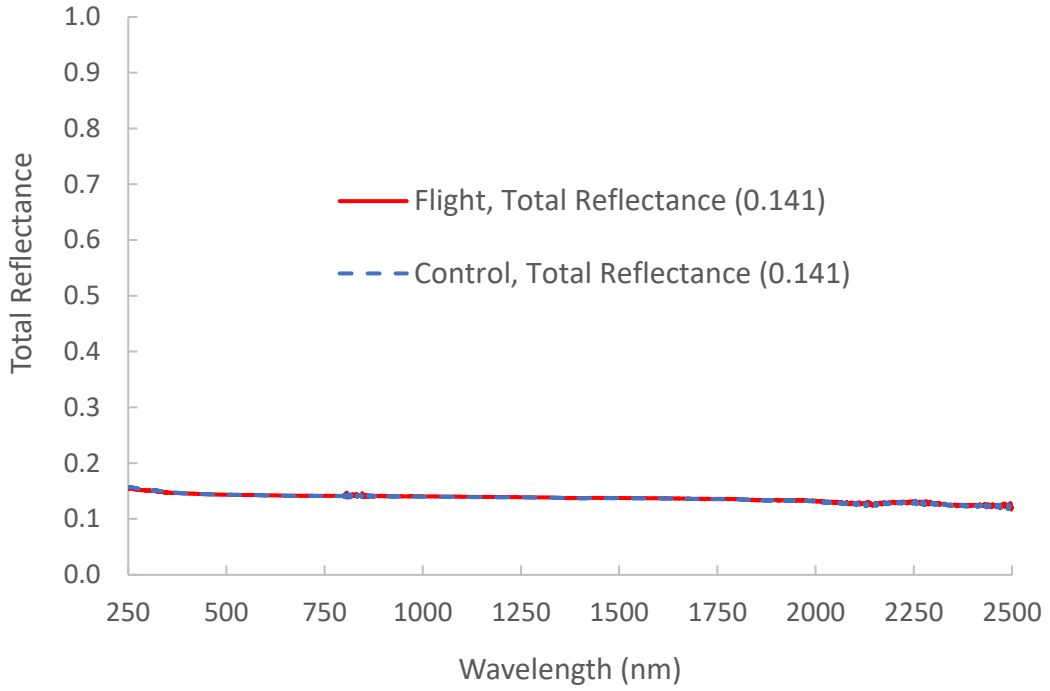

Fig. A9a. Total reflectance curves and integrated AM0 values for the MISSE-12 ram alumina flight (M12R-C3 F) and control (M12R-C3/M12W-C3 B) samples.

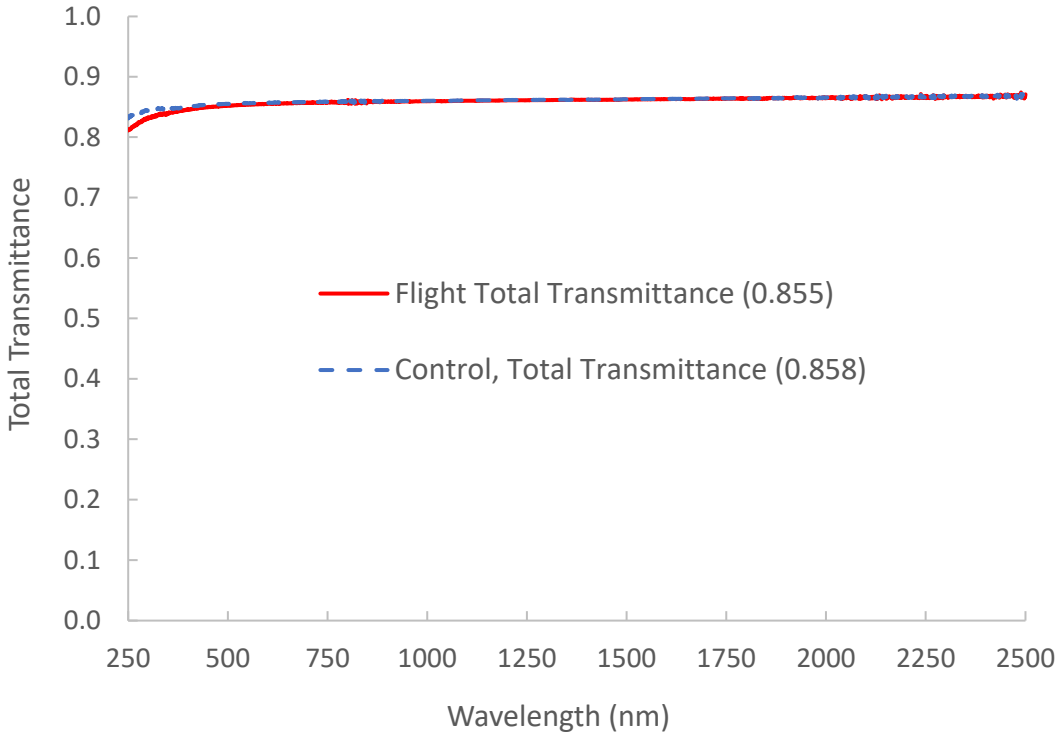

Fig. A9b. Total transmittance curves and integrated AM0 values for the MISSE-12 ram alumina flight (M12R-C3 F) and control (M12R-C3/M12W-C3 B) samples.

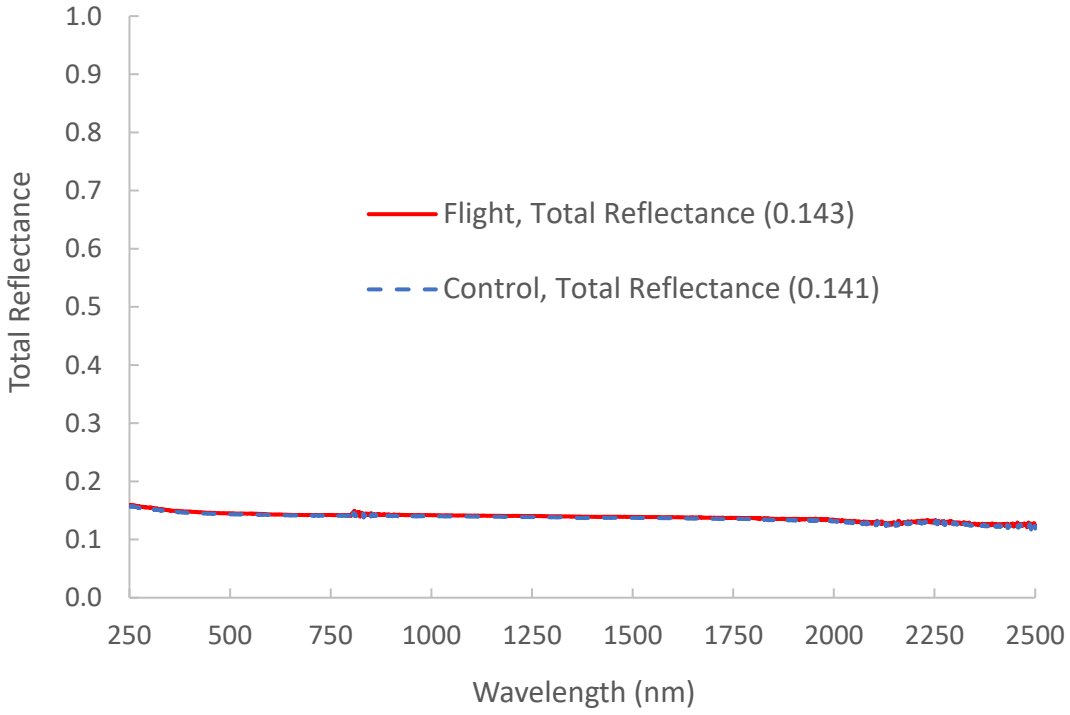

Fig. A10a. Total reflectance curves and integrated AM0 values for the MISSE-12 wake alumina flight (M12W-C3 F) and control (M12R-C3/M12W-C3 B) samples.

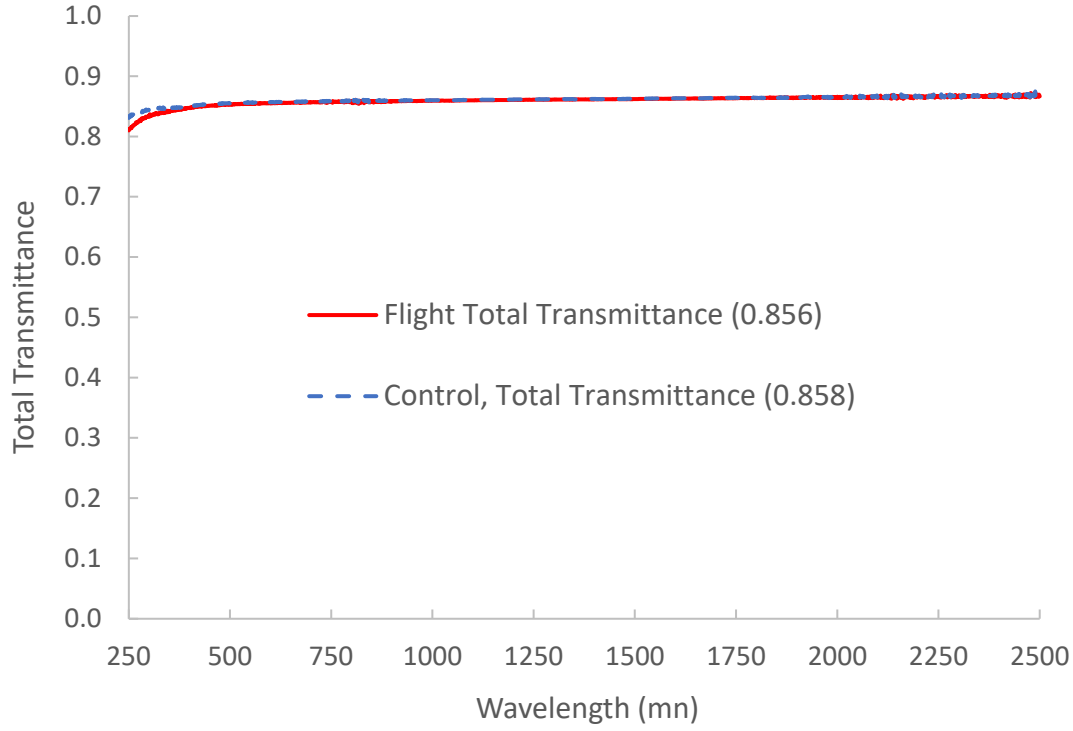

Fig. A10b. Total transmittance curves and integrated AM0 values for the MISSE-12 wake alumina flight (M12W-C3 F) and control (M12R-C3/M12W-C3 B) samples.

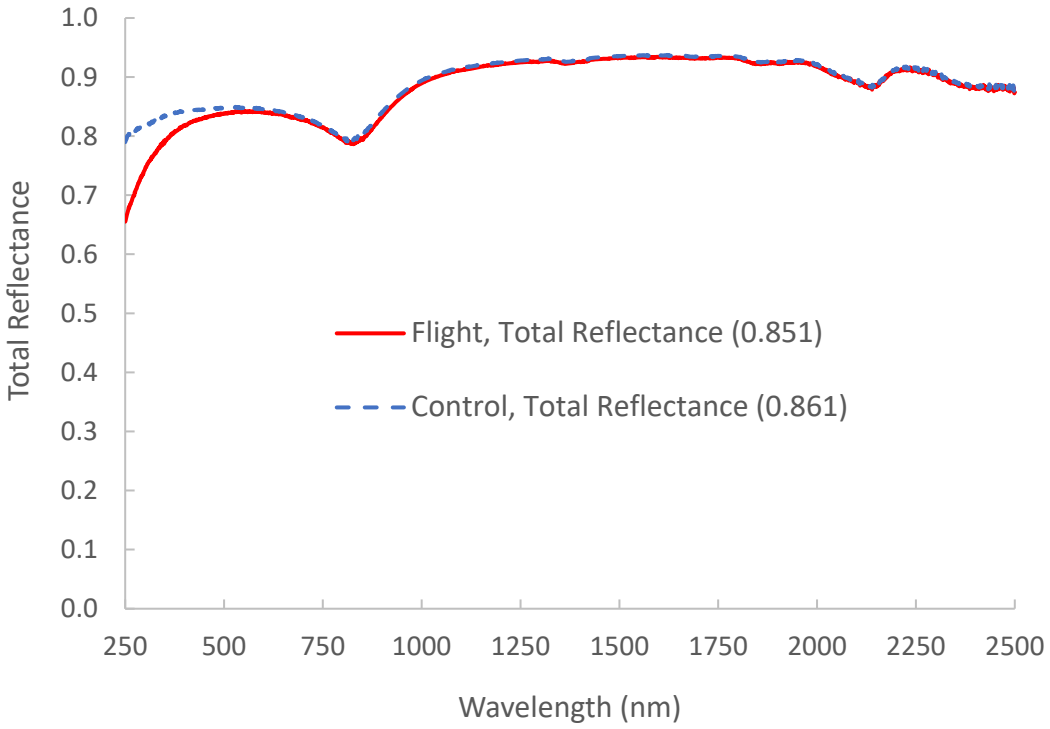

Fig. A11a. Total reflectance curves and integrated AM0 values for the MISSE-13 ram aluminized-Teflon FEP flight (M13W-C4 F) and control (M13W-C4 B) samples.

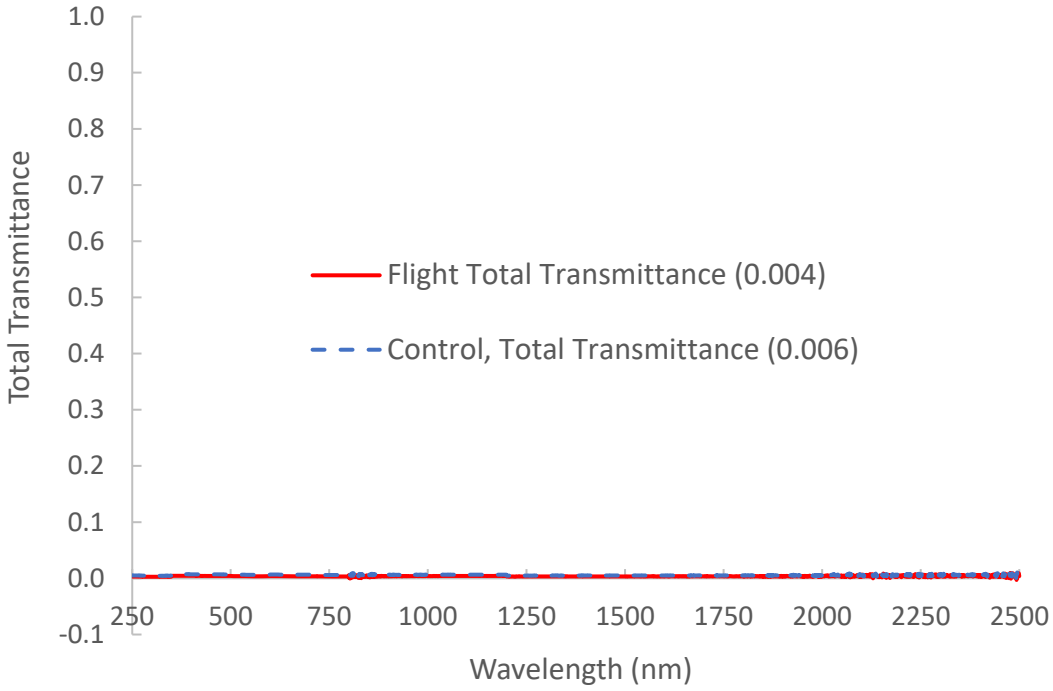

Fig. A11b. Total transmittance curves and integrated AM0 values for the MISSE-13 ram aluminized-Teflon FEP flight (M13W-C4 F) and control (M13W-C4 B) samples.

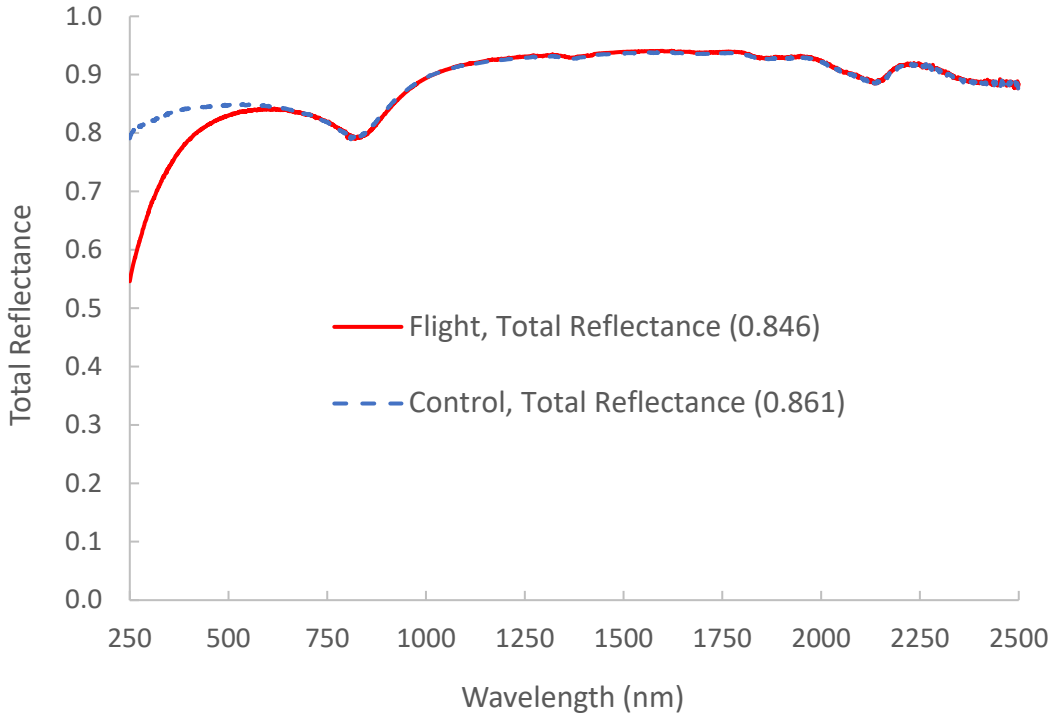

Fig. A12a. Total reflectance curves and integrated AM0 values for the MISSE-13 zenith aluminized-Teflon FEP flight (M13Z-C4 F) and control (M13Z-C4 B) samples.

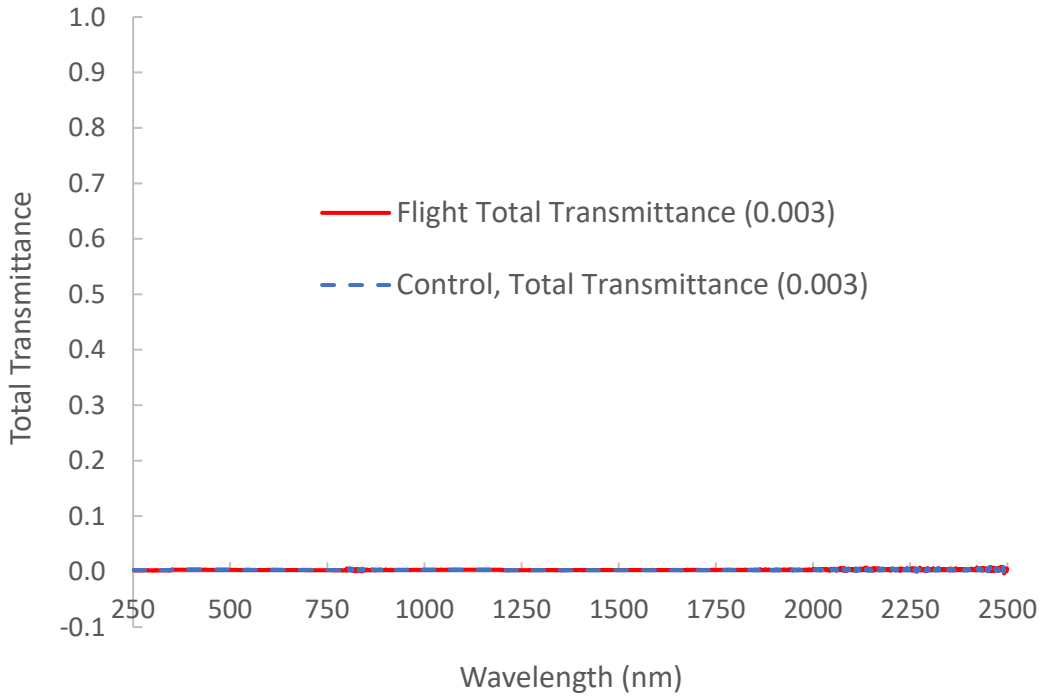

Fig. A12b. Total transmittance curves and integrated AM0 values for the MISSE-13 zenith aluminized-Teflon FEP flight (M13Z-C4 F) and control (M13Z-C4 B) samples.

References

1. de Groh, K.K., Banks, B.A., Miller, S.K.R., and Dever, J.A., Degradation of Spacecraft Materials (Chapter 28), Handbook of Environmental Degradation of Materials, Myer Kutz (editor), William Andrew Publishing, pp. 601–645, 2018.
2. de Groh, K.K. and McCollum, T.A., "Low Earth Orbit Durability of Protected Silicone for Refractive Photovoltaic Concentrator Arrays," *Journal of Spacecraft and Rockets*, Vol. 32, No. 1, Jan-Feb 1995, pp. 103–109.
3. de Groh, K.K., Banks, B.A., and Ma, D., "Ground-to-Space Effective Atomic Oxygen Fluence Correlation for DC 93-500 Silicone," *Journal of Spacecraft and Rockets*, Vol. 43, No. 2, March-April 2006, 414–420.
4. Banks, B.B., Dever, J.A., Gebauer L., and Hill, C.M., "Atomic Oxygen Interactions with FEP Teflon and Silicones on LDEF," LDEF-69 Months in Space, First Post-Retrieval Symposium, NASA Conference Publication 3134, Part 2 (of 3), 1991, pp. 801–815.
5. Banks, B.A., de Groh, K.K., Rutledge, S.K., and Haytas, C.A., "Consequences of Atomic Oxygen Interaction with Silicones and Silicone Contamination on Surfaces in Low Earth Orbit," Proceedings of SPIE, Vol. 3784, Rough Surface Scattering and Contamination, 1999; also NASA TM-1999-209179.
6. de Groh, K.K. and McCue, T.R., "Analyses of Contaminated Solar Array Handrail Samples Retrieved from Mir," Proceedings of the IECEC-99 Conference, August 1999, Vancouver Canada (99IECEC-25, SAE 1999-01-2694); also NASA TM-1999-209399, October 1999.
7. Kimoto, Y., Yano, K., Ishizawa, J., and Miyazaki, E., "Post Retrieval Analyses of Space Environment Monitoring Samples: Radiation Effects, UV, and Atomic Oxygen Fluence" Proc. of International Symposium on "SM/MPAC&SEED Experiment," Tsukuba, Japan, 10–11 March 2008.
8. de Groh, K.K. and Banks, B.A., "MISSE-Flight Facility Polymers and Composites Experiment 1-4 (PCE 1-4)," NASA/TM-20205008863, February 2021.
9. de Groh, K.K. and Banks, B.A., "Space Environmental Exposure of the MISSE 9–15 Polymers and Composites Experiment 1-4 (PCE 1-4)," NASA/TM-20240000755, February 2024.
10. Aegis Aerospace - Commercial Space (2023): //aegisaero.com/commercial-space-services/.
11. ASTM E490-22 "Standard Solar Constant and Zero Air Mass Solar Spectral Irradiance Tables," (May 2022).
12. Dever, J.A., Miller, S.K., Sechkar, E.A., and Wittberg, T.N., "Space Environment Exposure of Polymer Films on the Materials International Space Station Experiment: Results from MISSE 1 and MISSE 2," *High Performance Polymers*, 20 (2008), pp. 371–387.
13. Dawson, T.T., Hill, C.A., Rowell, A.F., Leavor, K.R., and Hawley, S.A., "SAGE III/ISS Contamination Monitoring Package: Observations in Orbit," NASA/TM-20205001963, June 2020.
14. de Groh, K.K. and Banks, B.A., "Atomic Oxygen Erosion Data from the MISSE 2-8 Missions," NASA/TM-2019-219982, May 2019.